

# MECHANISMS OF REHEATING AFTER INFLATION

A DISSERTATION  
SUBMITTED TO THE DEPARTMENT OF PHYSICS  
AND THE COMMITTEE ON GRADUATE STUDIES  
OF STANFORD UNIVERSITY  
IN PARTIAL FULFILLMENT OF THE REQUIREMENTS  
FOR THE DEGREE OF  
DOCTOR OF PHILOSOPHY

Gary Felder  
April 2001

© Copyright by Gary Felder 2001  
All Rights Reserved

I certify that I have read this dissertation and that in my opinion it is fully adequate, in scope and quality, as a dissertation for the degree of Doctor of Philosophy.

---

Andrei Linde  
(Principal Adviser)

I certify that I have read this dissertation and that in my opinion it is fully adequate, in scope and quality, as a dissertation for the degree of Doctor of Philosophy.

---

Savas Dimopoulos

I certify that I have read this dissertation and that in my opinion it is fully adequate, in scope and quality, as a dissertation for the degree of Doctor of Philosophy.

---

Robert Wagoner

Approved for the University Committee on Graduate Studies:

# Abstract

For the last two decades the dominant paradigm in early-universe cosmology has been the theory of inflation. According to this theory the universe underwent a brief period of exponential expansion during which it became nearly homogeneous on scales much larger than those we can observe today. The theory also states that the density of matter during this period nearly vanished, and all the matter we observe in the universe today was produced after inflation in a process known as reheating. Although the basic mechanisms of inflation are well understood and accepted, many unresolved problems remain concerning the production of matter after inflation and the subsequent transition to a more traditional, hot big bang model of the evolution of the universe. These problems are particularly difficult because we do not know the correct effective theory of physics for the energy scales relevant to inflationary theory, and because most models that we can consider involve non-perturbative, nonlinear interactions that can only be fully studied using numerical techniques.

The research described here consists of a combination of analytical and numerical work aimed at describing the possible mechanisms of reheating. My collaborators and I have studied the effects of parametric resonance, symmetry breaking and phase transitions, gravitational particle production, tachyonic (aka spinodal) instability, and a novel mechanism of reheating that we call "instant preheating." We investigated these effects in the context of single field inflation models with polynomial potentials, single field models with no minima, and multi-field hybrid inflation models. We found that many inflationary models could be ruled out on the basis of cosmologically unacceptable consequences such as domain walls, moduli fields, or excessive isocurvature fluctuations. Conversely we found that some seemingly impossible models could be

rescued by means of a secondary stage of inflation, or by instant preheating.

Much of this work required the use of numerical calculations, and in many cases only full scale lattice simulations could capture the nonlinear dynamics. Over the past several years I have been one of the two developers of a C++ lattice program for simulating the evolution of interacting scalar fields. This program, called LATTICEEASY, has been a key element of the research described in this thesis. The program is now available on the World Wide Web at

<http://physics.stanford.edu/gfelder/latticeeasy/>.

# Acknowledgements

First and foremost I would like to thank my advisor Andrei Linde, who has been a constant source of support to me both on an academic and a personal level. I was drawn to him by his love of physics, his profound intuition, his interest in the deepest questions in our field, and his willingness to share that interest with me and others. Since I first formed those impressions I have never been disappointed by him. I also sincerely thank Lev Kofman, who has functioned very much as a second advisor to me through much of my graduate career. In addition to working with me on many projects over the years he also graciously invited me to come work with him for a year in Toronto, which was an invaluable experience for me both scientifically and personally. I thank the Canadian Institute for Theoretical Astrophysics for their hospitality and for providing a stimulating and pleasant working environment. I also thank Lev and CITA for offering me a postdoc position, which I was delighted to accept.

Thanks are also due to the many other great physicists that have helped me throughout this process, including Patrick Greene, Igor Tkachev, Juan Garcia-Bellido, and Nemanja Kaloper. These people have collaborated with me and provided useful sounding boards for both my ideas and for my confusion. Thanks go to Robert Wagoner for putting up with my incessant questions, which he was always willing to take time for. And for making my education at Stanford many times more useful and abundantly more enjoyable than it would have been without them I would like to thank my study partners Aaron Birch, Travis Brooks, Amanda Weinstein, and Yue Chen. Special thanks go to Aaron Miller for a seemingly endless supply of rides and other favors, to Yonatan Zunger for keeping my computer running all these years,

and to Danna Rosenberg for being there for me when I most needed it. Thanks go also to Marcia Keating, who helped me out in almost every aspect of learning to deal with the bureaucracy and regulations at Stanford.

To Mom and Dad, Marty and Rebecca, Kenny and Elena, and all the other members of my family I want to say that I have never in my life known a more loving and supportive family than ours. The opportunity to live near my sister Elena has been one of the greatest joys of being in graduate school. And to Rosemary McNaughton, my personal candidate for the most wonderful woman in the world, thank you for being there for me in so many ways.

I dedicate this work to the memory of Johnny Charlton: Dear friend, you will always be missed.





We are a bit of stellar matter gone wrong. We are physical machinery - puppets that strut and talk and laugh and die as the hand of time pulls the strings beneath. But there is one elementary inescapable answer. We are that which asks the question.

-Sir Arthur Eddington

As an adolescent I aspired to lasting fame, I craved factual certainty, and I thirsted for a meaningful vision of human life - so I became a scientist. This is like becoming an archbishop so you can meet girls.

- Matt Cartmill

Let's start at the very beginning. A very good place to start.

- Julie Andrews in "The Sound of Music"



# Contents

<b>Abstract</b>	<b>iv</b>
<b>Acknowledgements</b>	<b>vi</b>
<b>I Introduction</b>	<b>1</b>
1 Motivation	2
2 Outline of the Thesis	5
3 A Primer on Inflation	7
3.1 The Big Bang Model . . . . .	7
3.1.1 Overview of the Model . . . . .	7
3.1.2 Initial Condition Problems . . . . .	9
3.1.3 Relic Problems . . . . .	11
3.1.4 Summary of the Problems With the Big Bang Model . . . . .	11
3.2 Inflation . . . . .	12
3.2.1 Why Inflation Occurs . . . . .	13
3.2.2 Some Basic Consequences of Inflation . . . . .	16
3.3 Reheating . . . . .	18
<b>II Mechanisms of Reheating</b>	<b>20</b>
4 Introduction to the Research	21

<b>5</b>	<b>Instant Preheating</b>	<b>25</b>
5.1	Introduction . . . . .	26
5.2	Instant preheating: The basic idea . . . . .	27
5.3	The simplest models . . . . .	29
5.4	Fat wimpzillas . . . . .	34
5.5	Instant Preheating and NO Models . . . . .	36
5.6	Conclusions . . . . .	36
<b>6</b>	<b>Inflation and Preheating in NO Models</b>	<b>39</b>
6.1	Introduction . . . . .	40
6.2	Isocurvature perturbations in NO Models . . . . .	41
6.3	Cosmological production of gravitinos and moduli fields . . . . .	46
6.4	Saving NO models: Instant preheating . . . . .	49
6.4.1	Initial conditions for inflation and reheating in the model with interaction $\frac{g^2}{2}\phi^2\chi^2$ . . . . .	50
6.4.2	Instant preheating in NO models . . . . .	52
6.5	Other versions of NO models . . . . .	56
<b>7</b>	<b>Gravitational Particle Production and the Moduli Problem</b>	<b>58</b>
7.1	Chapter Abstract . . . . .	58
7.2	Introduction . . . . .	59
7.3	Moduli problem . . . . .	61
7.4	Generation of light particles from and after inflation . . . . .	66
7.5	Light moduli from inflation . . . . .	71
<b>8</b>	<b>Inflation After Preheating</b>	<b>77</b>
8.1	Introduction . . . . .	78
8.2	Theory of the phase transition . . . . .	79
8.3	Simulation Results and Their Interpretation . . . . .	83
8.4	Nonthermal phase transitions and production of topological defects . . . . .	89
8.5	Conclusions . . . . .	93

<b>9</b>	<b>The Development of Equilibrium After Preheating</b>	<b>94</b>
9.1	Introduction . . . . .	95
9.2	Calculations in Chaotic Inflation . . . . .	97
9.2.1	Model . . . . .	97
9.2.2	The Output Variables . . . . .	98
9.2.3	Results . . . . .	101
9.3	Other Models of Inflation and Interactions . . . . .	107
9.3.1	Variations on Chaotic Inflation With a Quartic Potential . . .	107
9.3.2	Chaotic Inflation with a Quadratic Potential . . . . .	108
9.3.3	Hybrid Inflation . . . . .	109
9.4	The Onset of Chaos, Lyapunov Exponents and Statistics . . . . .	111
9.5	Rules of Thermalization . . . . .	117
9.6	Discussion . . . . .	118
<b>10</b>	<b>Dynamics of Symmetry Breaking and Tachyonic Preheating</b>	<b>123</b>
10.1	Introduction . . . . .	124
10.2	Tachyonic Instability and symmetry breaking . . . . .	125
10.2.1	Quadratic potential . . . . .	125
10.2.2	Cubic potential . . . . .	130
10.3	Tachyonic preheating in hybrid inflation . . . . .	133
<b>III</b>	<b>LATTICEEASY: Lattice Simulations of Scalar Field Dynamics</b>	<b>138</b>
<b>11</b>	<b>Introduction to LATTICEEASY</b>	<b>139</b>
11.1	Lattice Simulations and Cosmology . . . . .	140
11.2	My Contributions to LATTICEEASY . . . . .	141
<b>12</b>	<b>Equations</b>	<b>143</b>
12.1	Evolution Equations . . . . .	143
12.1.1	Field Equations and Coordinate Rescalings . . . . .	143
12.1.2	Scale Factor Evolution . . . . .	144

12.2	Initial Conditions on the Lattice . . . . .	145
12.2.1	Initial Conditions for Field Fluctuations . . . . .	145
12.2.2	Initial Conditions for Field Derivative Fluctuations . . . . .	148
12.2.3	Standing Waves . . . . .	149
12.2.4	The Adiabatic Approximation . . . . .	151
12.3	Renormalization . . . . .	153
<b>13</b>	<b>Computational Methods Used by LATTICEEASY</b>	<b>155</b>
13.1	Time Evolution: The Staggered Leapfrog	
	Method . . . . .	155
13.2	Correction to the Scale Factor Evolution Equation to Account for Stag-	
	gered Leapfrog . . . . .	156
13.3	Spatial Derivatives . . . . .	157
13.4	The Accuracy of the Simulations . . . . .	158
13.4.1	The Classical Approximation . . . . .	158
13.4.2	Numerical Accuracy . . . . .	160
<b>IV</b>	<b>Conclusion: My Philosophical Ramblings</b>	<b>163</b>
	<b>Bibliography</b>	<b>167</b>

# List of Figures

7.1	Fluctuations vs. mode frequency at a late time. The lower plots show runs that started close to the end of inflation, with initial conditions $f_k = \frac{1}{\sqrt{2k}}e^{-ikt}$ . The starting times range from $\phi_0 = 1.5M_p$ (lowest curve) up through $\phi_0 = 2M_p$ . The highest curve shows the Hankel function solutions given by eqs. (7.20) and (7.21) As we see, calculations with $f_k = \frac{1}{\sqrt{2k}}e^{-ikt}$ produce the correct spectrum at large $k$ but underestimate the level of quantum fluctuations at small $k$ . . . . .	69
8.1	The spatial average of the inflation field $\phi$ as a function of time. The field $\phi$ is shown in units of $v$ , the symmetry breaking parameter. Time is shown in Planck units. . . . .	84
8.2	The spatial average of the inflation field $\phi$ as a function of time in the vicinity of the phase transition. The left figure shows the field just before the phase transition and at the moment of the transition. The field oscillates with an amplitude approaching $10^{-3}v$ . The right figure shows the field $\phi$ after the phase transition, when it oscillates near the (time-dependent) position of the minimum of the effective potential at $\phi \approx v$ . Time is shown in Planck units. . . . .	86
8.3	These plots show the region of space in which symmetry breaking has occurred at four successive times. . . . .	87
8.4	The scale factor $a$ as a function of time. In the beginning $a \sim \sqrt{t}$ , which is a curve with negative curvature, but then at some stage it begins to turn upwards, indicating a short stage of inflation. . . . .	88

8.5	The second derivative of the scale factor, $\ddot{a}$ . A universe dominated by ordinary matter (relativistic or nonrelativistic) will always have $\ddot{a} < 0$ , whereas in an inflationary universe $\ddot{a} > 0$ . We see that starting from the moment $t \sim 2 \times 10^{12}$ (in Planck units) the universe experiences accelerated (inflationary) expansion. . . . .	89
8.6	The ratio of pressure to energy density $p/\rho$ . (Values were time averaged over short time scales to make the plot smoother and more readable.)	90
9.1	Number density $n$ for $V = \frac{1}{4}\lambda\phi^4 + \frac{1}{2}g^2\phi^2\chi^2$ . The plots are, from bottom to top at the right of the figure, $n_\phi$ , $n_\chi$ , and $n_{tot}$ . The dashed horizontal line is simply for comparison. The end of exponential growth and the beginning of turbulence (i.e. the moment $t_*$ ) occurs around the time when $n_{tot}$ reaches its maximum. . . . .	102
9.2	Evolution of the spectrum of $\chi$ in the model $V = \frac{1}{4}\lambda\phi^4 + \frac{1}{2}g^2\phi^2\chi^2$ . Red plots correspond to earlier times and blue plots to later ones. For black and white viewing: The sparse, lower plots all show early times. In the thick bundle of plots higher up the spectrum is rising on the right and falling on the left as time progresses. . . . .	103
9.3	Variances for $V = \frac{1}{4}\lambda\phi^4 + \frac{1}{2}g^2\phi^2\chi^2$ . The upper plot shows $\langle(\phi - \bar{\phi})^2\rangle$ and the lower plot shows $\langle(\chi - \bar{\chi})^2\rangle$ . . . . .	104
9.4	Effective masses for $V = \frac{1}{4}\lambda\phi^4 + \frac{1}{2}g^2\phi^2\chi^2$ as a function of time in units of comoving momentum. The lower plot is $m_\phi$ and the upper one is $m_\chi$ .	106
9.5	Time evolution of the effective masses for the model $V = \frac{1}{4}\lambda\phi^4 + \frac{1}{2}g^2\phi^2\chi^2 + \frac{1}{2}h^2\chi^2\sigma^2$ . From bottom to top on the right hand side the plots show $m_\phi$ , $m_\sigma$ , and $m_\chi$ . . . . .	107
9.6	Evolution of variances of fields in the model (9.25). The two fields that grow at late times, in order of their growth, are $\chi$ and $Im(\Phi)$ . . . . .	111
9.7	The Lyapunov exponent $\lambda$ for the fields $\phi$ (lower curve) and $\chi$ (upper curve). The vertical axis is $\lambda t$ . . . . .	113
9.8	The Lyapunov exponent $\lambda'$ for the fields $\phi$ and $\chi$ using the normalized distance function $\Delta$ . . . . .	114



9.9	The probability distribution function for the field $\chi$ after preheating. Dots show a histogram of the field and the solid curve shows a best-fit Gaussian. . . . .	115
9.10	Deviations from Gaussianity for the field $\phi$ as a function of time. The solid, red line shows $3\langle\delta\phi^2\rangle^2/\langle\delta\phi^4\rangle$ and the dashed, blue line shows $3\langle\delta\dot{\phi}^2\rangle^2/\langle\delta\dot{\phi}^4\rangle$ . . . . .	116
9.11	Deviations from Gaussianity for the field $\chi$ as a function of time. The solid, red line shows $3\langle\delta\chi^2\rangle^2/\langle\delta\chi^4\rangle$ and the dashed, blue line shows $3\langle\delta\dot{\chi}^2\rangle^2/\langle\delta\dot{\chi}^4\rangle$ . . . . .	116
9.12	$V = 1/4\lambda\phi^4$ . (Note that the vertical scale is larger than for the subsequent plots.) . . . . .	120
9.13	$V = 1/4\lambda\phi^4 + 1/2g^2\phi^2\chi^2$ , $g^2/\lambda = 200$ . The upper curve represents $n_\chi$ . . . . .	120
9.14	$V = 1/4\lambda\phi^4 + 1/2g^2\phi^2\chi^2 + 1/2h^2\chi^2\sigma^2$ , $g^2/\lambda = 200$ , $h^2 = 100g^2$ . The highest curve is $n_\phi$ . The number density of $\chi$ diminishes when $n_\sigma$ grows. . . . .	120
9.15	$V = 1/4\lambda\phi^4 + 1/2g^2\phi^2\chi^2 + 1/2h_i^2\chi^2\sigma_i^2$ , $g^2/\lambda = 200$ , $h_1^2 = 200g^2$ , $h_2^2 = 100g^2$ . The pattern is similar to the three-field case until the growth of $\sigma_2$ . . . . .	120
9.16	$V = 1/4\lambda\phi^4$ . . . . .	121
9.17	$V = 1/4\lambda\phi^4 + 1/2g^2\phi^2\chi^2$ , $g^2/\lambda = 200$ . The spectra of $\phi$ and $\chi$ are nearly identical. . . . .	121
9.18	$V = 1/4\lambda\phi^4 + 1/2g^2\phi^2\chi^2 + 1/2h^2\chi^2\sigma^2$ , $g^2/\lambda = 200$ , $h^2 = 100g^2$ . The $\chi$ and $\sigma$ spectra are similar, but $\sigma$ rises in the infrared). The spectrum of $\phi$ is markedly different from the others. . . . .	121
9.19	$V = 1/4\lambda\phi^4 + 1/2g^2\phi^2\chi^2 + 1/2h_i^2\chi^2\sigma_i^2$ , $g^2/\lambda = 200$ , $h_1^2 = 200g^2$ , $h_2^2 = 100g^2$ . All fields other than the inflaton have nearly identical spectra. . . . .	121
9.20	$V = 1/2m^2\phi^2 + 1/2g^2\phi^2\chi^2$ , $g^2M_p^2/m^2 = 2.5 \times 10^5$ . The upper curve represents $n_\chi$ . . . . .	122
9.21	$V = 1/2m^2\phi^2 + 1/2g^2\phi^2\chi^2 + 1/2h^2\chi^2\sigma^2$ , $g^2M_p^2/m^2 = 2.5 \times 10^5$ , $h^2 = 100g^2$ . The highest curve is $n_\chi$ . The field that grows latest is $\sigma$ . . . . .	122
9.22	$V = 1/2m^2\phi^2 + 1/2g^2\phi^2\chi^2$ , $g^2M_p^2/m^2 = 2.5 \times 10^5$ . The upper curve represents the spectrum of $\chi$ . . . . .	122

9.23	$V = 1/2m^2\phi^2 + 1/2g^2\phi^2\chi^2 + 1/2h^2\chi^2\sigma^2$ , $g^2M_p^2/m^2 = 2.5 \times 10^5$ , $h^2 = 100g^2$ The $\chi$ and $\sigma$ spectra are similar, while the spectrum of $\phi$ rises much higher in the infrared. . . . .	122
10.1	The process of symmetry breaking in the model (10.1) for $\lambda = 10^{-4}$ . In the beginning the distribution is very narrow. Then it spreads out and shows two maxima that oscillate about $\phi = \pm v$ with an amplitude much smaller than $v$ . These maxima never come close to the initial point $\phi = 0$ . The values of the field are shown in units of $v$ . . . . .	129
10.2	Growth of quantum fluctuations in the process of symmetry breaking in the quadratic model (10.1). . . . .	130
10.3	The development of domain structure in the quadratic model (10.1). . . . .	131
10.4	The process of symmetry breaking in the model (10.1) for a complex field $\phi$ . The field distribution falls down to the minimum of the effective potential at $ \phi  = v$ and experiences only small oscillations with rapidly decreasing amplitude $ \Delta\phi  \ll v$ . . . . .	132
10.5	The distribution of strings in the model (10.1) for a complex field $\phi$ . . . . .	133
10.6	Fast growth of the peaks of the distribution of the field $\phi$ in the cubic model (10.4). It should be compared with Fig. 10.2 for the quadratic model (10.1). . . . .	134
10.7	Histograms describing the process of symmetry breaking in the model (10.4) for $\lambda = 10^{-2}$ . After a single oscillation the distribution acquires the form shown in the last frame and after that it practically does not oscillate. . . . .	135
10.8	The process of symmetry breaking in the hybrid inflation model (10.6) for $g^2 \ll \lambda$ . The field distribution moves along the ellipse $g^2\phi^2 + \lambda\sigma^2 = g^2\phi_c^2$ from the bifurcation point $\phi = \phi_c$ , $\sigma = 0$ . . . . .	136

# **Part I**

## **Introduction**

# Chapter 1

## Motivation

The topic of this thesis is reheating after inflation. Put in a more general way, I intend to talk about where all the matter we see in the universe (including dark matter) came from. Cosmologists today generally believe that this matter was produced about 15 billion years ago following a period of rapid expansion known as inflation. The theory of inflation, including this period of matter production known as reheating, is a modification of the standard big bang model of cosmology developed early in this century by Einstein, Hubble, Friedmann, and others.

Much of the thesis is fairly technical and assumes a basic knowledge of general relativity and quantum field theory. For the sake of completeness, however, I have written a self-contained “inflation primer” outlining the basic structure of the big bang model, the motivations for inflation as a modification of that model, and some of the key ideas in the theory of inflation and reheating.

Subsequent chapters will explain work I have done exploring different mechanisms by which reheating can occur. The wide variety of models being considered is a reflection of our current state of ignorance about the early universe. On the one hand we have no direct observational knowledge of any processes that occurred before the time of nucleosynthesis, i.e. the formation of nuclei of the light elements such as deuterium, helium, and lithium. Inflation was certainly over long before this period. On the other hand we have very little theoretical guidance as to what model to use for describing physics at the high energy scales that prevailed during the time of inflation.

Most theorists agree that the standard model of particle physics that describes all of physics at the energy scales we can observe is almost certainly not valid at energy scales much higher than our current observations. We have many ideas about possible elements of a theory of high energy physics, including supersymmetry, Grand Unified Theories, and string theory, but no specific model has been formulated and tested for physics at high energies.<sup>1</sup>

So the physics of the early universe has not been observed, and the theory describing it is not known. Given such a dearth of knowledge it might seem that research into inflation would be hopeless. It turns out, however, that many results can be formulated that seem to be generic across a wide spectrum of possible models. Some of the generic predictions of inflation have already been tested and others are likely to be tested in the next 5-10 years, mostly by experiments testing in detail the properties of the microwave background radiation.

Moreover, a lot of important work has been done and continues to be done exploring the parameter space of possible inflationary models. On the observational side we can use currently available data to constrain the space of inflationary models, and over the last decade this technique has allowed us to eliminate many candidate models. On the theoretical side we can use ideas such as supersymmetry and supergravity to guide our searches for inflationary models and explore some of the consequences of models that incorporate those theoretical ideas. As better experimental and theoretical results become available our modeling will be more tightly constrained. Of course the hope is to eventually have a clear theoretical knowledge of what fields and interactions exist at high energies, use our knowledge of inflation to make detailed, testable predictions within that model, and have the experimental sophistication to test those predictions. We are still a long way from accomplishing any of those three goals, but progress is being made on all three.

---

<sup>1</sup>By high energies I mean anything from the scale of our current observations, roughly 1000 GeV, up to the Planck scale at about  $10^{19}$  GeV. Within this range it is still likely that physics is described by some quantum field theory, but we don't know the specific fields and interactions involved. At energies above the Planck scale quantum field theory itself may break down because quantum fluctuations of spacetime become important. Unless I specify otherwise I will always use "high energy theory" to mean something in the range from  $10^3$  to  $10^{19}$  GeV. Essentially all inflationary models involve typical energy scales within this range.

Given all of this, I view the role of inflationary theorists in the following way. We need to understand what mechanisms and predictions hold generically in inflation. We need to explore the space of models and figure out what observational signatures, if any, would allow us to distinguish between these models. Finally we need to develop techniques of analysis, both analytical and numerical, that are general enough to be of use as the theoretical and observational foundation of our work changes. It is in the spirit of these goals that the work presented here was done.

## Chapter 2

### Outline of the Thesis

This thesis is divided into three main sections. The first section contains general introductory material (including this outline), followed by a short inflation primer. The material in the primer does not assume any knowledge of advanced physics and it should serve as a general introduction for anyone not familiar with the field of cosmology. It describes the standard big bang theory that has held sway for most of this century, why many people came to believe this theory was in need of modification, and how inflationary theory has been able to address some of the problems with the standard big bang cosmology. Finally, the introduction ends with a brief discussion of reheating, the process by which we believe all the matter in the observable universe was generated.

The following section, part II, constitutes the main bulk of the thesis. The chapters in this section are adapted from the papers that I have co-authored as part of my graduate research. In general, these chapters describe different mechanisms by which reheating can occur and the consequences of those different processes. A more detailed outline of the material in the chapters and my specific role in the different aspects of the research is presented at the beginning of part II.

A good deal of the research described here has been done with the help of lattice simulations. Building on a program originally written by Igor Tkachev I developed a C++ program for performing such simulations of fields in the early universe. Much of my graduate work has been devoted to developing this program. This work has

included aspects of physics, mathematics, and programming. The final section of the thesis is thus a description of these lattice simulations. The website I created for the lattice program contains detailed documentation on the internal functioning and the use of the program itself. In this thesis I concentrate instead on the physics underlying the simulations. I also describe in more detail there the separate contributions that Dr. Tkachev and I each made to this work.



# Chapter 3

## A Primer on Inflation

### 3.1 The Big Bang Model

#### 3.1.1 Overview of the Model

For most of this century our view of the large scale structure and history of the universe has been dominated by the big bang model. According to this model the universe at early times was a nearly homogeneous expanding collection of high energy particles in thermal equilibrium. As the universe expanded and cooled very small inhomogeneities were then amplified by gravity and collapsed to form the structures we see today such as clusters, and galaxies. Extrapolating backwards, on the other hand, that homogeneous fireball would have had higher temperatures and densities at earlier times, ultimately reaching infinite density at a time called the big bang, about 15 billion years ago.

This model is in perfect accord with the theory of general relativity, which predicts that a universe with the initial conditions specified by the model will expand and cool in exactly that way. Moreover there have been many observational confirmations of the big bang model. These confirmations include the apparent motions of distant objects relative to us, the electromagnetic radiation emitted in the early universe and detectable now in the form of microwaves, and the abundances of light elements predicted by the theory of nucleosynthesis.

I want to focus in particular on the latter of these. Nuclear theory is well tested and understood, and by applying this theory to a homogeneous, expanding medium at high temperature we can predict what relative abundances of hydrogen, deuterium, helium, and lithium nuclei should have emerged when these nuclei were formed in the early universe. These predictions accurately match the observational data. This match is particularly important because it provides the earliest observational evidence we have for the big bang model. We have no direct measurements of any processes that occurred before nucleosynthesis. So in that sense we are free to imagine any deviations we wish from the big bang model before that point. However, since it seems unlikely that a very different scenario would give the same predictions for these abundances, any such models are constrained to reduce to the big bang scenario by the time of nucleosynthesis.

Given how successful the big bang model has been in matching essentially every observation to date one might legitimately wonder why we would want to modify it at all, rather than just accepting it straight back to the moment of the big bang. Such a complete extrapolation of the theory is not possible, however, because of certain limitations of our theories of high energy physics. When we talk about extrapolating backwards in the big bang model we are referring to running the equations of general relativity backwards to earlier times and higher densities. We know, however, that general relativity ceases to be valid when we try to describe a region of spacetime whose density exceeds a certain value known as the Planck density, roughly  $10^{96} \frac{\text{kg}}{\text{m}^3}$ . If we try to consistently apply quantum mechanics and general relativity at such a density we find that quantum fluctuations of spacetime should be important, and we have no theory that describes such a situation.

So the best we can do in using the big bang model to describe the very early universe is the following. At some point in the past the density of the universe was above the Planck density. We don't know what physics governs such a case so we can make no predictions based on it. Somehow this super-Planckian state (sometimes called *spacetime foam*) gave rise to at least one region of sub-Planckian density with the right initial conditions to produce the universe we currently see. From now on when I refer to the "initial conditions" for our universe I will mean the state that the

observable part of the universe was in after the density first became sub-Planckian and the universe (or at least this region of it) could thus be described classically.

Even in this more limited sense, however, there are certain problems with extending the big bang model back to the beginning of the universe. These problems can be categorized into “initial condition problems” and “relic problems.” I define what each of these are in the following two sections.

### 3.1.2 Initial Condition Problems

These problems consist of a number of seemingly fine-tuned aspects of the early universe in the big bang model. For example, we know that the universe was almost perfectly homogeneous at early times. Such statements are, to one way of thinking, not problems at all. As I discussed in the previous section, we do not know what physics gave rise to these initial conditions, so they are free parameters of the theory. Put another way, we can imagine that somewhere in the ultra-high energy physics theory that we don’t yet know is an explanation for why our universe emerged from the spacetime foam with exactly the right initial conditions to produce the kind of universe we see. It would be more satisfying if we could find an explanation for these features within known physics, but nature is not obliged to satisfy us. As it happens, we do know of such an explanation. Before discussing this solution, however, I want to describe some of these initial condition problems.

#### Homogeneity

The universe we observe today is very lumpy on small scales, e.g. those of people or galaxies, but on sufficiently large scales appears to be smooth and uniform. We know from our observations of the microwave background radiation that at much earlier times the universe was almost completely uniform even on smaller scales, with a mean variation  $\delta\rho/\rho \approx 10^{-5}$ .<sup>1</sup> If the initial conditions were random it might seem strange that there should be such good homogeneity, but of course the initial conditions were

---

<sup>1</sup>The Greek letter  $\rho$  is often used to mean density. So the meaning of this equation is that the energy density of any two points in the universe differed on average by less than one part in 100,000.

presumably not random but set by some unknown physics. It's not hard to imagine that some physical mechanism drove the universe to a state of high homogeneity. However, this mechanism must have been imperfect because the universe retained a small amount of inhomogeneity. If it weren't for these small inhomogeneities there would have been no seeds for galaxy formation and hence no structure formation. A mechanism that would drive the universe to near-perfect uniformity while still leaving these small but observable fluctuations seems a little stranger.

### Flatness

General relativity relates the curvature of spacetime to the matter in that spacetime. In the case of an expanding, nearly homogeneous universe such as ours the curvature depends on the overall density of matter and energy. If this density is above a critical value then the universe will be “open,” meaning parallel lines will diverge. If the density is sub-critical the universe will be “closed,” meaning parallel lines will converge. Finally, if the universe is exactly at critical density the universe will be “flat,” i.e. Euclidean. Typically the ratio of the density in the universe to the critical density moves away from one over time. A perfectly flat universe will always remain so but a curved universe will become more curved over time, whether it's open or closed.

Currently we can measure that the universe is within a factor of two or three of critical density. (Based on recent measurements it's probably within about 10% of critical density.) For this to be true now  $\rho/\rho_{crit}$  must have been  $1 \pm 10^{-59}$  at the time when the universe had Planck density. If the deviation had been a few orders of magnitude greater than that the universe would either have recollapsed long ago, or would have a nearly vanishing energy density by now. Was there some mechanism that drove the universe to such near-perfect (or possibly perfect) flatness?

### Horizon

This problem is related to the homogeneity problem described above. According to the theory of relativity no causal effect can propagate faster than the speed of light. If we believe that the universe had a beginning a finite time ago, then there is a finite

radius across which causal effects could have propagated by now. At the time when the microwave background was emitted there should have been roughly a million causally disconnected regions within the region of the universe we can currently observe. What could have caused such strong homogeneity over such a vast region before any causal signals could have spread information throughout this space?

### 3.1.3 Relic Problems

Another set of problems with the big bang model has to do with the production of exotic particles at high energies. By “high energies” in this context I mean energies below the Planck scale but above the prevalent scale at nucleosynthesis. We don’t have a clear understanding of physics at these energies, but we do know some theoretical ideas that are likely to be part of such high energy theory, including Grand Unified Theories (“GUT’s”), supersymmetry, and supergravity. All such theories tend to include species of particles that can only be produced at energies far above what we can produce today or what was present during nucleosynthesis. If we believe that the big bang model was valid back to the Planck era then the universe must have passed through a stage where the energies were high enough for these particles to have been produced.

In many cases these particles have long lifetimes. Some of them could, if produced, last until nucleosynthesis and spoil the predictions of light element abundances. Others could survive to the present and would be expected to dominate the current energy density. Particles in either of these two groups are known as relic particles because they persist from an earlier and higher energy epoch. For those familiar with theories of particle physics, such particles include moduli, gravitinos, monopoles, and more.

### 3.1.4 Summary of the Problems With the Big Bang Model

As I said before, every testable prediction of the big bang model to date has been verified, and it is almost certain that this model gives an accurate description of the universe back at least as far as the time of nucleosynthesis. The earliest it could possibly be applied would be the Planck era. If this extrapolation were valid then we

would have to suppose that all the very fine-tuned initial conditions we observe such as homogeneity and flatness were present from the beginning, presumably as a result of some unknown quantum gravity effects. Even given this assumption, however, it is unclear how the theory could avoid the production of relic particles that would destroy the successful description it has made of the later universe.

It would be wonderful if a theory existed that with a minimum of assumptions could explain the initial conditions such as flatness and homogeneity, provide a causal mechanism for propagating information over all the seemingly causally disconnected regions in the early universe, eliminate all high energy relic particles, and then segue into the big bang model itself by the time of nucleosynthesis. Fortunately such a theory exists. It's known as *inflation*.

## 3.2 Inflation

The basic idea of inflation is extremely simple, and has to do with the rate at which the universe is expanding. In the standard big bang model the universe experiences “power-law expansion,” meaning the distance between any two distant objects grows like  $t^p$  where  $t$  is the time since the big bang and  $p$  is a number that depends on what the universe is made of. Typically  $p$  will be either  $1/2$  or  $2/3$ , or possibly something in between the two. According to inflationary theory, before this power law expansion there was a brief period of exponential expansion. In other words distances during this time grew as  $e^{Ht}$  where  $t$  is once again time and  $H$  can be any number.<sup>2</sup> Exponential growth can be much faster than power-law growth. During this time the universe expanded by at least 60 e-folds, i.e. by a factor of at least  $e^{60}$  (roughly  $10^{26}$ , or nearly a billion billion billion). There are two obvious questions raised by this idea: What mechanism would cause such an expansion to occur and what would be the consequences if it did? In the next section I will explain how inflation can come about in the context of basic field theory. I will argue that inflation is a very natural occurrence that may be expected to take place within a wide variety of high energy

---

<sup>2</sup>The symbol  $e$  just refers to a number, roughly 2.8, that is typically used for convenience. You could also write this law as  $10^{Ht}$  and you would simply get a different value for  $H$ .

physics models. In the following section I will describe some of the basic consequences of inflation, including the resolution of all the problems raised in the previous section on the big bang model.

### 3.2.1 Why Inflation Occurs

In this section I am going to use a little more math and physics than in the rest of the primer. For any non-technical readers who find this section confusing you should be able to skip it, take my word that inflation does occur naturally in the context of many models of physics, and go on to the section on the consequences of inflation.

In general relativity the expansion of a homogeneous patch of the universe is described by the Friedmann equations

$$H^2 + \frac{k}{a^2} = \frac{8\pi}{3M_p^2} \rho \quad (3.1)$$

$$\ddot{a} = -\frac{4\pi}{3M_p^2} (\rho + 3p) a. \quad (3.2)$$

The scale factor  $a$  is proportional to the distance between two objects comoving with the expansion. The constant  $k$  indicates the curvature of the universe;  $k = -1, 0$ , or  $1$  for an open, flat, or closed universe respectively. The Hubble parameter  $H$  is defined as  $H \equiv \frac{\dot{a}}{a}$  and the other terms in the equations are the energy density  $\rho$ , the pressure  $p$ , and the Planck mass  $M_p = 1/\sqrt{G} \approx 1.22 \times 10^{19} \text{GeV}$ .

Starting from the first Friedmann equation, the second one is equivalent to the statement of energy conservation,  $dE = -pdV$ , applied to a local patch of the universe. Taking  $E = \rho V$  and  $V \propto a^3$  this energy conservation equation becomes the equation of continuity

$$\dot{\rho} = -3H (\rho + p). \quad (3.3)$$

For an equation of state of the form  $p = \alpha\rho$  the solution to the equation of continuity is

$$\rho \propto a^{-3(1+\alpha)}. \quad (3.4)$$

For the two most common cases of nonrelativistic particles (“matter”) and relativistic

particles (“radiation”) the values of  $\alpha$  are 0 and  $1/3$ , meaning that  $\rho$  decreases as  $a^{-3}$  and  $a^{-4}$  respectively in these two cases. Note that in both of these cases the energy density is decreasing faster than the curvature term in equation [3.1]. This is why in a matter or radiation dominated universe curvature tends to increase.

What would happen if the universe were dominated by a form of energy with  $\alpha = -1$ , i.e.  $p = -\rho$ ? In this case the energy density wouldn’t decrease at all as the universe expanded. The curvature would quickly become negligible and equation [3.1] would reduce to

$$H^2 = \frac{8\pi}{3M_p^2}\rho, \quad (3.5)$$

which for a constant  $\rho$  gives a constant  $H$ . Recalling that  $H \equiv \frac{\dot{a}}{a}$  this equation implies

$$a = e^{Ht}, \quad (3.6)$$

in other words inflation.

Having said this, however, we are still faced with the question of what would give rise to such a strange equation of state. One possibility is a “cosmological constant,” i.e. an energy density associated with the vacuum. Because this density wouldn’t change as the universe expanded (the vacuum presumably still being the same) it would behave as we have just described. (There are other, more direct ways to show that in general relativity the only consistent way to have a frame-independent vacuum energy would be for it to have the equation of state  $p = -\rho$ .) A cosmological constant term would not be a useful way to have inflation, however, because in this case inflation would never end.

A simple way to mimic the effects of a cosmological constant, however, would be to have a potential dominated scalar field. The energy density and pressure for a scalar field with potential  $V$  minimally coupled to gravity in a FRW universe are

$$\rho = \frac{1}{2}\dot{\phi}^2 + \frac{1}{2}|\nabla\phi|^2 + V \quad (3.7)$$

$$p = \frac{1}{2}\dot{\phi}^2 - \frac{1}{6}|\nabla\phi|^2 - V. \quad (3.8)$$



So if the dominant energy term is  $V$  the equation of state will be  $p = -\rho$  and the field  $\phi$  will act like a cosmological constant, maintaining a constant energy density as the universe expands. This behavior can be intuitively understood simply by noting that for a given potential function  $V(\phi)$ , if  $\phi$  is not changing the energy density  $V$  should not change.

The term “inflation” was coined by Alan Guth [1], who developed a model where a scalar field was trapped in a local minimum of its potential with  $V > 0$ . In such a case the field would remain potential dominated until it tunneled to its true minimum, thus ending inflation. Unfortunately this model suffered from a number of problems. For example, it failed to produce the right level of inhomogeneities. It was also far from obvious what would have driven the field to be trapped in this minimum in the first place, so to some degree the model simply traded one set of fine-tunings for another.

Since Guth’s paper came out there have been many different versions of inflation devised, including “new inflation,” “chaotic inflation,” “hybrid inflation,” “extended inflation,” and on and on. Most plausible models, however, are based on some variant of the following idea, first developed by Andrei Linde in 1983 [2].

The evolution equation for a homogeneous scalar field in an expanding universe is

$$\ddot{\phi} + 3H\dot{\phi} + \frac{\partial V}{\partial \phi} = 0. \quad (3.9)$$

Note that  $H$  plays the role of a friction term in this equation, slowing the motion of  $\phi$ . If  $\phi$  starts out at a value with a large potential, then by equation [3.1]  $H$  will be large and  $\phi$  will tend to roll very slowly. In this case the potential term will dominate over the kinetic term and both  $V$  and  $H$  will vary slowly. The universe will thus expand quasi-exponentially, i.e. inflation will occur. Eventually, however,  $\phi$  will roll to a small enough value that  $H$  will no longer overdamp the system,  $\dot{\phi}$  will become important, and inflation will end.

Linde showed that for simple potentials such as  $V \propto \phi^2$  or  $V \propto \phi^4$  such inflation can occur. If you assume that the field  $\phi$  had chaotic initial conditions when the universe first began with sub-Planckian energy density then there will in general be

some patch where the potential energy of  $\phi$  dominates over the kinetic and gradient terms enough to cause inflation. If in the entire universe there is one patch, even a Planck size one, with these conditions, then inflation will drive the size of this patch to exponentially large values. Such inflationary regions will quickly come to dominate the volume of the universe. In fact, using the assumption of chaotic initial conditions an inflationary region will typically expand by at least about  $10^{10^7}$  times, and often much more.

So the requirements for having inflation are fairly simple. Provided the quantum field theory governing sub-Planckian physics has a scalar field with a reasonable potential and somewhere in the universe a region exists where the potential energy of that field is large and dominates the overall energy density, inflation will occur in that region. Regions where inflation occurs will then fill nearly all of space. The scalar field that drives inflation in this way is often referred to as the “inflaton”. Note that a “reasonable potential” includes the polynomial potentials mentioned above as well as others. At present we have never directly observed a scalar field, but at least one such field must exist in nature if the standard model is correct, and supersymmetry predicts the existence of many scalar fields. So although we don’t know the correct fundamental physics model that would give rise to the inflaton, it seems at the very least reasonable to suppose that such a field might exist.

### 3.2.2 Some Basic Consequences of Inflation

The impact of inflation on the initial condition problems mentioned before is quite simple. If the universe undergoes exponential expansion then any local patch of it will come to be very homogeneous and flat, like the surface of a balloon being blown up very rapidly. Mathematically this can be seen from the argument above explaining why curvature tends to grow in a matter or radiation dominated universe but decrease in an inflationary universe. Given the enormous expansion that occurs during inflation, the growth of the curvature that has occurred since then should be completely negligible and we would expect to see an essentially perfectly flat universe now.

Inflation can also solve the horizon problem. The statement that the observable universe at the Planck era consisted of many causally disconnected regions comes from extrapolating back assuming matter and/or radiation domination. During inflation, however, a single, Planck size, causally connected region can expand to become many times bigger than the current observable universe, thus creating causal correlations on scales much bigger than we can hope to observe.

Inflation also solves the problem of relic particles because during inflation the density of all particles will be exponentially suppressed. When inflation ends and the universe moves towards a state of thermal equilibrium, the temperature may be low enough to avoid reproducing these relic particles.

All of these results of inflation are theoretically attractive as explanations of the features we observe in the universe at large scales. Probably the most important success of inflation, however, is its explanation of the origin of inhomogeneities in the universe. At first this idea might seem contradictory given that I said inflation flattens the universe and reduces to effectively zero the density of anything that was in it. It turns out, however, that small inhomogeneities can be generated during inflation. The fluctuations that are generated in this way early in inflation are typically stretched out by the exponential expansion to scales much greater than we can observe (although see chapter 7 for some possible consequences of these large scale fluctuations). The fluctuations generated at the last stages of inflation, however, form the seeds of the inhomogeneities that we observe in the CMB, and which subsequently gave rise to the structures we observe in the universe.

The origin of these inhomogeneities is in quantum fluctuations that are stretched out during inflation. As the wavelength of these fluctuations grows larger than the Hubble radius  $H^{-1}$  they cease oscillating and get frozen in as classical waves. The fluctuations on the scales we can observe today were all generated during the last 60 or so e-folds of inflation. See [3] for more details on this process.

The overall amplitude of these fluctuations depends on the parameters in the inflaton potential, so these parameters must be adjusted to match the observed CMB anisotropy. The form of the fluctuations, however, is a robust prediction of inflation.

In almost all versions of inflation these fluctuations have the form of Gaussian, adiabatic perturbations with a nearly scale-invariant spectrum.<sup>3</sup> So far the predictions of inflation have fit the CMB data excellently, and no other theory has been able to reproduce these predictions.

### 3.3 Reheating

Although inflation produces a universe with many of the features we observe in our own, such as near-homogeneity with small fluctuations, the universe immediately after inflation is in one sense almost completely empty. While inflation gets rid of all relic particles such as gravitinos and monopoles, it also gets rid of all other particles as well. After inflation nearly all the energy density in the universe is in the homogeneous inflaton field. Once inflation ends this field must somehow decay and give its energy to other fields, eventually giving rise to the panoply of particles we see around us today. The process by which the inflaton decays into other forms of energy is known as reheating.

The issue of reheating has been explored for almost as long as inflationary theory itself (see e.g. [4]). In the earliest papers on the subject it was noted that after inflation ends the homogeneous inflaton field would oscillate about its minimum. Assuming the inflaton were coupled to other fields it would then decay, leading to a cascade of energy density into many different forms. Several methods were developed for perturbatively investigating this decay.

In 1994 it was realized that there is in general a much more efficient mechanism by which the inflaton could decay, namely parametric resonance [5]. To see how this works consider the simple case of a field  $\chi$  coupled to the inflaton  $\phi$  via an interaction term

$$V_{interaction} = \frac{1}{2}g^2\phi^2\chi^2. \quad (3.10)$$

The equation of motion for  $\chi$  will be that of an oscillator whose frequency depends on  $\phi$ . As  $\phi$  oscillates this frequency will change, causing fluctuations of  $\chi$  to be

---

<sup>3</sup>There are many introductions and reviews about the CMB available. See for example <http://cfa-www.harvard.edu/mwhite/htmlpapers.html>.

rapidly amplified in bands of resonant frequencies. (For a more complete discussion of parametric resonance in general see [6] and for a discussion of parametric resonance during reheating see [7, 8].) This effect is known as *preheating* because it rapidly transfers much of the inflaton's energy to fluctuations of the field  $\chi$  before the slower, perturbative mechanisms of reheating can occur.

Since the discovery of preheating a great deal of work has been done to understand the consequences of nonperturbative effects in reheating. These effects can include phase transitions, the production of topological defects, the production and/or elimination of various kinds of relic particles, and secondary stages of inflation. Such nonperturbative effects often involve strong, nonlinear interactions between fields far from thermal equilibrium in an expanding universe. Thus progress in this field has in many cases required large-scale numerical simulations.

The work described in this thesis forms part of the ongoing investigation into different mechanisms by which reheating can occur and the consequences of those mechanisms within various models of inflationary cosmology.

## **Part II**

# **Mechanisms of Reheating**

# Chapter 4

## Introduction to the Research

This part of the thesis is adapted from the papers I have published in the course of my graduate research. All of these papers deal with probing mechanisms of reheating after inflation. Collectively they, along with my work on lattice simulations described in part III, form the essential content of this thesis.

Before presenting this research it is appropriate that I should say a few words about my contributions to the work presented here. Of course most of the work done in scientific collaboration is the result of numerous discussions, arguments, and other forms of give and take that make it impossible to separate out individual contributions in a meaningful way. Nonetheless I can note in a general sense that all of the lattice calculations reported in these chapters were done by me. I also performed various other numerical calculations such as the linear calculations described in chapter 7. The interpretation of these results was collaborative. The development of the lattice simulations, and in particular the physics (as opposed to computational) aspects of them, has continually evolved over the last several years as a result of discussions between me and several of my collaborators. The program itself was originally written by Igor Tkachev and has subsequently been rewritten and extended by me. Part III contains a more detailed discussion of our respective contributions to the simulations. The theoretical parts of the research, including the discussions and conclusions, was worked out in so many exchanges between so many people that I don't think individual contributions can meaningfully be attributed.

The rest of this introduction consists of a brief summary of the subject matter of the chapters in this part. This summary is not intended as a full, pedagogical account of the content of the research, and it will be presented in a technical form most suitable for people familiar with inflationary cosmology. The details of the work are contained in the chapters themselves and this section is merely intended as a quick reference to those results.

## Summary of Papers

Chapter 5, “Instant Preheating” explains a novel mechanism by which the decay of the inflaton can produce particles many orders of magnitude heavier than the inflaton particles themselves. My collaborators and I call this mechanism instant preheating because it can lead to essentially complete decay within a single oscillation. The basic idea is that if the inflaton field  $\phi$  is coupled to another field  $\chi$ , e.g. through a  $g^2\phi^2\chi^2$  coupling, then the mass of the  $\chi$  particles will depend on  $\phi$ . In particular, as  $\phi$  passes through zero the  $\chi$  particles will be momentarily massless. The resulting nonadiabatic change of the  $\chi$  mass will lead to the production of a certain number density of  $\chi$  particles. All of this has been understood for many years. What wasn’t appreciated, however, was the effect that the continued movement of the  $\phi$  field would have on the  $\chi$  particles. In particular, as  $\phi$  moves away from zero these particles would become massive. In most typical inflationary models  $\phi$  will continue to roll to a value of the order of a Planck mass, meaning that if  $g^2 = O(1)$  the  $\chi$  particles will acquire masses of the order of the Planck mass, irrespective of the mass of  $\phi$ . If  $\phi$  then rolls back and settles near zero this changing  $\chi$  mass will be relatively unimportant. If, however,  $\chi$  can in turn decay to another species of massive particles then it can effectively drain all the energy from the  $\phi$  field in a single oscillation while producing particles with near Planckian masses. If  $\phi$  doesn’t oscillate but continues rolling (as for example in some quintessence models) then this mechanism will be even more efficient, an issue that is taken up in more detail in chapter 6.

Chapter 6 on NO models describes a class of inflationary models in which the inflaton field has no minimum, but rather continues rolling in an asymptotically flat



potential. Such models generated a lot of interest for a while because of their possible relevance to the theory of quintessence. Because the usual mechanisms of reheating don't work in these models it had been proposed by several authors that reheating could occur in these cases via gravitational particle production. My collaborators and I showed that such scenarios suffer from serious problems involving the production of isocurvature fluctuations and relic particles such as moduli and gravitinos. We explained how these problems can be avoided, however, by introducing a coupling between the inflaton and one or more light fields and invoking the instant preheating mechanism described above.

Chapter 7 on moduli fields reconsiders an old problem, namely the production of large values of moduli fields during inflation. Moduli, i.e. light, weakly coupled fields, appear generically in string and supersymmetry motivated models of particle physics. In this chapter I show that the problems associated with their production in the early universe are more severe than had been previously realized. In particular, even if no classical displacement of the moduli fields occur there will be long wavelength quantum fluctuations of these fields amplified during inflation. The amplitude of these fluctuations will depend on the duration of inflation and for typical chaotic inflation models these will be large enough to disrupt nucleosynthesis and in many cases even cause a new stage of inflation dominated by these light fields. Inflation driven by such light fields would be in serious conflict with CMB observations. I discuss how these effects can depend on the details of the models, but do not present a general solution to the problem.

Chapter 8, "Inflation After Preheating," also deals with a secondary stage of inflation, but one of a very different sort. It was known from previous work that if the inflaton has a symmetry breaking potential and couples to another field then fluctuations of this second field created during preheating can temporarily lead to symmetry restoration, followed by a first order phase transition. It was speculated that such symmetry restoration could lead to a very brief secondary stage of inflation, perhaps alleviating some problems of relic production during inflation and preheating. In this chapter I report the results of lattice simulations in which my collaborators and I verified this prediction. In particular we found that after symmetry was restored

in our simulations there was a brief period where the pressure was negative and the expansion of the universe was accelerating, i.e. a period of inflation.

Chapter 9 on the development of equilibrium considers what happens to the inflaton and the products of its decay after the explosive stage of particle production associated with preheating. I report here the results of a series of lattice simulations in different models. My collaborator and I used these results to derive a set of empirical rules that seem to govern the process of thermalization. Most notably, we argued that in most models of inflation there is some mechanism that leads to rapid particle production, with the excitation concentrated in the infrared modes of the produced fields. Following this initial excitation all fields that are directly or indirectly coupled to the excited sector also get excited exponentially rapidly. The fields then form into groups, in which all of the fields within a particular group have identical spectra and time evolution. Within each group, the fields then thermalize by spreading their energy to the ultraviolet end of the spectrum. The composition of these groups depends strongly on the detailed interactions between the fields.

Finally, chapter 10 on tachyonic preheating describes a new mechanism by which the inflaton can rapidly decay. If the inflaton sector includes a direction in field space with negative curvature then fluctuations can be rapidly produced via a spinodal instability. Such potentials occur generically in models of hybrid inflation. Essentially the process being described is just spontaneous symmetry breaking. The existence of spinodal instabilities has long been known in condensed matter physics, and of course spontaneous symmetry breaking has been studied extensively in condensed matter and particle physics. However, so far as I know nobody had previously realized that in the context of the sudden appearance of a negative curvature (as occurs in hybrid inflation) this mechanism of decay is so efficient as to lead to a complete decay of the homogeneous field(s) within a single oscillation. We found this result to be generic for a wide variety of models and parameters.

# Chapter 5

## Instant Preheating

*Note: This chapter is based on a paper by Gary Felder, Lev Kofman, and Andrei Linde, available on the Los Alamos eprint server as hep-ph/9812289. The full citation appears in the bibliography [9].*

### Chapter Abstract

I describe here a new efficient mechanism of reheating. Immediately after rolling down the rapidly moving inflaton field  $\phi$  produces particles  $\chi$ , which may be either bosons or fermions. This is a nonperturbative process that occurs almost instantly; no oscillations or parametric resonance are required. The effective masses of the  $\chi$  particles may be very small at the moment when they are produced, but they “fatten” when the field  $\phi$  increases. When the particles  $\chi$  become sufficiently heavy, they rapidly decay to other, lighter particles. This leads to an almost instantaneous reheating accompanied by the production of particles with masses which may be as large as  $10^{17} - 10^{18}$  GeV. This mechanism works in the usual inflationary models where  $V(\phi)$  has a minimum, where it takes only a half of a single oscillation of the inflaton field  $\phi$ , but it is especially efficient in models with effective potentials slowly decreasing at large  $\phi$  as in the theory of quintessence.

## 5.1 Introduction

As discussed in the introduction to the thesis, the first stages of preheating are typically governed by nonperturbative effects. In particular, the most efficient mechanism of reheating known before the publication of the research in this chapter was based on the theory of the nonperturbative decay of the inflaton field due to the effect of broad parametric resonance [5, 7, 8]. To distinguish this stage of nonperturbative particle production from the stage of particle decay and thermalization which can be described using perturbation theory [10, 11, 12] (see also [13, 4]), it was called *preheating*.

This process can rapidly transfer the energy of a coherently oscillating scalar field to the energy of other fields or elementary particles. Because of the nonperturbative nature of the process, it may lead to many unusual effects, such as nonthermal cosmological phase transitions [14, 15, 16, 17]. Another unusual feature of preheating discovered in [5, 7, 8] is the possibility of the production of a large amount of superheavy particles with masses one or two orders of magnitude greater than the inflaton mass. In the simplest versions of chaotic inflation with the inflaton mass  $m \sim 10^{13}$  GeV this can lead to the copious production of particles with masses up to  $10^{14} - 10^{15}$  GeV [5, 7, 8, 18, 19, 20, 21, 22, 23]. This issue is rather important since interactions and decay of superheavy particles may lead to baryogenesis at the GUT scale [18, 19].

However, GUT baryogenesis was only marginally possible in previously studied models of preheating because the masses of produced particles just barely approached the GUT scale. Moreover, in some models the particles created by the resonance strongly interact with each other, or rapidly decay. This may take them out of the resonance band, in which case parametric resonance does not last long or does not happen at all. Also, there are some models where the effective potential does not have a minimum, but instead slowly decreases at large  $\phi$  [24, 25, 26, 27, 28, 29]. In these models the scalar field does not oscillate at all after inflation, so neither parametric resonance nor the standard perturbative mechanism of inflaton decay works there. Such models are discussed at more length in chapter 6.

In this chapter I show how my collaborators and I turned these potential problems

into an advantage. I describe a new mechanism of preheating, which works even in the models where parametric resonance cannot develop. The new mechanism is also nonperturbative but very simple. It leads to an almost instantaneous reheating accompanied by the production of superheavy particles with masses which may be as great as  $10^{17} - 10^{18}$  GeV. In some cases it may even lead to the production of black holes of a Planckian mass, which immediately evaporate.

## 5.2 Instant preheating: The basic idea

To explain the main idea of the new scenario I will consider the simplest model of chaotic inflation with the effective potential  $\frac{m^2}{2}\phi^2$  or  $\frac{\lambda}{4}\phi^4$  and assume that the inflaton field  $\phi$  interacts with some other scalar field  $\chi$  with the interaction term  $V = \frac{1}{2}g^2\phi^2\chi^2$ . In these models inflation occurs at  $|\phi| \gtrsim 0.3M_p$  [3]. Suppose for definiteness that initially  $\phi$  is large and negative, and inflation ends at  $\phi \sim -0.3M_p$ . After that the field  $\phi$  rolls to  $\phi = 0$ , then it grows up to  $10^{-1}M_p \sim 10^{18}$  GeV, and finally rolls back and oscillates about  $\phi = 0$  with a gradually decreasing amplitude. If the coupling constant  $g$  is large enough ( $g \gtrsim 10^{-4}$ ), then, according to [5, 7, 8], the production of particles  $\chi$  occurs for the first time when the scalar field  $\phi$  reaches the point  $\phi = 0$  after the end of inflation. With each subsequent oscillation, particle creation occurs as  $\phi$  crosses zero. This mechanism of particle production is described by the theory of preheating in the broad resonance regime [5, 7, 8]. But now I will concentrate on the first instant of this process. Remarkably, in certain cases this is all that we need for efficient reheating.

Usually only a small fraction of the energy of the inflaton field  $\sim 10^{-2}g^2$  is transferred to the particles  $\chi$  at that moment (see Eq. (5.7) in the next section). The role of parametric resonance was to increase this energy exponentially within several oscillations of the inflaton field. But suppose that the particles  $\chi$  interact with fermions  $\psi$  with the coupling  $h\bar{\psi}\psi\chi$ . If this coupling is strong enough, then  $\chi$  particles may decay to fermions before the oscillating field  $\phi$  returns back to the minimum of the effective potential. If this happens, parametric resonance does not occur. However, as I will show, something equally interesting may occur instead of it: The energy

density of the  $\chi$  particles at the moment of their decay may become much greater than their energy density at the moment of their creation.

Indeed, prior to their decay the number density of  $\chi$  particles,  $n_\chi$ , remains practically constant [5, 7, 8], whereas the effective mass of each  $\chi$  particle grows as  $m_\chi = g\phi$  when the field  $\phi$  rolls up from the minimum of the effective potential. Therefore their total energy density grows. One may say that  $\chi$  particles are “fattened,” being fed by the energy of the rolling field  $\phi$ . The fattened  $\chi$  particles tend to decay to fermions at the moment when they have the greatest mass, i.e. when  $\phi$  reaches its maximal value  $\sim 10^{-1}M_p$ , just before it begins rolling back to  $\phi = 0$ .

At that moment  $\chi$  particles can decay to two fermions with mass up to  $m_\psi \sim \frac{g}{2}10^{-1}M_p$ , which can be as large as  $5 \times 10^{17}$  GeV for  $g \sim 1$ . This is two orders of magnitude greater than the masses of the particles that can be produced by the usual mechanism based on parametric resonance [5, 7, 8]. As a result, the total energy density of the produced particles also becomes two orders of magnitude greater than their energy density at the moment of their production. Thus the chain reaction  $\phi \rightarrow \chi \rightarrow \psi$  considerably enhances the efficiency of transfer of energy of the inflaton field to matter.

More importantly, superheavy particles  $\psi$  (or the products of their decay) may eventually dominate the total energy density of matter even if in the beginning their energy density was relatively small. For example, the energy density of the oscillating inflaton field in the theory with the effective potential  $\frac{\lambda}{4}\phi^4$  decreases as  $a^{-4}$  in an expanding universe with a scale factor  $a(t)$ . Meanwhile the energy density stored in the nonrelativistic particles  $\psi$  (prior to their decay) decreases only as  $a^{-3}$ . Therefore their energy density rapidly becomes dominant even if originally it was small. A subsequent decay of such particles leads to a complete reheating of the universe.

Since the main part of the process of preheating in this scenario (production of  $\chi$  and  $\psi$  particles) occurs immediately after the end of inflation, within less than one oscillation of the inflaton field, we called it *instant preheating*. I should emphasize that instant preheating is a completely nonperturbative effect, which can lead to the production of particles with momenta and masses many orders of magnitude greater than the inflaton mass. This would be impossible in the context of the elementary

theory of reheating developed in [10, 11, 12]. In what follows I will give a more detailed description of the instant preheating scenario.

### 5.3 The simplest models

Consider first the simplest model of chaotic inflation with the effective potential  $V(\phi) = \frac{m^2}{2}\phi^2$ , and with the interaction Lagrangian  $-\frac{1}{2}g^2\phi^2\chi^2 - h\bar{\psi}\psi\chi$ . I will take  $m = 10^{-6}M_p$ , as required by microwave background anisotropy [3], and in the beginning I will assume for simplicity that  $\chi$  particles do not have a bare mass, i.e.  $m_\chi(\phi) = g|\phi|$ . Reheating in this model is efficient only if  $g \gtrsim 10^{-4}$  [5, 7, 8]<sup>1</sup>, which implies  $gM_p \gtrsim 10^2 m$  for the realistic value of the mass  $m \sim 10^{-6}M_p$ . Thus, immediately after the end of inflation, when  $\phi \sim M_p/3$ , the effective mass  $g|\phi|$  of the field  $\chi$  is much greater than  $m$ . It decreases when the field  $\phi$  moves down, but initially this process remains adiabatic,  $|\dot{m}_\chi| \ll m_\chi^2$ .

The adiabaticity condition becomes violated and particle production occurs when  $|\dot{m}_\chi| \sim g|\dot{\phi}|$  becomes greater than  $m_\chi^2 = g^2\phi^2$ . For a harmonic oscillator one has  $|\dot{\phi}_0| = m\Phi$ , where  $|\dot{\phi}_0|$  is the velocity of the field in the minimum of the effective potential, and  $\Phi \sim 10^{-1}M_p$  is the amplitude of the first oscillation. This implies that the process becomes nonadiabatic for  $g\phi^2 \lesssim m\Phi$ , i.e. for  $-\phi_* \lesssim \phi \lesssim \phi_*$ , where  $\phi_* \sim \sqrt{\frac{m\Phi}{g}}$  [5, 7, 8]. Here  $\Phi \sim 10^{-1}M_p$  is the initial amplitude of the oscillations of the inflaton field. Note that under the condition  $g \gg 10^{-4}$  which is necessary for efficient reheating, the interval  $-\phi_* \lesssim \phi \lesssim \phi_*$  is very narrow:  $\phi_* \ll \Phi$ . As a result, the process of particle production occurs nearly instantaneously, within the time

$$\Delta t_* \sim \frac{\phi_*}{|\dot{\phi}_0|} \sim (gm\Phi)^{-1/2}. \quad (5.1)$$

This time interval is much smaller than the age of the universe, so all effects related to the expansion of the universe can be neglected during the process of particle production. The uncertainty principle implies in this case that the created particles will

---

<sup>1</sup>Note that if one takes  $g > 10^{-3}$ , radiative corrections to the effective potential may considerably change its shape [3]. However, this does not happen in supersymmetric theories where the contributions of fermions and bosons nearly cancel each other.

have typical momenta  $k \sim (\Delta t_*)^{-1} \sim (gm\Phi)^{1/2}$ . The occupation number  $n_k$  of  $\chi$  particles with momentum  $k$  is equal to zero all the time when it moves toward  $\phi = 0$ . When it reaches  $\phi = 0$  (or, more exactly, after it moves through the small region  $-\phi_* \lesssim \phi \lesssim \phi_*$ ) the occupation number suddenly (within the time  $\Delta t_*$ ) acquires the value [5, 7, 8]

$$n_k = \exp\left(-\frac{\pi k^2}{gm\Phi}\right), \quad (5.2)$$

and this value does not change until the field  $\phi$  rolls to the point  $\phi = 0$  again.

A detailed description of this process including the derivation of Eq. (5.2) was given in Ref. [7]; see in particular Eq. (55) there. This equation (5.2) can be written in a more general form. First of all, the shape of the effective potential does not play any role in its derivation. The essential point of the derivation of Eq. (5.2) is that  $\chi$  particles are produced in a small vicinity of the point  $\phi = 0$ , when  $\phi(t)$  can be represented as  $\phi(t) \approx \dot{\phi}_0(t - t_0)$ . The only thing which one needs to know is not  $V(\phi)$ ,  $m$  or  $\Phi$ , but the velocity of the field  $\phi$  at the time when it passes the point  $\phi = 0$ . Therefore one can replace  $m\Phi$  by  $|\dot{\phi}_0|$  in this equation. Also, the same equation is valid for massive particles  $\chi$  as well, if one replaces  $k^2$  by  $k^2 + m_\chi^2$ , where  $m_\chi$  is the bare mass of the particles  $\chi$  at  $\phi = 0$ . (A similar result is valid for fermions and for vector particles.) Therefore Eq. (5.2) in a general case (for any  $m_\chi$  and  $V(\phi)$ ) can be written as follows:

$$n_k = \exp\left(-\frac{\pi(k^2 + m_\chi^2)}{g|\dot{\phi}_0|}\right). \quad (5.3)$$

This can be integrated to give the density of  $\chi$  particles

$$n_\chi = \frac{1}{2\pi^2} \int_0^\infty dk k^2 n_k = \frac{(g\dot{\phi}_0)^{3/2}}{8\pi^3} \exp\left(-\frac{\pi m_\chi^2}{g|\dot{\phi}_0|}\right). \quad (5.4)$$

Numerical investigation of inflation in the theory  $\frac{m^2}{2}\phi^2$  with  $m = 10^{-6} M_p$  gives  $|\dot{\phi}_0| = 10^{-7} M_p^2$ , whereas in the theory  $\frac{\lambda}{4}\phi^4$  with  $\lambda = 10^{-13}$  one has a somewhat smaller value  $|\dot{\phi}_0| = 6 \times 10^{-9} M_p^2$ . This implies, in particular, that if one takes  $g \sim 1$ , then in the theory  $\frac{m^2}{2}\phi^2$  there is no exponential suppression of production of  $\chi$  particles unless their mass is greater than  $m_\chi \sim 2 \times 10^{15}$  GeV. This agrees with a similar conclusion



obtained in [5, 7, 8, 18, 19, 20, 21, 22, 23].

Let us now concentrate on the case  $m_\chi^2 \lesssim g|\dot{\phi}_0|$ , when the number of produced particles is not exponentially suppressed. In this case

$$n_\chi \approx \frac{(g\dot{\phi}_0)^{3/2}}{8\pi^3} . \quad (5.5)$$

According to Eq. (5.3), a typical initial energy (momentum) of each particle  $\chi$  at the moment of their production is  $\sim (g|\dot{\phi}|/\pi)^{1/2}$ , so their total energy density is

$$\rho_\chi \sim \frac{(g\dot{\phi}_0)^2}{8\pi^{7/2}} . \quad (5.6)$$

The ratio of this energy to the total energy density  $\rho_\phi = \dot{\phi}_0^2/2$  of the scalar field  $\phi$  at this moment gives

$$\frac{\rho_\chi}{\rho_\phi} \sim 5 \times 10^{-3} g^2 . \quad (5.7)$$

This result is practically model-independent, given the interaction term  $-\frac{1}{2}g^2\phi^2\chi^2$ . In particular, it does not depend on the inflaton mass  $m$  in the theory  $\frac{m^2}{2}\phi^2$ . The same result can be obtained in the theory  $\frac{\lambda}{4}\phi^4$  independently of the value of  $\lambda$ .

An interesting possibility appears if one has  $m_\chi^2 \sim g|\dot{\phi}_0|$ . Then the probability of production of such particles is not exponentially suppressed during the first oscillation, but it is exponentially suppressed during all subsequent oscillations because  $|\dot{\phi}|$  decreases due to the expansion of the universe, and the condition  $m_\chi^2 \lesssim g|\dot{\phi}|$  becomes violated. In this case new particles  $\chi$  are not created. However, as we already explained, these new particles may not even be necessary. For example, in the theory  $\frac{\lambda}{4}\phi^4$  the energy density of the inflaton field  $\rho_\phi$  decreases as  $a^{-4}$ , whereas the energy density stored in the nonrelativistic particles  $\chi$  (prior to their decay) decreases only as  $a^{-3}$ . Therefore their energy density rapidly becomes dominant even if originally it was small. Their subsequent decay makes the process of reheating complete.

But preheating in this model becomes much more efficient if one uses the mechanism described in the beginning of this chapter. Indeed, let us assume that the particles  $\chi$  survive until the field  $\phi$  rolls up from  $\phi = 0$  to the point  $\phi_1$  from which

it returns back to  $\phi = 0$ . In the theory  $\frac{m^2}{2}\phi^2$  one has  $\phi_1 \approx 0.07 M_p$ , whereas in the theory  $\frac{\lambda}{4}\phi^4$  one has  $\phi_1 \approx 0.12 M_p$ . I will take  $\phi_1 \approx 0.07 M_p$  in my estimates. At that time the mass of each particle  $\chi$  will be  $g\phi_1 \sim 10^{-1}gM_p$ , they will be nonrelativistic, and their total energy density (for the case of the theory  $\frac{m^2}{2}\phi^2$ ) will be

$$\rho_\chi = m_\chi n_\chi \approx 10^{-1}gM_p \frac{(g\dot{\phi}_0)^{3/2}}{8\pi^3} \sim 10^{-14}g^{5/2}M_p^4. \quad (5.8)$$

Therefore the ratio of the energy density of  $\chi$  particles to the energy density of the inflaton field  $\sim \dot{\phi}_0^2/2$  will be

$$\frac{\rho_\chi}{\rho_\phi} \sim 10^{-3}|\dot{\phi}_0|^{-1/2}M_pg^{5/2} \sim 2g^{5/2}. \quad (5.9)$$

The last result follows from the relation  $|\dot{\phi}_0| \sim 10^{-1}mM_p \sim 10^{-7}M_p^2$  for  $m \sim 10^{-6}M_p$ . Under the condition  $g \gtrsim 10^{-4}$ , which is the standard condition for efficient preheating [5, 7, 8], this ratio is much greater than the one in Eq. (5.7).

If the particles  $\chi$  do not decay when the field  $\phi$  reaches  $\phi_1$ , then their energy will decrease again in parallel with  $|\phi|$ , until it reaches the value given by Eq. (5.7). Thus, preheating is most efficient if all particles  $\chi$  can decay at the moment when the field  $\phi$  reaches its maximal value  $\phi_1$ . This is possible if the lifetime of the particles  $\chi$  created at the moment  $t_0$  is close to  $\Delta t \sim \pi m^{-1}/4$ . Particles  $\chi$  in this model can decay to fermions, with the decay rate [5, 7, 8]

$$\Gamma(\chi \rightarrow \psi\psi) = \frac{h^2 m_\chi}{8\pi} = \frac{h^2 g |\phi|}{8\pi}. \quad (5.10)$$

Note that the decay rate grows with the growth of the field  $|\phi|$ , so particles tend to decay at large  $|\phi|$ . One can easily check that the particles  $\chi$  decay when the field  $\phi$  reaches its maximal value  $|\phi| \approx 0.07M_p$  if

$$h^2 g \sim \frac{500m}{M_p} \sim 5 \times 10^{-4}. \quad (5.11)$$

At the moment when  $|\phi|$  reaches  $0.07M_p$ , the particles  $\chi$  have effective mass  $m_\chi =$

$g|\phi| \sim 0.07gM_p$ . Such particles can decay to two fermions  $\psi$  if  $m_\psi < 0.035gM_p$ . This implies that after the first half of an oscillation, the scalar field  $\phi$  can produce fermions with mass up to  $0.035gM_p$ . For example, in the theory with  $g \sim 10^{-1}$ ,  $h \sim 7 \times 10^{-2}$  one can produce fermions with mass up to  $m_\psi \sim 4 \times 10^{16}$  GeV, and in the theory with  $g \sim 1$ ,  $h \sim 2 \times 10^{-2}$  one can produce particles with mass up to  $4 \times 10^{17}$  GeV.

As we have found, initially the ratio  $\frac{\rho_\chi}{\rho_\phi}$  is suppressed by the factor  $2g^{5/2}$ , see Eq. (5.9). But this suppression is not very strong, and if the energy density of the  $\psi$  particles during some short period of the evolution of the universe decreases not as fast as the energy density of the inflaton field and other products of its subsequent decay, then very soon the universe will be dominated by the products of decay of the particles  $\psi$ , and reheating will be complete.

If  $h^2g \gg 5 \times 10^{-4}$ , the  $\chi$  particles may decay before the oscillating field  $\phi$  reaches its maximal value  $\phi_1 \sim 10^{-1}M_p$ . This can make our mechanism somewhat less efficient. However, the decay cannot occur until  $m_\chi = g|\phi|$  becomes greater than  $2m_\psi$ . If, for example, the fermions have mass  $\sim 0.03gM_p$ , then the decay occurs only when the field  $\phi$  reaches its maximal value  $\phi_1$  even if  $h^2g \gg 5 \times 10^{-4}$ . This preserves the efficiency of our mechanism even for very large  $h^2g$ .

On the other hand, for  $h^2g \ll 5 \times 10^{-4}$ , the particles  $\chi$  do not decay within a single oscillation. In this case the parametric resonance regime becomes possible, which again leads to efficient preheating according to [5, 7, 8]. Moreover, superheavy fermions still will be produced in this regime, because the oscillating field will spend a certain amount of time at  $\phi \sim \phi_1$ . During this time superheavy particles will be produced, and their number may not be strongly suppressed.

The mechanism of particle production described above can work in a broad class of theories. For example, one can consider models with the interaction  $\frac{g^2}{2}\chi^2(\phi+v)^2$ . Such interaction terms appear, for example, in supersymmetric models with superpotentials of the type  $W = g\chi^2(\phi+v)$  [30]. In such models the mass  $m_\chi$  vanishes not at  $\phi_1 = 0$ , but at  $\phi_1 = -v$ , where  $v$  can take any value. Correspondingly, the production of  $\chi$  particles occurs not at  $\phi = 0$  but at  $\phi = -v$ . When the inflaton field reaches the minimum of its effective potential at  $\phi = 0$ , one has  $m_\chi \sim gv$ , which may be very

large. If one takes  $v \sim M_p$ , one can get  $m_\chi \sim gM_p$ , which may be as great as  $10^{18}$  GeV for  $g \sim 10^{-1}$ , or even  $10^{19}$  GeV for  $g \sim 1$ . If, however, one takes  $v \gg M_p$ , the density of  $\chi$  particles produced by this mechanism will be exponentially suppressed by the subsequent stage of inflation. This possibility will be discussed in the next section.

Since parametric amplification of particle production is not important in the context of the instant preheating scenario, it will work equally well if the inflaton field couples not to bosons but to fermions [31, 32]. Indeed, the creation of fermions with mass  $g|\phi|$  also occurs because of the nonadiabaticity of the change of their mass at  $\phi = 0$ . The theory of this effect at  $g \gtrsim 10^{-4}$  is very similar to the theory of the creation of  $\chi$  particles described above; see in this respect [32]. The efficiency of preheating will be enhanced if the fermions  $\psi$  with a growing mass  $g|\phi|$  can decay into other fermions and bosons, as in the scenario described in the previous section.

It is amazing that oscillations of the field  $\phi$  with mass  $m = 10^{13}$  GeV can lead to the copious production of superheavy particles with masses 4 - 5 orders of magnitude greater than  $m$ . The previously known mechanism of preheating was barely capable of producing particles of mass  $\sim 10^{15}$  GeV, which is somewhat below the GUT scale, and even that was possible only in the strong coupling limit  $g = O(1)$ . This new mechanism allows for the production of particles with mass greater than  $10^{16}$  GeV even if the coupling constants are relatively small. This fact may play an important role in the theory of baryogenesis in GUTs.

## 5.4 Fat wimpzillas

There have been a number of papers published on the possibility of the production of superheavy WIMPS after inflation [33, 34, 35, 36, 37, 38, 23]. Such particles (which have been proudly called WIMPZILLAS [39]) could be responsible for the dark matter content of the universe, and, if they have a very large but finite decay time, they can also be responsible for cosmic rays with energies greater than the Greisen–Zatsepin–Kuzmin limit [40, 41]. The focus of these works in a certain sense was opposite to that of the theory of preheating: It was necessary to find a mechanism for the production

of stable (or nearly stable) particles which would survive until now. For that purpose, the mechanism of their production must be extremely *inefficient*, since otherwise the present density of such relics would be unacceptably large.

As one could expect, it is much easier to make the mechanism inefficient rather than the other way around. For example, Eq. (5.4) implies that the probability of production of superheavy  $\chi$  particles is suppressed by a factor of  $\exp\left(-\frac{\pi m_\chi^2}{g|\dot{\phi}_0|}\right)$ . In the theory  $\frac{m^2}{2}\phi^2$  with  $m = 10^{-6}M_p$  we have  $|\dot{\phi}_0| = 10^{-7}M_p^2$ , so this suppression factor is given by  $\exp\left(-\frac{10^7\pi m_\chi^2}{gM_p^2}\right)$ . This implies that for  $g \sim 1$  the production of particles with  $m_\chi \sim 10^{16}$  GeV is suppressed approximately by  $10^{-10}$ , and this suppression becomes as strong as  $10^{-40}$  for  $m_\chi = 2 \times 10^{16}$  GeV. This same level of suppression can be achieved, for example, with  $g = 10^{-2}$  and  $m_\chi = 2 \times 10^{15}$ . Thus, by fine-tuning of the parameters  $m_\chi$  and  $g$  one can obtain any value of the density of WIMPS at the present stage of the evolution of the universe. This result agrees with the result obtained in [23] by a different method.

This suppression mechanism is equally operative for the process  $\phi \rightarrow \chi \rightarrow \psi$  discussed here. If the particles  $\chi$  are heavy at  $\phi = 0$ , their number will be exponentially suppressed. When the field  $\phi$  grows, their masses grow as follows:  $m_\chi^2(\phi) = m_\chi^2 + g^2\phi^2$ . At the moment of their decay these particles can have mass of the order  $10^{17} - 10^{18}$  GeV. The main advantage of this new mechanism is that the process of fattening of the particles  $\chi$  described above allows for the production of particles  $\psi$  which can be  $10^2$  times heavier than their cousins discussed in [33, 34, 35, 36, 37, 38, 23]. In the absence of established terminology, one can call such superheavy particles FAT WIMPZILLAS.

Another way to produce an exponentially small number of superheavy WIMPS is to produce them at the last stages of inflation. This is possible in theories with the interaction term  $\frac{g^2}{2}\chi^2(\phi + v)^2$ , as described in the previous section. If one takes  $v \gtrsim M_p$ , then the particles  $\chi$  will be created during inflation. The number of  $\chi$  particles produced during inflation in the simplest theory with  $V(\phi) = \frac{m^2}{2}\phi^2$  does not depend on  $v$  because  $\dot{\phi}$  does not depend on  $\phi$  and on  $v$  in this scenario:  $\dot{\phi} = \frac{mM_p}{2\pi}$  [3]. However, their density will subsequently be exponentially suppressed by inflation. This is exactly what we need if the  $\chi$  particles or the products of their decay are

WIMPS. For example, in the theory with  $V(\phi) = \frac{m^2}{2}\phi^2$  the universe inflates by a factor of  $\exp(2\pi v^2/M_p^2)$  after the creation of  $\chi$  particles [3], so their density at the end of inflation becomes smaller by a factor of  $\exp(6\pi v^2/M_p^2)$ . This leads to a desirable suppression for  $v \sim 2M_p$ . (The exact number depends on the subsequent thermal history of the universe.) Meanwhile the masses of WIMPS produced by this mechanism can be extremely large, of order  $gM_p$ . If the  $\chi$  particles are stable, they themselves may serve as superheavy WIMPS with nearly Planckian mass. If they decay to fermions, then the fermions may play a similar role.

## 5.5 Instant Preheating and NO Models

The mechanism of instant preheating works most efficiently in models where the inflaton potential becomes flat at large values of  $\phi$ . Such non-oscillatory (NO) models have been the subject of a great deal of interest recently because of their potential application to the theory of quintessence, i.e. the possibility that a rolling scalar field with a nearly flat potential could mimic the role of a cosmological constant in the current universe. The application of instant preheating in these models will be discussed in detail in chapter 6. Here I will simply note that if the mass of the particles  $\chi$  grows with  $\phi$  and  $\phi$  has a flat potential then the mass of  $\chi$  can become essentially arbitrarily large.

## 5.6 Conclusions

The theory of reheating after inflation is already rather old. For many years it was thought that the classical oscillating inflaton field could be represented as a collection of scalar particles of mass  $m \lesssim 10^{13}$  GeV, that each particle decayed to particles of smaller mass, and that the final goal was to calculate the reheating temperature  $T_r$ .

During the last decade we have learned that this simple picture in certain cases can be very useful, but typically one must use the nonperturbative theory of reheating for the description of the first stages of reheating. The main ingredient of this theory was the theory of broad parametric resonance. Particle production in this scenario could

be represented as a series of successive acts of creation, during which the number of produced particles increased exponentially. It seems now that this was only a first step towards a complete understanding of nonperturbative mechanisms of reheating after inflation. It may be sufficient to consider a single act of creation, especially if one takes into account the relative increase of energy of produced particles during the subsequent evolution of the classical inflaton field, and the possibility of the chain reaction  $\phi \rightarrow \chi \rightarrow \psi$ . This new mechanism is capable of producing particles of nearly Planckian energy, which was impossible in the previous versions of the theory of reheating.

One of the key ingredients of the nonperturbative mechanism of preheating described above is a nonadiabatic change of the mass  $m_\chi(\phi)$  near the point where it vanishes (or at least strongly decreases). Such situations occur very naturally in supersymmetric theories of elementary particles if one identifies  $\phi$  and  $\chi$  with moduli fields that correspond to flat directions of the effective potential. Indeed, in supersymmetric theories the effective potential often has several flat directions, which may intersect. When one of the moduli fields (the inflaton) moves along a flat direction and reaches the intersection, the mass of another field vanishes. A simple example of this situation was described in section 5.3. The change of the number of massless degrees of freedom is a generic phenomenon which is under intense investigation in the context of supersymmetric gauge theories, supergravity and string theory, where it is associated with the points of enhanced gauge symmetry, see e.g. [42, 43, 44, 45, 46].

Masses of elementary particles may also change nonadiabatically during cosmological phase transitions. At the moment of a phase transition masses of some particles vanish and may even temporarily become tachyonic. In this case particle production may become even more intense. See chapter 10.

The main conclusion of this work is that with an account taken of the new possibilities discussed above the scenario of preheating becomes more robust. In the cases where parametric resonance may occur, it provides a very efficient mechanism of preheating. Now we have found that efficient preheating is possible even in models where parametric resonance does not happen because of the rapid decay of produced

particles. Instant preheating occurs in the usual inflationary models where the inflaton field oscillates near the minimum of its effective potential. But this mechanism works especially well in models with effective potentials which slowly decrease at large  $\phi$ , as in the theory of quintessence. The conversion of the energy of the inflaton field to the energy of elementary particles in these models occurs very rapidly, and it is always 100% efficient. The next chapter discusses such scenarios.



## Chapter 6

# Inflation and Preheating in NO Models

*Note: This chapter is based on a paper by Gary Felder, Lev Kofman, and Andrei Linde, available on the Los Alamos eprint server as hep-ph/9903350. The full citation appears in the bibliography [47].*

### Chapter Abstract

In this chapter I discuss inflationary models in which the effective potential of the inflaton field does not have a minimum, but rather gradually decreases at large  $\phi$ . In such models the inflaton field does not oscillate after inflation, and its effective mass becomes vanishingly small, so the standard theory of reheating based on the decay of the oscillating inflaton field does not apply. For a long time the only known mechanism of reheating in such non-oscillatory (NO) models was based on gravitational particle production in an expanding universe. This mechanism is very inefficient. I will show that it may lead to cosmological problems associated with large isocurvature fluctuations and overproduction of dangerous relics such as gravitinos and moduli fields. These problems can be resolved in the context of the scenario of instant preheating described in chapter 5 if there exists an interaction  $g^2\phi^2\chi^2$  of the inflaton field  $\phi$  with another scalar field  $\chi$ . I show that the mechanism of instant preheating in

NO models is much more efficient than the usual mechanism of gravitational particle production even if the coupling constant  $g^2$  is extremely small,  $10^{-14} \ll g^2 \ll 1$ .

## 6.1 Introduction

Usually it is assumed that the inflaton field  $\phi$  after inflation rolls down to the minimum of its effective potential  $V(\phi)$ , oscillates, and eventually decays. The stage of oscillations of the inflaton field is a necessary part of the standard mechanism of reheating of the universe [10, 11, 12, 5, 7, 8].

However, there exist some models where the inflaton potential  $V(\phi)$  gradually decreases at large  $\phi$  and does not have a minimum. In such theories the inflaton field  $\phi$  does not oscillate after inflation, so the standard mechanism of reheating does not work there.

Investigation of inflationary models of this type has been rather sporadic [24, 25, 26, 27, 28], and each new author has given them a new name, such as deflation [25], kination [26, 27], and quintessential inflation [28]. However, the universe does not deflate in these models, and in general they are not related to the theory of quintessence. The main distinguishing feature of inflationary models of this type is the non-oscillatory behavior of the inflaton field, which makes the standard mechanism of reheating inoperative. Therefore we decided to call such models “non-oscillatory models,” or simply “NO models.” In addition to describing the most essential feature of this class of theories which makes reheating problematic, this name reflects the rather negligent attitude towards these models which existed until recently.

One of the reasons why NO models have not attracted much attention was the absence of an efficient mechanism of reheating. For a long time it was believed that the only mechanism of reheating possible in NO models was gravitational particle production [24, 25, 26, 27, 28], which occurs because of the changing metric in the early universe [48, 49, 50, 51, 52, 53]. This mechanism is very inefficient, which may lead to certain cosmological problems.

However, recently the situation changed. The mechanism of instant preheating described in the previous chapter is very efficient, and it works in NO models even

better than in the models where  $V(\phi)$  has a minimum.

In this chapter I will describe various features of NO models. First of all, I will discuss the problem of initial conditions in these models, which had not been properly addressed before. The standard assumption made in [24, 25, 26, 27, 28] is that at the end of inflation in NO models one has a large and heavy inflaton field  $\phi$  that rapidly changes and creates light particles  $\chi$  minimally coupled to gravity from a state where the classical value of the field  $\chi$  vanishes. We showed that this setting of the problem needed to be reconsidered. If the fields  $\phi$  and  $\chi$  do not interact (which was the standard assumption of Refs. [24, 25, 26, 27, 28]), then at the end of inflation the field  $\chi$  typically does not vanish. Usually the last stages of inflation are driven by the light field  $\chi$  rather than by the heavy field  $\phi$ . But in this case reheating occurs due to oscillations of the field  $\chi$ , as in the usual models of inflation.

In addition to reexamining the problem of initial conditions, we will point out potential difficulties associated with isocurvature perturbations and gravitational production of gravitinos and moduli fields in NO models.

In order to provide a consistent setting for the NO models one needs to introduce interaction between the fields  $\phi$  and  $\chi$ . This resolves the problem of initial conditions in these models and makes it possible to have a non-oscillatory behavior of the inflaton field after inflation. We show that all of these problems can be resolved in the context of the recently proposed scenario of instant preheating [9] if there is an interaction  $\frac{g^2}{2}\phi^2\chi^2$  of the inflaton field  $\phi$  with another scalar field  $\chi$ , with  $g^2 \gg 10^{-14}$ . In this case the mechanism of instant preheating in NO models is much more efficient than the usual mechanism of gravitational particle production studied in [24, 25, 26, 27, 28].

## 6.2 Isocurvature perturbations in NO Models

In chapter 7 I show that if inflation begins with a large value of the inflaton  $\phi$  and a vanishing value of a light field  $\chi$  then typically large fluctuations of the field  $\chi$  will be generated by the end of inflation. These fluctuations are largest at long wavelengths, well outside the horizon, and thus appear effectively homogeneous on subhorizon scales. For a sufficiently long period of inflation these fluctuations will

grow large enough to initiate a new inflationary stage driven by the light field  $\chi$ . Thus the standard assumption that reheating begins with a light field  $\chi$  having vanishing amplitude is generically incorrect.

Here I will consider a more general question: If the two fields  $\phi$  and  $\chi$  do not interact, then why should we assume that one of them should vanish at the beginning of inflation? And if it does not vanish, then how does it change the whole picture?

Suppose for example that the field  $\chi$  is a Higgs field [28] with a relatively small mass and with a large coupling constant  $\lambda_\chi \gg \lambda_\phi$ . The total effective potential in this theory (for  $\phi < 0$ ) is given by

$$V(\phi, \chi) = \frac{\lambda_\phi}{4}\phi^4 + \frac{\lambda_\chi}{4}(\chi^2 - v^2)^2. \quad (6.1)$$

Here  $v$  is the amplitude of spontaneous symmetry breaking,  $v \ll M_p$ . During inflation and at the first stages of reheating this term can be neglected, so we will study the simplified model

$$V(\phi, \chi) = \frac{\lambda_\phi}{4}\phi^4 + \frac{\lambda_\chi}{4}\chi^4. \quad (6.2)$$

This model was first analyzed in [54]. It is directly related to the Peebles-Vilenkin model [28] if the field  $\chi$  is the Higgs boson field with a small mass  $m$ .

In general, at the beginning of inflation one has both  $\phi \neq 0$  and  $\chi \neq 0$ . Thus we will not assume that  $\chi = 0$ , and instead of studying quantum fluctuations of this field which can make it large, I will assume that it could be large from the very beginning.

Even though the fields  $\phi$  and  $\chi$  do not interact with each other directly, they move towards the state  $\phi = 0$  and  $\chi = 0$  in a coherent way. The reason is that the motion of these fields is determined by the same value of the Hubble constant  $H$ .

The equations of motion for both fields during inflation look as follows:

$$3H\dot{\phi} = -\lambda_\phi\phi^3. \quad (6.3)$$

$$3H\dot{\chi} = -\lambda_\chi\chi^3. \quad (6.4)$$

These equations imply that

$$\frac{d\phi}{\lambda_\phi \phi^3} = \frac{d\chi}{\lambda_\chi \chi^3}, \quad (6.5)$$

which yields the general solution

$$\frac{1}{\lambda_\phi \phi^2} = \frac{1}{\lambda_\chi \chi^2} + \frac{1}{\lambda_\phi \phi_0^2} - \frac{1}{\lambda_\chi \chi_0^2}, \quad (6.6)$$

Since the initial values of these fields are much greater than the final values, at the last stages of inflation one has [54]

$$\frac{\phi}{\chi} = \sqrt{\frac{\lambda_\chi}{\lambda_\phi}}. \quad (6.7)$$

Suppose  $\lambda_\phi \ll \lambda_\chi$ . In this case the “heavy” field  $\chi$  rapidly rolls down, and then from the last equation it follows, rather paradoxically, that the Hubble constant at the end of inflation is dominated by the “light” field  $\phi$ . Thus we can consistently consider the creation of fluctuations of the field  $\chi$  ( $\chi$  particles) at the end of and after the last inflationary stage driven by the  $\phi$  field. But now these fluctuations occur on top of a nonvanishing classical field  $\chi$ .

To study the behavior of the classical fields  $\phi$  and  $\chi$  and their fluctuations analytically, one should remember that during the inflationary stage driven by  $\phi$  one has  $H = \sqrt{\frac{2\lambda_\phi \pi}{3}} \frac{\phi^2}{M_p}$ . In this case, as before, the solution for the equation of motion of the field  $\phi$  is given by [2]

$$\phi = \phi_0 \exp \left( -\sqrt{\frac{\lambda_\phi}{6\pi}} M_p t \right). \quad (6.8)$$

Meanwhile, according to Eq. (6.7),

$$\chi = \phi_0 \sqrt{\frac{\lambda_\phi}{\lambda_\chi}} \exp \left( -\sqrt{\frac{\lambda_\phi}{6\pi}} M_p t \right), \quad (6.9)$$

whereas for perturbations of the field  $\chi$  one has:

$$\delta\chi = \delta\chi_0 \exp\left(-3\sqrt{\frac{\lambda_\phi}{6\pi}}M_p t\right). \quad (6.10)$$

Let us consider, for example, the behavior of the fields and their fluctuations at the end of inflation, starting from the moment  $\phi = \phi_i$ . One may take, for example,  $\phi_i \sim 4M_p$ , which corresponds to a point approximately 60 e-folds before the end of inflation. The fluctuations  $\delta\chi_i \sim H(\phi_i)/2\pi$  decrease according to (6.10), and at the end of inflation one gets

$$\frac{\delta\chi}{\chi} = \frac{H(\phi_i)}{2\pi\chi_i} \exp\left(-2\sqrt{\frac{\lambda_\phi}{6\pi}}M_p t\right) = \frac{\sqrt{\lambda_\chi}\phi_i}{\sqrt{6\pi}M_p} \frac{\phi_e^2}{\phi_i^2}. \quad (6.11)$$

Here  $\phi_e \sim 0.3M_p$  corresponds to the end of inflation.<sup>1</sup> After that moment the fields  $\phi$  and  $\chi$  begin oscillating, and the ratio of  $\delta\chi$  to the amplitude of oscillations of the field  $\chi$  remains approximately constant. This gives the following estimate for the amplitude of isocurvature perturbations in this model:

$$\frac{\delta V(\chi)}{V(\chi)} \sim 4 \frac{\delta\chi}{\chi} = 2 \times 10^{-2} \sqrt{\lambda_\chi}. \quad (6.12)$$

Initially perturbations of  $V(\chi)$  give a negligibly small contribution to perturbations of the metric because  $V(\chi) \ll V(\phi)$ ; that is why they are called isocurvature perturbations. However, the main idea of preheating in NO models is that eventually  $\chi$  fields or the products of their decay will give the dominant contribution to the energy-momentum tensor because the energy density of the field  $\phi$  rapidly vanishes due to the expansion of the universe ( $\rho_\phi \sim a^{-6}$ ). However, because of the inhomogeneity of the distribution of the field  $\chi$  (which will be imprinted in the density distribution of the products of its decay on scales greater than  $H^{-1}$ ), the period of the dominance of matter over the scalar field  $\phi$  will happen at different times in different

---

<sup>1</sup>We are grateful to Peebles and Vilenkin for pointing out that the factor  $\frac{\phi_e^2}{\phi_i^2}$  should be present in this equation.

parts of the universe. In other words, the epoch when the universe begins expanding as  $a \sim \sqrt{t}$  or  $a \sim t^{2/3}$  instead of  $a \sim t^{1/3}$  will begin at different moments  $t$  (at different total densities) in different parts of the universe. Starting from this time the isocurvature fluctuations (6.12) will produce metric perturbations, and, as a result, perturbations of CMB radiation.

Note that if the equation of state of the field  $\chi$  or of the products of its decay coincided with the equation of state of the scalar field  $\phi$  after inflation, fluctuations of the field  $\chi$  would not induce any anisotropy of CMB radiation. For example, these fluctuations would be harmless if the field  $\chi$  decayed into ultrarelativistic particles with the equation of state  $p = \rho/3$  and if the equation of state of the field  $\phi$  at that time were also given by  $p = \rho/3$ . However, in our case the field  $\phi$  has equation of state  $p = \rho$ , which is quite different from the equation of state of the field  $\chi$  or of its decay products.

Isocurvature fluctuations lead to approximately 6 times greater large scale anisotropy of the cosmic microwave radiation as compared with adiabatic perturbations. To avoid cosmological problems, one would need to have  $\frac{\delta V(\chi)}{V(\chi)} \lesssim 5 \times 10^{-6}$ . If  $\chi$  is the Higgs field with  $\lambda_\chi \gtrsim 10^{-7}$ , then the perturbations discussed above will be unacceptably large. This may be a rather serious problem. Indeed, one may expect to have many scalar fields in realistic theories of elementary particles. To avoid large isocurvature fluctuations each of these fields must be extremely weakly coupled, with  $\lambda_\chi \lesssim 10^{-7}$ ,

The general conclusion is that the theory of reheating in NO models, as well as their consequences for the creation of the large-scale structure of the universe, may be quite different from what was anticipated in the first papers on this subject. In the simplest versions of such models inflation typically does not end in the state  $\chi = 0$ , and large isocurvature fluctuations are produced.

### 6.3 Cosmological production of gravitinos and moduli fields

If the inflaton field  $\phi$  is sterile, not interacting with any other fields, the elementary particles constituting the universe should be produced gravitationally due to the variation of the scale factor  $a(t)$  with time. This was one of the basic assumptions of all papers on NO models [24, 25, 26, 27, 28]. Not all species can be produced this way, but only those which are not conformally invariant. Indeed, the metric of the Friedmann universe is conformally flat. If one considers, for example, massless scalar particles  $\chi$  with an additional term  $-\frac{1}{12}\chi^2 R$  in the Lagrangian (conformal coupling), one can make conformal transformations of  $\chi$  simultaneously with transformations of the metric and find that the theory of  $\chi$  particles in the Friedmann universe is equivalent to their theory in flat space. That is why such particles would not be created in an expanding universe.

Since conformal coupling is a rather special requirement, one expects a number of different species to be produced. An apparent advantage of gravitational particle production is its universality [35, 36, 37]. There is a kind of “democracy” rule for all particles non-conformally coupled to gravity: the density of such particles produced at the end of inflation is  $\rho_X \sim \alpha_X H^4$ , where  $\alpha_X \sim 10^{-2}$  is a numerical factor specific for different species and  $H$  is the Hubble parameter at the end of inflation.

Unfortunately, democracy does not always work; there may be too many dangerous relics produced by this universal mechanism. One of the potential problems is related to the overproduction of gravitons mentioned in [28]. In order to solve it one needs to have models with a very large number of types of light particles. This is difficult but not impossible [28]. However, even more difficult problems will arise if NO models are implemented in supersymmetric theories of elementary particles.

For example, in supersymmetric theories one may encounter many flat directions of the effective potential associated with moduli fields. These fields usually are very stable. Moduli particles decay very late, so in order to avoid cosmological problems the energy density of the moduli fields must be many orders of magnitude smaller than the energy density of other particles [55, 56, 57, 58, 59, 60].



Moduli fields typically are not conformally invariant. There are several different effects that add up to give them masses  $CH$  during expansion of the universe, with  $C = O(1)$  (in general,  $C$  is not a constant) [55, 56, 57, 58, 59]. This is very similar to what happens if, for example, one adds a term  $-\frac{\xi}{2}R\phi^2$  to the lagrangian of a scalar field. Indeed, during inflation  $R = 12H^2$ , so this term leads to the appearance of a contribution to the mass of the scalar field  $\Delta m^2 = 12\xi H^2$ . Conformal coupling would correspond to  $m^2 = 2H^2$ .

According to [24], the energy density of scalar particles produced gravitationally at the end of inflation is given by  $10^{-2}H^4(1 - 6\xi)^2$ . Thus, unless the constant  $C$  is fine-tuned to mimic conformal coupling, we expect that in addition to the energy of classical oscillating moduli fields, at the end of inflation one has gravitational production of moduli particles with energy density  $\sim 10^{-2}H^4$ , just as for all other conformally noninvariant particles.

In usual inflationary models one also encounters the moduli problem if the energy of classical oscillating moduli fields is too large [55, 56, 57, 58, 59]. Here we are discussing an independent problem which appears even if there are no classical oscillating moduli. Indeed, in NO models all particles created by gravitational effects at the end of inflation will have similar energy density  $\sim 10^{-2}H^4$ . But if the energy density of moduli fields is not extremely strongly suppressed as compared with the energy density of other particles, then such models will be ruled out [55, 56, 57, 58, 59, 60]. See chapter 7 for further discussion of the moduli problem in inflation.

A similar problem appears if one considers the possibility of gravitational (non-thermal) production of gravitinos. Usually it is assumed that gravitinos have mass  $m_{3/2} = 10^2 - 10^3$  GeV, which is much smaller than the typical value of the Hubble constant at the end of inflation. Therefore naively one could expect that gravitinos, just like massless fermions of spin 1/2, are (almost exactly) conformally invariant and should not be produced due to expansion of the Friedmann universe.

However, in the framework of supergravity, the background metric is generated by inflaton field(s)  $\phi_j$  with an effective potential constructed from the superpotential  $W(\phi_j)$ . The gravitino mass in the early universe acquires a contribution proportional to  $W(\phi_j)$ . Depending on the model, the gravitino mass soon after the end of inflation

may be of the same order as  $H$  or somewhat smaller, but typically it is much greater than its present value  $m_{3/2}$ .

A general investigation of the behavior of gravitinos in the Friedmann universe shows that the gravitino field in a self-consistent Friedmann background supported by scalar fields is not conformally invariant [61]. For example, the effective potential  $\lambda\phi^4$  can be obtained from the superpotential  $\sqrt{\lambda}\phi^3$  in the global supersymmetry limit. This leads to a gravitino mass  $\sim \sqrt{\lambda}\phi^3/M_p^2$ . At the end of inflation  $\phi \sim M_p$ , and therefore the gravitino mass is comparable to the Hubble constant  $H \sim \sqrt{\lambda}\phi^2/M_p$ . This implies strong breaking of conformal invariance.

The theory of gravitational production of gravitinos is strongly model-dependent, and in some models it might be possible to achieve a certain suppression of their production as compared to the production of other particles. The problem is that, just like in the situation with the moduli fields, this suppression must be extraordinarily strong. Indeed, to avoid cosmological problems one should suppress the number of gravitinos as compared to the number of other particles by a factor of about  $10^{-15}$  [62, 63, 64, 65, 66, 67]. For a more detailed discussion of the cosmological production of gravitinos see [61].

The gravitino/moduli problem and the problem of isocurvature perturbations are interrelated in a rather nontrivial way. Indeed, the gravitino and moduli problems are especially severe if the density of gravitinos and/or moduli particles produced during reheating is of the same order of magnitude as the energy density of scalar fields  $\chi$ . In my previous calculations I assumed, following [24, 28], that the energy density of the fields  $\chi$  after inflation is  $O(10^{-2}H^4)$ . But this statement is not always correct. It was derived in [24] under an assumption that particle production occurs during a short time interval when the equation of state changes. Meanwhile in inflationary cosmology the long-wavelength fluctuations of the field  $\chi$  minimally coupled to gravity are produced during inflation all the time when the Hubble constant  $H(t)$  is smaller than the mass of the  $\chi$  particles  $m_\chi$ . The energy density of  $\chi$  particles produced during inflation will contain a contribution  $\rho_0 = \frac{m_\chi^2}{2}\langle\chi^2\rangle$ , which may be many orders of magnitude greater than  $10^{-2}H^4$ .

For the sake of argument, one may consider inflation in the theory  $\frac{\lambda}{4}\phi^4$  and take

$m_\chi$  equal to the value of  $H$  at the end of inflation,  $m_\chi \sim \sqrt{\lambda_\phi} M_p$ . Then, according to Eq. (7.29), after inflation one has  $\rho_0 \sim \frac{\lambda_\phi m_\chi^2 \phi_0^6}{36 M_p^4} \sim 10^{-2} H^4 \left( \frac{\phi_0}{M_p} \right)^6 \gg 10^{-2} H^4$ , because  $\phi_0 \gg M_p$ .

This is the same effect that I discuss in chapter 7: If  $\phi_0$  is large enough, we may even have a second stage of inflation driven by the large energy density of the fluctuations of the field  $\chi$ . But even if  $\phi_0$  is not large enough to initiate a second stage of inflation, it still must be much greater than  $M_p$  to drive the first stage of inflation, which makes the standard estimate  $\rho \sim 10^{-2} H^4$  incorrect [68].

There is one more effect that should be considered, in addition to gravitational particle production. The effective mass of the particles  $\phi$  at  $\phi < 0$  is given by  $\sqrt{3\lambda}\phi$ . At the end of inflation, at  $\phi \sim M_p$ , this mass is of the same order as the Hubble constant  $\sim \sqrt{\lambda}\phi^2/M_p$ . Then, within the Hubble time  $H^{-1}$  the field  $\phi$  rolls to the valley at  $\phi > 0$  and its mass vanishes. This is a non-adiabatic process; the mass of the scalar field changes by  $O(H)$  during the time  $O(H^{-1})$ . As a result, in addition to gravitational particle production there is an equally strong production of particles  $\phi$  due to the nonadiabatic change of their mass [68, 69].

This may imply that the fraction of energy in gravitinos will be much smaller than previously expected, simply because the fraction of energy in the fluctuations of the field  $\chi$  will be much larger. But there is no free lunch. For example, the production of large number of nearly massless particles  $\phi$  may lead to problems with nucleosynthesis. Large inflationary fluctuations of the field  $\chi$  can create large isocurvature fluctuations. One can avoid this problem if one assumes, for example, that the fields  $\chi$  acquire effective mass  $O(H)$  in an expanding universe. Then their fluctuations will not be produced during inflation. But in such a case their density after inflation will be given by  $10^{-2} H^4$ , and therefore we do not have any relaxation of the gravitino and the moduli problems.

## 6.4 Saving NO models: Instant preheating

As we will see, the problems discussed above will not appear in theories of a more general class, where the fields  $\phi$  and  $\chi$  can interact with each other. I will consider a

model with the interaction  $\frac{g^2}{2}\phi^2\chi^2$ . First I will show that in this case it really makes sense to study preheating assuming that  $\chi = 0$ . Then I will discuss how the instant preheating mechanism described in chapter 5 allows efficient energy transfer from the field  $\phi$  to particles of the field  $\chi$ .

### 6.4.1 Initial conditions for inflation and reheating in the model with interaction $\frac{g^2}{2}\phi^2\chi^2$

Consider a theory with an effective potential dominated by the term  $V(\phi, \chi) = \frac{g^2}{2}\phi^2\chi^2$ . This means that the constant  $g$  is large enough for me to temporarily neglect the terms  $\frac{\lambda_\phi}{4}\phi^4 + \frac{\lambda_\chi}{4}\chi^4$  in the discussion of initial conditions.

In this case the Planck boundary is given by the condition

$$\frac{g^2}{2}\phi^2\chi^2 \sim M_p^4, \quad (6.13)$$

which defines a set of four hyperbolas

$$g|\phi||\chi| \sim M_p^2. \quad (6.14)$$

At larger values of  $\phi$  and  $\chi$  the density is greater than the Planck density, so the standard classical description of space-time is impossible there. On the other hand, the effective masses of the fields should be smaller than  $M_p$ , and consequently the curvature of the effective potential cannot be greater than  $M_p^2$ . This leads to two additional conditions:

$$|\phi| \lesssim g^{-1}M_p, \quad |\chi| \lesssim g^{-1}M_p. \quad (6.15)$$

I assume that  $g \ll 1$ . Suppose for definiteness that initially the fields  $\phi$  and  $\chi$  belong to the Planck boundary (6.14) and that  $|\phi|$  is half-way towards its upper bound (6.15):  $|\phi| \sim g^{-1}M_p/2$ . The choice of the coefficient 1/2 here is not essential; we only want to make sure that the field  $\chi$  initially is of order  $M_p$ , but it can be slightly greater than  $M_p$ . This allows for an extremely short stage of inflation when the field  $\chi$  rolls down towards  $\chi = 0$ .

The equations for the two fields are

$$\ddot{\phi} + 3H\dot{\phi} = -g^2\phi\chi^2. \quad (6.16)$$

and

$$\ddot{\chi} + 3H\dot{\chi} = -g^2\phi^2\chi. \quad (6.17)$$

The curvature of the effective potential in the  $\phi$  direction initially is  $\sim g^2\chi^2 \sim g^2M_p^2$ , which is very small compared to the initial value of  $H^2 \sim M_p^2$ . Thus the field  $\phi$  will move very slowly, so one can neglect the term  $\ddot{\phi}$  in Eq. (6.16).

$$3H\dot{\phi} = -g^2\phi\chi^2. \quad (6.18)$$

If the field  $\phi$  changes slowly, then the field  $\chi$  behaves as in the theory  $\frac{m_\chi^2}{2}\chi^2$  with  $m_\chi \sim g|\phi|$  being slightly smaller than  $M_p$  and with the initial value of  $\chi$  being slightly greater than  $M_p$ . This leads to a very short stage of inflation that ends within a few Planck times. After this short stage the field  $\chi$  rapidly oscillates. During this stage the energy density of the oscillating field drops down as  $a^{-3}$ , the universe expands as  $a \sim t^{2/3}$ , and  $H = \frac{2}{3t}$ . Thus the square of the amplitude of the oscillations of the field  $\chi$  decreases as follows:  $\chi^2 \sim \chi_0^2 a^{-3} \sim t^{-2}$ . This leads to the following equation for the field  $\phi$ :

$$\frac{\dot{\phi}}{\phi} \sim -\frac{g^2}{t}. \quad (6.19)$$

The solution of this equation is  $\phi = \phi_0 \left(\frac{t}{t_0}\right)^{-g^2}$  with  $t_0 \sim M_p^{-1}$ , and  $\phi_0 \sim -M_p/g$ . (The condition  $t_0 \sim M_p^{-1}$  follows from the fact that the initial value of  $H = \frac{2}{3t}$  is not much below  $M_p$ .) This gives

$$\phi \sim -\frac{M_p}{g} (M_p t)^{-g^2}. \quad (6.20)$$

The inflaton field  $\phi$  becomes equal to  $-M_p$  after the exponentially large time

$$t \sim M_p^{-1} \left(\frac{1}{g}\right)^{g^{-2}}. \quad (6.21)$$

During this time the energy of oscillations of the field  $\chi$  becomes exponentially small, and the small term  $\frac{\lambda\phi}{4}\phi^4$  that I neglected until now becomes the leading term driving the scalar field  $\phi$ . At this stage we will have the usual chaotic inflation scenario with  $|\phi| > M_p$  and with the fields evolving along the direction  $\chi = 0$ .

Thus in the presence of the interaction term  $\frac{g^2}{2}\phi^2\chi^2$  one can indeed consider inflation and reheating with  $\chi = 0$ . As we have seen, this possibility was rather problematic in the models where  $\phi$  and  $\chi$  interacted only gravitationally.

The effective mass of the field  $\chi$  during inflation is  $g|\phi|$ , which is much greater than the Hubble constant  $\sim \frac{\sqrt{\lambda}\phi^2}{M_p}$  for  $\frac{g^2}{\lambda} \gg \frac{\phi^2}{M_p^2}$ . In realistic versions of this model one has  $\lambda \sim 10^{-13}$  [3], and  $g^2 \gg \lambda$ . Therefore long-wavelength fluctuations of the field  $\chi$  are not produced during the last stages of inflation, when  $\phi \sim M_p$ .

A similar conclusion is valid if at the last stages of inflation the effective potential of the field  $\phi$  is quadratic,  $V(\phi) = \frac{m^2}{2}\phi^2$ . In this case  $H \sim \frac{m\phi}{M_p}$ , and inflationary fluctuations of the field  $\chi$  are not produced for  $g \gg \frac{m}{M_p}$ . In realistic versions of this model one has  $m \sim 10^{-6}M_p$  [3], and fluctuations  $\delta\chi$  are not produced if  $g^2 \gg 10^{-12}$ . This means that the problem of isocurvature fluctuations does not appear.

### 6.4.2 Instant preheating in NO models

To explain the main idea of the instant preheating scenario in NO models, I will consider for simplicity a model where  $V(\phi) = \frac{m^2}{2}\phi^2$  for  $\phi < 0$ , and  $V(\phi)$  vanishes for  $\phi > 0$ . I will discuss a more general situation later. I will assume that the effective potential contains the interaction term  $\frac{g^2}{2}\phi^2\chi^2$ , and that  $\chi$  particles have the usual Yukawa interaction  $h\bar{\psi}\psi\chi$  with fermions  $\psi$ . For simplicity, we will assume here that  $\chi$  particles do not have any bare mass, so that their effective mass is equal to  $g|\phi|$ .

In chapter 5 I showed that for this case  $\chi$  particles are produced at the moment when  $\phi = 0$  with number density  $\frac{(g\dot{\phi}_0)^{3/2}}{8\pi^3}$ , which then decreases as  $a^{-3}(t)$  to give

$$n_\chi = \frac{(g\dot{\phi}_0)^{3/2}}{8\pi^3 a^3(t)} . \quad (6.22)$$

(See equation (5.5).) Here we take  $a_0 = 1$  at the moment of particle production.

Particle production occurs only in a small vicinity of  $\phi = 0$ . Then the field  $\phi$  continues rolling along the flat direction of the effective potential with  $\phi > 0$ , and the mass of each  $\chi$  particle grows as  $g\phi$ . Therefore the energy density of produced particles is

$$\rho_\chi = \frac{(g\dot{\phi}_0)^{3/2}}{8\pi^3} \frac{g\phi(t)}{a^3(t)}. \quad (6.23)$$

The energy density of the field  $\phi$  drops down much faster, as  $a^{-6}(t)$ . The reason is that if one neglects backreaction of produced particles, the energy density of the field  $\phi$  at this stage is entirely concentrated in its kinetic energy density  $\frac{1}{2}\dot{\phi}^2$ , which corresponds to the equation of state  $p = \rho$ . I will study this issue now in a more detailed way.

The equation of motion for the inflaton field after particle production looks as follows:

$$\ddot{\phi} + 3H\dot{\phi} = -g^2\phi\langle\chi^2\rangle \quad (6.24)$$

I will assume for simplicity that the field  $\chi$  does not have bare mass, i.e.  $m_\chi = g\phi$ . As soon as the field  $\phi$  becomes greater than  $\phi^*$  (and this happens practically instantly, when particle production ends), the particles  $\chi$  become nonrelativistic. In this case  $\langle\chi^2\rangle$  can be easily related to  $n_\chi$ :

$$\langle\chi^2\rangle \approx \frac{1}{2\pi^2} \int \frac{n_k k^2 dk}{\sqrt{k^2 + g^2\phi^2}} \approx \frac{n_\chi}{g\phi} \approx \frac{(g\dot{\phi}_0)^{3/2}}{8\pi^3 g\phi a^3(t)}. \quad (6.25)$$

Therefore the equation for the field  $\phi$  reads

$$\ddot{\phi} + 3H\dot{\phi} = -gn_\chi = -g \frac{(g\dot{\phi}_0)^{3/2}}{8\pi^3 a^3(t)}. \quad (6.26)$$

To analyze the solutions of this equation, I will first neglect backreaction. In this case one has  $a \sim t^{1/3}$ ,  $H = \frac{1}{3t}$ , and

$$\phi = \frac{M_p}{2\sqrt{3}\pi} \log \frac{t}{t_0}, \quad (6.27)$$

where  $t_0 = \frac{1}{3H_0} = \frac{M_p}{2\sqrt{3}\pi\dot{\phi}_0} \approx \frac{5}{\sqrt{3}\pi m}$ .

One can easily check that this regime remains intact and backreaction is unimportant for  $t < t_1 \sim \frac{8\pi^3}{\sqrt{g^5 \dot{\phi}_0}}$ , until the field  $\phi$  grows up to

$$\phi_1 \approx \frac{5M_p}{4\sqrt{3}\pi} \log \frac{1}{g} . \quad (6.28)$$

This equation is valid for  $g \ll 1$ . For example, for  $g = 10^{-3}$  one has  $\phi_1 \sim 3M_p$ . For  $g = 10^{-1}$  one has  $\phi_1 \sim M_p$ . Note that the terms in the left hand side of the Eq. (6.26) decrease as  $t^{-2}$  when the time grows, whereas the backreaction term goes as  $t^{-1}$ . As soon as the backreaction becomes important, i.e. as soon as the field  $\phi$  reaches  $\phi_1$ , it turns back, and returns to  $\phi = 0$ . When it reaches  $\phi = 0$ , the effective potential becomes large, so the field  $\phi$  cannot become negative, and it bounces towards large  $\phi$  again.

Now let us take into account interaction of the  $\chi$  field with fermions. This interaction leads to decay of the  $\chi$  particles with the decay rate [5, 7, 8]

$$\Gamma(\chi \rightarrow \psi\psi) = \frac{h^2 m_\chi}{8\pi} = \frac{h^2 g |\phi|}{8\pi} . \quad (6.29)$$

Note that the decay rate grows with the growth of the field  $|\phi|$ , so particles tend to decay at large  $\phi$ . In our case the field  $\phi$  spends most of the time prior to  $t_1$  at  $\phi \sim M_p$  (if it does not decay earlier, see below). The decay rate at that time is

$$\Gamma(\chi \rightarrow \psi\psi) \sim \frac{h^2 g M_p}{8\pi} . \quad (6.30)$$

If  $\Gamma_\chi^{-1} < t_1 \sim \frac{8\pi^3}{g^{5/2} \dot{\phi}_0}$ , then particles  $\chi$  will decay to fermions  $\psi$  at  $t < t_1$  and the force driving the field  $\phi$  back to  $\phi = 0$  will disappear before the field  $\phi$  turns back. In this case the field  $\phi$  will continue to grow, and its energy density will continue decreasing anomalously fast, as  $a^{-6}$ . This happens if

$$\frac{h^2 g M_p}{8\pi} \gtrsim \frac{g^{5/2} \dot{\phi}_0^{1/2}}{8\pi^3} . \quad (6.31)$$

Taking into account that in our case  $\dot{\phi}_0 \sim \frac{m M_p}{10}$  and  $m \sim 10^{-6} M_p$ , one finds that this



condition is satisfied if  $h \gtrsim 5 \times 10^{-3} g^{3/4}$ . This is a very mild condition. For example, it is satisfied for  $h > 5 \times 10^{-3}$  if  $g = 1$ , and for  $h > 5 \times 10^{-7}$  if  $g = 10^{-4}$ .

This scenario is always 100% efficient. The initial fraction of energy transferred to matter at the moment of  $\chi$  particle production is not very large, about  $10^{-2} g^2$  of the energy of the inflaton field [9]. However, because of the subsequent growth of this energy due to the growth of the field  $\phi$ , and because of the rapid decrease of kinetic energy of the inflaton field, the energy density of the  $\chi$  particles and of the products of their decay soon becomes dominant. This should be contrasted with the usual situation in the theories where  $V(\phi)$  has a minimum. As was emphasized in [5, 7, 8], efficient preheating is possible only in a subclass of such models. In many models where  $V(\phi)$  has a minimum the decay of the inflaton field is incomplete, and it accumulates an unacceptably large energy density compared with the energy density of the thermalized component of matter. The possibility of having very efficient reheating in NO models may have significant consequences for inflationary model building.

It is instructive to compare the density of particles produced by this mechanism to the density of particles created during gravitational particle production, which is given by  $\rho_\chi \sim 10^{-2} H^4 \sim \rho_\phi \frac{\rho_\phi}{M_p^4}$ , where  $\rho_\phi$  is the energy density of the field  $\phi$  at the end of inflation. In the model  $\frac{\lambda_\phi}{4} \phi^4$  one has  $\rho_\phi \sim 10^{-16} M_p^4$ , and, consequently,  $\rho_\chi \sim \rho_\phi \frac{\rho_\phi}{M_p^4} \sim 10^{-16} \rho_\phi$ . Meanwhile, as we just mentioned, at the first moment after particle production in our scenario the energy density of produced particles is of the order of  $10^{-2} g^2 \rho_\phi$  [9], and then it grows together with the field  $\phi$  because of the growth of the mass  $g\phi$  of each  $\chi$  particle. Thus, for  $g^2 \gtrsim 10^{-14}$  the number of particles produced during instant preheating is much greater than the number of particles produced by gravitational effects. Therefore one may argue that reheating of the universe in NO models should be described using the instant preheating scenario. Typically it is much more efficient than gravitational particle production. This means, in particular, that production of normal particles will be much more efficient than the production of gravitinos and moduli.

In order to avoid the gravitino problem altogether one may consider versions of NO models where the particles produced during preheating remain nonrelativistic

for a while. Then the energy density of gravitinos during this epoch decreases much faster than the energy density of usual particles. New gravitinos will not be produced if the resulting temperature of reheating is sufficiently small.

## 6.5 Other versions of NO models

In the previous section we considered the simplest model where  $V(\phi) = 0$  for  $\phi > 0$ . However, in general  $V(\phi)$  may become flat not at  $\phi = 0$ , but only asymptotically, at  $\phi \gtrsim M_p$ . Such theories have become rather popular now in relation to the theory of quintessence; for a partial list of references see e.g. [70, 71, 72, 73, 74, 75, 76, 29, 77, 78, 79]. In such a case the backreaction of created particles may never turn the scalar field  $\phi$  back to  $\phi = 0$ . Therefore the decay of the particles  $\chi$  may occur very late, and one can have very efficient preheating for any values of the coupling constants  $g$  and  $h$ .

On the other hand, if the  $\chi$  particles are stable, and if the field  $\phi$  continues rolling for a very long time, one may encounter a rather unusual regime. If the particle masses  $g|\phi|$  at some moment approach  $M_p$ , the  $\chi$  particles may convert to black holes and immediately evaporate.

Indeed, in conventional quantum field theory, an elementary particle of mass  $M$  has a Compton wavelength  $M^{-1}$  smaller than its Schwarzschild radius  $2M/M_p^2$  if  $M \gtrsim M_p$ . Therefore one may expect that as soon as  $m_\chi = g|\phi|$  becomes greater than  $M_p$ , each  $\chi$  particle becomes a Planck-size black hole, which immediately evaporates and reheats the universe. If this regime is possible, it should be avoided. Indeed, black holes of Planck mass may produce similar amounts of all kinds of particles, including gravitinos. Therefore if reheating occurs because of black hole evaporation, then we will return to the gravitino problem again.

Thus, the best possibility is to consider those versions of the instant preheating scenario that do not lead to the creation of stable particles of Planckian mass. It may seem paradoxical that one needs to be careful about this constraint. Several years ago it would have seemed impossible to produce particles of mass greater than  $5 \times 10^{12}$  GeV during the decay of an inflaton field of mass  $m_\phi \sim 10^{13}$  GeV. Here I have described

a nonperturbative mechanism of preheating that may produce particles 5 orders of magnitude heavier than  $m_\phi$ . It is interesting that the mechanism of instant preheating works especially well in the context of NO models where all other mechanisms are rather inefficient.

# Chapter 7

## Gravitational Particle Production and the Moduli Problem

*Note: This chapter is based on a paper by Gary Felder, Lev Kofman, and Andrei Linde, available on the Los Alamos eprint server as hep-ph/9909508. The full citation appears in the bibliography [68].*

### 7.1 Chapter Abstract

A theory of gravitational production of light scalar particles during and after inflation is investigated. In the most interesting cases where long-wavelength fluctuations of light scalar fields can be generated during inflation, these fluctuations rather than quantum fluctuations produced after inflation give the dominant contribution to particle production. In such cases a simple analytical theory of particle production can be developed. Application of these results to the theory of quantum creation of moduli fields demonstrates that if the moduli mass is smaller than the Hubble constant then these fields are copiously produced during inflation. This gives rise to the cosmological moduli problem even if there is no homogeneous component of the classical moduli field in the universe. To avoid this version of the moduli problem it is necessary for the Hubble constant  $H$  during the last stages of inflation and/or the reheating temperature  $T_R$  after inflation to be extremely small.

## 7.2 Introduction

Recently there has been a renewal of interest in gravitational production of particles in an expanding universe. This was a subject of intensive study many years ago, see e.g. [48, 49, 50, 51, 52, 53]. However, with the invention of inflationary theory the issue of the production of particles due to gravitational effects became less urgent. Indeed, gravitational effects are especially important near the cosmological singularity, at the Planck time. But the density of the particles produced at that epoch becomes exponentially small due to inflation. New particles are produced only after the end of inflation when the energy density is much smaller than the Planck density. Production of particles due to gravitational effects at that stage is typically very inefficient.

There are a few exceptions to this rule that have motivated the recent interest in gravitational particle production. First of all, there are some models where the main mechanism of reheating during inflation is due to gravitational production. Even though this mechanism is very inefficient, in the absence of other mechanisms of reheating it may do the job. For example, in the NO models discussed in the previous chapter the inflaton field  $\phi$  does not oscillate after inflation, so the standard mechanism of reheating does not work [24, 25, 26, 27, 28, 47]. Usually gravitational particle production in such models lead to dangerous cosmological consequences, such as large isocurvature fluctuations and overproduction of gravitinos. In order to overcome these problems, it was necessary to modify the NO models and to use the non-gravitational mechanism of instant preheating for the description of particle production. See chapters 5 and 6 for more details.

There are some other cases where even very small but unavoidable gravitational particle production may lead either to useful or to catastrophic consequences [35, 37, 57, 61, 80]. For example, it has recently been found that the production of gravitinos by the oscillating inflaton field is not suppressed by the small gravitational coupling. As a result, gravitinos can be copiously produced in the early universe even if the reheating temperature always remains smaller than  $10^8$  GeV [61, 80]. Another important example is related to moduli production. 15 years ago Coughlan *et al* realized that string theory and supergravity give rise to a cosmological moduli

problem associated with the existence of a large homogeneous classical moduli field in the early universe [81]. Soon afterwards Goncharov, Linde and Vysotsky showed that quantum fluctuations of moduli fields produced at the last stages of inflation lead to the moduli problem even if initially there were no classical moduli fields [57]. Thus the cosmological moduli problem may appear either because of the existence of a large long-living homogeneous classical moduli field or because of quantum production of excitations (particles) of the moduli fields. In [47] it was pointed out that the problem of moduli production is especially difficult in the context of NO models, where moduli are produced as abundantly as usual particles.

Recently the problem of moduli production in the early universe was studied by numerical methods in [80], with conclusions similar to those of Ref. [57]. As I am going to demonstrate, the main source of gravitational production of light moduli in inflationary cosmology is very simple, and one can study the theory of moduli production not only numerically but also analytically by the methods developed in [57, 47]. This fact allowed us to generalize and considerably strengthen the results of Refs. [57, 80].

In particular, we will see that in the leading approximation the problem of overproduction of light moduli particles is *equivalent* to the problem of large homogeneous classical moduli fields [57]. I will show that the ratio of the number density of light moduli produced during inflation to the entropy of the universe after reheating satisfies the inequality

$$\frac{n_\chi}{s} \gtrsim \frac{T_R H_0^2}{3mM_p^2} . \quad (7.1)$$

Here  $m$  is the moduli mass,  $M_p \sim 2.4 \times 10^{18}$  GeV is the reduced Planck mass, and  $H_0$  is the Hubble constant at the moment corresponding to the beginning of the last 60 e-foldings before the end of inflation.

In the simplest versions of inflationary theory with potentials  $M^2\phi^2/2$  or  $\lambda\phi^4/4$  one has  $H_0 \sim 10^{14}$  GeV. In such models our result implies that in order to satisfy the cosmological constraint  $\frac{n_\chi}{s} \lesssim 10^{-12}$  one needs to have an abnormally small reheating temperature  $T_R \lesssim 1$  GeV. Alternatively one may consider inflationary models where the Hubble constant at the end of inflation is very small. But I will argue that even

this may not help, so one may need either to invoke thermal inflation or to use some other mechanisms that can make the moduli problem less severe, see e.g. [82, 83, 84].

In the next section I outline the classical and quantum versions of the moduli problem and explain how each of them can arise in inflationary theory. In section 7.4 I describe the results of our numerical simulations of gravitational production of light scalar fields during and after preheating. In particular these results verify our prediction that the dominant contribution to particle production comes from long-wavelength modes that are indistinguishable from homogeneous classical moduli fields. Finally in section 7.5 I analytically compute the production of these long wavelength modes and derive Eq.(7.1). This section also contains a concluding discussion.

### 7.3 Moduli problem

String moduli couple to standard model fields only through Planck scale suppressed interactions. Their effective potential is exactly flat in perturbation theory in the supersymmetric limit, but it may become curved due to nonperturbative effects or because of supersymmetry breaking. If these fields originally are far from the minimum of their effective potential, the energy of their oscillations will decrease in an expanding universe in the same way as the energy density of nonrelativistic matter,  $\rho_m \sim a^{-3}(t)$ . Meanwhile the energy density of relativistic plasma decreases as  $a^{-4}$ . Therefore the relative contribution of moduli to the energy density of the universe may quickly become very significant. They are expected to decay after the stage of nucleosynthesis, violating the standard nucleosynthesis predictions unless the initial amplitude of the moduli oscillations  $\chi_0$  is sufficiently small. The constraints on the energy density of the moduli field  $\rho_\chi$  and the number of moduli particles  $n_\chi$  depend on details of the theory. The most stringent constraint appears because of the photodissociation and photoproduction of light elements by the decay products of the moduli fields. For  $m \sim 10^2 - 10^3$  GeV one has

$$\frac{n_\chi}{s} \lesssim 10^{-12} - 10^{-15} . \quad (7.2)$$

see [60, 85, 86] and references therein. In this chapter I use a conservative version of this constraint,  $\frac{n_\chi}{s} \lesssim 10^{-12}$ .

If the field  $\chi$  is a classical homogeneous oscillating scalar field, then this constraint applies to it as well if one defines the corresponding number density of nonrelativistic particles  $\chi$  by the following obvious relation:

$$n_\chi = \frac{\rho_\chi}{m} = \frac{m\chi^2}{2}. \quad (7.3)$$

Let us first consider moduli  $\chi$  with a constant mass  $m \sim 10^2 - 10^3$  GeV and assume that reheating of the universe occurs after the beginning of oscillations of the moduli. This is indeed the case if one takes into account that in order to avoid the gravitino problem one should have  $T_R < 10^8$  GeV. I will also assume for definiteness that the minimum of the effective potential for the field  $\chi$  is at  $\chi = 0$ ; one can always achieve this by an obvious redefinition of the field  $\chi$ .

Independent of the choice of inflationary theory, at the end of inflation the main fraction of the energy density of the universe is concentrated in the energy of an oscillating scalar field  $\phi$ . Typically this is the same field that drives inflation, but in some models such as hybrid inflation this may not be the case. I will consider here the simplest (and most general) model where the effective potential of the field  $\phi$  after inflation is quadratic,

$$V(\phi) = \frac{M^2}{2}\phi^2. \quad (7.4)$$

After inflation the field  $\phi$  oscillates. If one keeps the notation  $\phi$  for the amplitude of oscillations of this field, then one can say that the energy density of this field is given by  $\rho(\phi) = \frac{M^2}{2}\phi^2$ .

To simplify my notation, I take the scale factor at the end of inflation to be  $a_0 = 1$ . The amplitude of the oscillating field in the theory with the potential (7.4) changes as

$$\phi(t) = \phi_0 a^{-3/2}(t). \quad (7.5)$$

The field  $\chi$  does not oscillate and almost does not change its magnitude until the



moment  $t_1$  when  $H^2(t) = \frac{\rho_\phi}{3M_p^2}$  becomes smaller than  $m^2/3$ . At that time one has

$$\frac{\rho_\chi}{\rho_\phi} \sim \frac{m^2 \chi_0^2}{6H^2(t)M_p^2} \sim \frac{\chi_0^2}{2M_p^2} \quad (7.6)$$

This ratio, which can also be obtained by a numerical investigation of oscillations of the moduli fields, does not change until the time  $t_R$  when reheating occurs because  $\rho_\chi$  and  $\rho_\phi$  decrease in the same way: they are proportional to  $a^{-3}$ .

At the moment of reheating one has  $\rho_\phi(t_R) = \pi^2 N(T) T_R^4/30$ , and the entropy of produced particles  $s = 2\pi^2 N(T) T_R^3/45$ , where  $N(T)$  is the number of light degrees of freedom. This yields

$$\frac{n_\chi}{s} \sim \frac{\rho_\chi}{ms} \sim \frac{\chi_0^2 T_R}{3mM_p^2} \quad (7.7)$$

Usually one expects  $T_R \gg m \sim 10^2$  GeV. Then in order to have  $\frac{n_\chi}{s} < 10^{-12}$  one would need  $\chi_0 \ll 10^{-6} M_p$ . However, it is hard to imagine why the value of the moduli field at the end of inflation should be so small. If one takes  $\chi_0 \sim M_p$ , which looks natural, then one violates the bound  $\frac{n_\chi}{s} < 10^{-12}$  by more than 12 orders of magnitude. This is the essence of the cosmological moduli problem [81].

In general, the situation is more complex. During the expansion of the universe the effective potential of the moduli acquires some corrections. In particular, quite often the effective mass of the moduli (the second derivative of the effective potential) can be represented as

$$m_\chi^2 = m^2 + c^2 H^2, \quad (7.8)$$

where  $c$  is some constant and  $H$  is the Hubble parameter [55, 56]. Higher derivatives of the effective potential may acquire corrections as well. This leads to a different version of the moduli problem discussed in [57], see also [58, 59]. The position of the minimum of the effective potential of the moduli field in the early universe may occur at a large distance from the position of the minimum at present. This may fix the initial position of the field  $\chi$  and lead to its subsequent oscillations.

A simple toy model illustrating this possibility was given in [82, 83]:

$$V = \frac{1}{2}m_\chi^2\chi^2 + \frac{c^2}{2}H^2(\chi - \chi_0)^2. \quad (7.9)$$

At large  $H$  the minimum appears at  $\chi = \chi_0$ ; at small  $H$  the minimum is at  $\chi = 0$ . Thus one would expect that initially the field should stay at  $\chi_0$ , and later, when  $H$  decreases, it should oscillate about  $\chi = 0$  with an initial amplitude approximately equal to  $\chi_0$ . The only natural value for  $\chi_0$  in supergravity is  $\chi_0 \sim M_p$ . This may lead to a strong violation of the bound (7.2).

A more detailed investigation of this situation has shown [84] that one should distinguish between three different possibilities:  $c \gg 1$ ,  $c \sim 1$  and  $c \ll 1$ .

If  $c > O(10)$ , the field  $\chi$  is trapped in the (moving) minimum of the effective potential, its oscillations have very small amplitudes, and the moduli problem does not appear at all [84]. This is the simplest resolution of the problem, but it is not simple to find realistic models where the condition  $c > O(10)$  is satisfied.

The most natural case is  $c \sim 1$ . It requires a complete study of the behavior of the effective potential in an expanding universe. There may exist some cases where the minimum of the effective potential does not move in this regime, but in general the effects of quantum creation of moduli in this scenario [57, 80] are subdominant with respect to the classical moduli problem discussed above [57, 58, 59], so I will not discuss this regime.

Here I study the case  $c \ll 1$ . In this case the effective mass of the moduli at  $H \gg m$  is always much smaller than  $H$ , so the field does not move towards its minimum, regardless of its position. Thus if there is any classical field  $\chi_0$  it simply stays at its initial position until  $H$  becomes smaller than  $m$ , just as in the case considered above, and the resulting ratio  $\frac{n_\chi}{s}$  is given by Eq. (7.7).

The moduli problem in this scenario has two aspects. First of all, in order to avoid the classical moduli problem one needs to explain why  $\chi_0 \sim 10^{-6} \sqrt{\frac{m}{T_R}} M_p$ , which is necessary (but not sufficient) to have  $n_\chi/s < 10^{-12}$ . Then one should study quantum creation of moduli in an expanding universe and check whether their contribution to  $n_\chi$  violates the bound  $n_\chi/s < 10^{-12}$ . This last aspect of the moduli problem was

studied in [57, 80].

In inflationary cosmology these two contributions (the contributions to  $n_\chi$  from the classical field  $\chi$  and from its quantum fluctuations) are almost indistinguishable. Indeed, the dominant contribution to the number of moduli produced in an expanding universe is given by the fluctuations of the moduli field produced during inflation. These fluctuations have exponentially large wavelengths and for all practical purposes they have the same consequences as a homogeneous classical field of amplitude  $\chi_0 = \sqrt{\langle \chi^2 \rangle}$ .

To be more accurate, these fluctuations behave in the same way as the homogeneous classical field  $\phi$  only if their wavelength is greater than  $H^{-1}$ . During inflation this condition is satisfied for all inflationary fluctuations, but after inflation the size of the horizon grows and eventually becomes larger than the wavelength of some of the modes. Then these modes begin to oscillate and their amplitude begins to decrease even if at that stage  $m < H$ . To take this effect into account one may simply exclude from consideration those modes whose wavelengths become smaller than  $H^{-1}$  prior to the moment  $t \sim m^{-1}$  when  $H$  drops down to  $m$ . It can be shown that in the context of our problem this is a relatively minor correction, so one can use the simple estimate  $\chi_0 = \sqrt{\langle \chi^2 \rangle}$ .

In order to evaluate this quantity I will assume that  $c \ll 1$  and  $m \ll H$  during and after inflation. This reduces the problem to the investigation of the production of massless (or nearly massless) particles during and after inflation. In the next section I study this issue and show that in the most interesting cases where inflationary long-wavelength fluctuations of a scalar field can be generated during inflation, they give the dominant contribution to particle production. This allowed us to reduce a complicated problem of gravitational particle production to a simple problem that could be easily solved analytically.

## 7.4 Generation of light particles from and after inflation

In this section I will present the results of a numerical study of the gravitational creation of light scalar particles in the context of inflation. Consider a scalar field  $\chi$  with the potential

$$V(\chi) = \frac{1}{2} (m^2 - \xi R) \chi^2 \quad (7.10)$$

where  $R$  is the Ricci scalar. In a Friedmann universe  $R = -\frac{6}{a^2}(\ddot{a}a + \dot{a}^2)$ . The scalar field operator can be represented in the form

$$\chi(x, t) = \frac{1}{(2\pi)^{-3/2}} \int d^3k \left[ \hat{a}_k \chi_k(t) e^{ikx} + \hat{a}_k^\dagger \chi_k^*(t) e^{-ikx} \right] \quad (7.11)$$

where the eigenmode functions  $\chi_k$  satisfy

$$\ddot{\chi}_k + 3\frac{\dot{a}}{a}\dot{\chi}_k + \left[ \left( \frac{k}{a} \right)^2 + m^2 - \xi R \right] \chi_k = 0, \quad (7.12)$$

By introducing conformal time and field variables defined as  $\eta \equiv \int \frac{dt}{a}$ ,  $f_k \equiv a\chi_k$  eq. (7.12) can be simplified to

$$f_k'' + \omega_k^2 f_k = 0 \quad (7.13)$$

where primes denote differentiation with respect to  $\eta$  and

$$\omega_k^2 = k^2 + a^2 m^2 + \left( \frac{1}{6} - \xi \right) \frac{\ddot{a}}{a}. \quad (7.14)$$

The growth of the scale factor is determined by the evolution of the inflaton field  $\phi$  with potential  $V(\phi)$ . In conformal time

$$\ddot{a} = \frac{\dot{a}^2}{a} - \frac{8\pi a}{3} (\phi'^2 - a^2 V(\phi)) \quad (7.15)$$

$$\phi'' + 2\frac{\dot{a}}{a}\phi' + a^2 \frac{\partial V(\phi)}{\partial \phi} = 0. \quad (7.16)$$

For initial conditions for the modes  $f_k$ , in the first approximation one can use positive frequency vacuum fluctuations  $f_k = \frac{1}{\sqrt{2k}}e^{-ikt}$ , see e.g. [37]. However, when describing fluctuations produced at the last stages of a long inflationary period, one should begin with fluctuations that have been generated during the previous stage of inflation. For example, for massless scalar fields minimally coupled to gravity instead of  $f_k = \frac{1}{\sqrt{2k}}e^{-ikt}$  one should use Hankel functions [3]:

$$f_k(t) = \frac{ia(t)H}{k\sqrt{2k}} \left( 1 + \frac{k}{iH}e^{-Ht} \right) \exp \left( \frac{ik}{H}e^{-Ht} \right), \quad (7.17)$$

where  $H$  is the Hubble constant at the beginning of calculations. To make the calculations even more accurate, one should take into account that long-wavelength perturbations were produced at early stages of inflation when  $H$  was greater than at the beginning of the calculations. If the stage of inflation is very long, then the final results do not change much if instead of the Hankel functions (7.17) one uses  $f_k = \frac{1}{\sqrt{2k}}e^{-ikt}$ . However, if the inflationary stage is short, then using the functions  $f_k = \frac{1}{\sqrt{2k}}e^{-ikt}$  considerably underestimates the resulting value of  $\langle \chi^2 \rangle$ .

At late times the solutions to Eq. (7.13) can be represented in terms of WKB solutions as

$$f_k(\eta) = \frac{\alpha_k(\eta)}{\sqrt{2\omega_k}}e^{-i\int^\eta \omega_k d\eta} + \frac{\beta_k(\eta)}{\sqrt{2\omega_k}}e^{+i\int^\eta \omega_k d\eta}, \quad (7.18)$$

where  $\alpha_k(\eta)$  and  $\beta_k(\eta)$  play the role of coefficients of a Bogolyubov transformation. This form is often used to discuss particle production because the number density of particles in a given mode is given by  $n_k = |\beta_k(\eta)|^2$  and their energy density is  $\omega_k n_k$ . As we will see, though, the main contribution to the number density of  $\chi$  particles at late times comes from long-wavelength modes that are far outside the horizon during reheating. As long as they remain outside the horizon these modes do not manifest particle-like behaviour, i.e. the mode functions do not oscillate. In this situation the coefficients  $\alpha$  and  $\beta$  have no clear physical meaning. I therefore present our results in terms of the mode amplitudes  $|f_k(\eta)|^2$ , which as I will show contain all the information relevant to number density and energy density at late times.

At late times when  $\frac{a''}{a} \sim H < m$  the long wavelength modes of  $\chi$  will be nonrelativistic and their number density will simply be given by Eq. (7.3). Moreover the very long wavelength modes which are still outside the horizon at late times (e.g. at nucleosynthesis) will act like a classical homogeneous field whose amplitude is given by

$$\langle \chi^2 \rangle = \frac{1}{2\pi^2 a^2} \int dk k^2 |f_k|^2. \quad (7.19)$$

It is these very long wavelength modes which will dominate and therefore the quantity of interest for us is the amplitude of these fluctuations.

In our calculations we assumed that  $m^2 = c^2 H^2$  with  $c \ll 1$ ; the results shown are for  $c = 0$  but we also did the calculations with  $c = .01$  and found that the results were independent of  $c$  in this range.

Figure 7.1 shows the results of solving Eq. (7.13) for a model with the inflaton potential  $V(\phi) = \frac{1}{4}\lambda\phi^4$ . These data were taken after ten oscillations of the inflaton field. The vertical axis shows  $k^2 |f_k|^2$  as a function of the momentum  $k$ . The momentum is shown in units of the Hubble constant at the end of inflation.

The different plots represent runs with different starts of inflation, i.e. with different initial values of  $\phi$ . They all coincide in the ultraviolet part of the spectrum, but the runs that started towards the end of inflation show a significant suppression in the infrared. This shows that fluctuations produced during inflation are the primary source of the infrared modes, which in turn dominate the number density.

The curve on top shows the Hankel function solutions (7.17), which give

$$|f_k|^2 = \frac{a^2 H^2}{2k^3} \quad (7.20)$$

for de Sitter space, i.e. for a constant  $H$ . In the figure, we have corrected this expression by using for each mode the value of the Hubble constant at the moment when that mode crossed the horizon. For the  $\lambda\phi^4$  model shown here the appropriate Hubble parameter for each mode can be approximated as

$$H_k = \sqrt{\frac{2\pi\lambda}{3}} \left( \phi_e^2 - \frac{1}{\pi} \ln \left( \frac{k}{H_e} \right) \right) \quad (7.21)$$

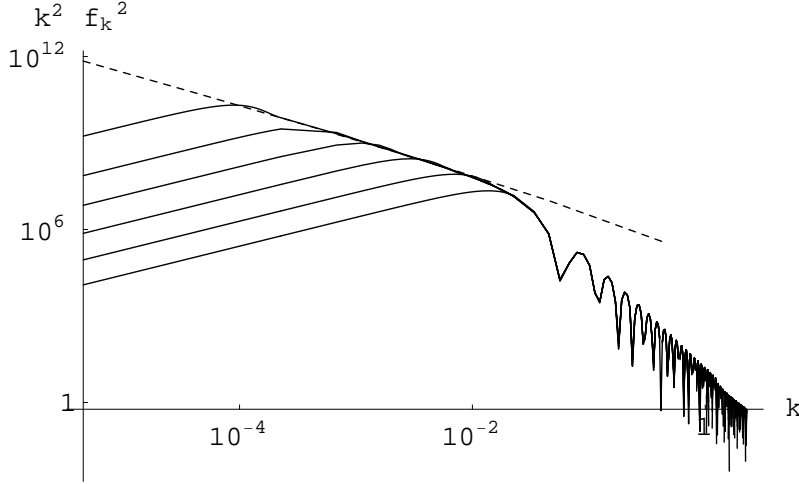


Figure 7.1: Fluctuations vs. mode frequency at a late time. The lower plots show runs that started close to the end of inflation, with initial conditions  $f_k = \frac{1}{\sqrt{2k}}e^{-ikt}$ . The starting times range from  $\phi_0 = 1.5M_p$  (lowest curve) up through  $\phi_0 = 2M_p$ . The highest curve shows the Hankel function solutions given by eqs. (7.20) and (7.21). As we see, calculations with  $f_k = \frac{1}{\sqrt{2k}}e^{-ikt}$  produce the correct spectrum at large  $k$  but underestimate the level of quantum fluctuations at small  $k$ .

where  $\phi_e$  and  $H_e$  are the values of the inflaton and the Hubble parameter respectively at the end of inflation.

Note that if the Hankel function solutions (7.17) are used as initial conditions for a numerical run then they do not change as the modes cross the horizon, so the upper curve of the plot can also be obtained from such a run. Relative to this upper curve it's easy to see how the numerical runs show suppression in the infrared due to starting inflation at late times and choosing the initial conditions in the form  $f_k = \frac{1}{\sqrt{2k}}e^{-ikt}$ , and suppression in the ultraviolet due to the end of inflation. The latter suppression is physically realistic. The infrared suppression should occur at a wavelength corresponding to the Hubble radius at the beginning of inflation.

The different regions of the graph illustrate effects that occurred at different times. During inflation long wavelength modes crossed the horizon at early times. Thus the far left portion of the plot shows the modes that crossed earliest. They have the highest amplitudes both because they were frozen in earliest and because the Hubble constant was higher at earlier times when they were produced. The lower plots don't

show these high amplitudes because inflation began too late for these modes to cross outside the horizon and be amplified. Farther to the right the curve shows modes that were only slightly if at all amplified during inflation. The far right modes were produced during the fast rolling and oscillatory stages. These modes are not frozen and can be described meaningfully in terms of  $\alpha$  and  $\beta$  coefficients. The regularized expression

$$|f_k|^2 = \frac{1}{\omega_k} \left[ |\beta_k|^2 + \text{Re} \left( \alpha_k \beta_k^* e^{-2i \int \omega_k d\eta} \right) \right] \quad (7.22)$$

shows why the amplitudes of these modes oscillate as a function of  $k$ .

In short inflationary fluctuations are primarily responsible for producing infrared modes and post-inflationary effects account for ultraviolet modes, but it is the infrared modes that were outside the horizon at the end of inflation that dominate the number density at late times. The earlier inflation began the farther this distribution will extend into the infrared, and the long wavelength end of this spectrum will always give the greatest contribution to the number density of  $\chi$  particles.

Our numerical calculations were similar to those of Kuzmin and Tkachev [37]. However, they took a rather small initial value of the classical scalar field  $\phi$ , which resulted in less than 60 e-folds of inflation. As initial conditions for the fluctuations they used  $f_k = \frac{1}{\sqrt{2k}} e^{-ikt}$ . They pointed out that the results of such calculations can give only a lower bound on the number of  $\chi$  particles produced during inflation. Consequently, similar calculations performed in [80] could give only a lower bound on the number of moduli fields produced in the early universe.

Our goal is to find not a lower bound but the complete number of particles produced at the last stages of inflation in realistic inflationary models, where the total duration of inflation typically is much greater than 60 e-foldings. One result revealed by our calculations is that the effects of an arbitrarily long stage of inflation can be mimicked by the correct choice of “initial” conditions chosen for the modes  $\chi_k$  after inflation. Instead of using the Minkowski space fluctuations  $f_k = \frac{1}{\sqrt{k}} e^{-ikt}$  used in [37] as well as in our numerical calculations, one should use the de Sitter space solutions (7.17), with  $H$  corrected to the value it had for each mode at horizon crossing. Using these modes at the end of inflation is equivalent to running a simulation with a long



stage of inflation.

Our numerical calculations confirmed the result that I am going to derive analytically in the next section: The number of  $\chi$  particles ( $n_\chi \sim m\langle\chi^2\rangle$ ) produced during the stage of inflation beginning at  $\phi = \phi_0$  in the simplest model  $M^2\phi^2/2$  is proportional to  $\phi_0^4$ , whereas in the model  $\lambda\phi^4/4$  it is proportional to  $\phi_0^6$ . Thus the total number of particles produced during inflation is *extremely* sensitive to the choice of initial conditions. If one considers  $\phi_0$  corresponding to the beginning of the last 60 e-folds of inflation, the total number of particles produced at that stage appears to be much greater than the lower bound obtained in [37]. As we will see, this allowed us to put a much stronger constraint on the moduli theories than the constraint obtained in [80].

## 7.5 Light moduli from inflation

The numerical results obtained in the previous section confirmed our expectation that in the most interesting cases where long-wavelength inflationary fluctuations of light scalar fields can be generated during inflation, they give the dominant contribution to particle production. In particular, in the case of  $c \ll 1$ ,  $m \ll H$  most moduli field fluctuations are generated during inflation rather than during the post-inflationary stage. These fluctuations grow at the stage of inflation in the same way as if the moduli field  $\chi$  were massless [3]:

$$\frac{d\langle\chi^2\rangle}{dt} = \frac{H^3}{4\pi^2}. \quad (7.23)$$

If the Hubble constant does not change during inflation, one obtains the well-known relation

$$\langle\chi^2\rangle = \frac{H^3 t}{4\pi^2}. \quad (7.24)$$

However, in realistic inflationary models the Hubble constant changes in time, and fluctuations of the light fields  $\chi$  with  $m \ll H$  behave in a more complicated way.

As an example, let us consider the case studied in the last section. Here inflation is driven by a field  $\phi$  with an effective potential  $V(\phi) = \frac{\lambda}{4}\phi^4$  at  $\phi > 0$ . This potential

could be oscillatory or flat for  $\phi < 0$ . We consider a light scalar field  $\chi$  that is not coupled to the inflaton field  $\phi$ , and that is minimally coupled to gravity.

The field  $\phi$  during inflation obeys the following equation:

$$3H\dot{\phi} = -\lambda\phi^3. \quad (7.25)$$

Here

$$H = \frac{1}{2}\sqrt{\frac{\lambda}{3}} \frac{\phi^2}{M_p}. \quad (7.26)$$

These two equations yield the solution [3]

$$\phi = \phi_0 \exp\left(-2\sqrt{\frac{\lambda}{3}}M_p t\right), \quad (7.27)$$

where  $\phi_0$  is the initial value of the inflaton field  $\phi$ . In this case Eq. (7.23) reads:

$$\frac{d\langle\chi^2\rangle}{dt} = \frac{\lambda\sqrt{\lambda}}{96\sqrt{3}\pi^2} \frac{\phi_0^6}{M_p^3} \exp\left(-12\sqrt{\frac{\lambda}{3}}M_p t\right) \quad (7.28)$$

The result of integration at large  $t$  converges to

$$\langle\chi^2\rangle = \frac{\lambda}{2} \left(\frac{\phi_0^3}{24\pi M_p^2}\right)^2. \quad (7.29)$$

This result agrees with the results of our numerical investigation described in the previous section.

From the point of view of the moduli problem, these fluctuations lead to the same consequences as a classical scalar field  $\chi$  that is homogeneous on the scale  $H^{-1}$  and that has a typical amplitude

$$\chi_0 = \sqrt{\langle\chi^2\rangle} = \sqrt{\frac{\lambda}{2}} \frac{\phi_0^3}{24\pi M_p^2}. \quad (7.30)$$

A similar result can be obtained in the model  $V(\phi) = \frac{M^2}{2}\phi^2$ . In this case one has

[3]

$$\phi(t) = \phi_0 - \sqrt{\frac{2}{3}} M_p M t. \quad (7.31)$$

The time-dependent Hubble parameter is given by

$$H = \frac{M}{\sqrt{6} M_p} \phi(t), \quad (7.32)$$

which yields

$$\chi_0 = \sqrt{\langle \chi^2 \rangle} = \frac{M \phi_0^2}{8\pi \sqrt{3} M_p^2}. \quad (7.33)$$

As we see, the value of  $\chi_0$  depends on the initial value of the field  $\phi$ . This result has the following interpretation. One may consider an inflationary domain of initial size  $H^{-1}(\phi_0)$ . This domain after inflation becomes exponentially large. For example, its size in the model with  $V(\phi) = \frac{M^2}{2} \phi^2$  becomes [3]

$$l \sim H^{-1}(\phi_0) \exp\left(\frac{\phi_0^2}{4M_p^2}\right). \quad (7.34)$$

In order to achieve 60 e-folds of inflation in this model one needs to take  $\phi_0 \sim 15M_p$ . This implies that a typical value of the (nearly) homogeneous scalar field  $\chi$  in a universe that experienced 60 e-folds of inflation in this model is given by

$$\chi_0 = \sqrt{\langle \chi^2 \rangle} \sim 5M. \quad (7.35)$$

In realistic versions of this model one has  $M \sim 5 \times 10^{-6} M_p \sim 10^{13}$  GeV [3]. Substitution of this result into Eq. (7.7) gives

$$\frac{n_\chi}{s} \sim 2 \times 10^{-10} \frac{T_R}{m}. \quad (7.36)$$

This implies that the condition  $n_\chi/s \lesssim 10^{-12}$  requires that the reheating temperature in this model should be at least two orders of magnitude smaller than  $m$ . For example, for  $m \sim 10^2$  GeV one should have  $T_R \lesssim 1$  GeV, which looks rather problematic.

This result confirms the basic conclusion of Ref. [57] that the usual models of inflation do not solve the moduli problem. Our result is similar to the result obtained in [80] by numerical methods, but it is approximately two orders of magnitude stronger. The reason for this difference is that the authors of Ref. [80] used a much smaller value of  $\phi_0$  in their numerical calculations. Consequently, they took into account only the particles produced at the very end of inflation, whereas the leading effect occurs at earlier stages of inflation, i.e. at larger  $\phi$ .

In general one can get a simple estimate of  $\chi_0 = \sqrt{\langle \chi^2 \rangle}$  by assuming that the universe expanded with a constant Hubble parameter  $H_0$  during the last 60 e-folds of inflation. To make this estimate more accurate one should take the value of the Hubble constant not at the end of inflation but approximately 60 e-foldings before it, at the time when the fluctuations on the scale of the present horizon were produced. The reason is that the largest contribution to the fluctuations is given by the time when the Hubble constant took its greatest values. Also, at that stage the rate of change of  $H$  was relatively slow, so the approximation  $H = H_0 = \text{const}$  is reasonable. Thus one can write

$$\chi_0 = \sqrt{\langle \chi^2 \rangle} \gtrsim \frac{H_0}{2\pi} \sqrt{H_0 t} \sim \frac{H_0}{2\pi} \sqrt{60} \sim H_0 . \quad (7.37)$$

This gives

$$\frac{n_\chi}{s} \gtrsim \frac{T_R H_0^2}{3m M_p^2} . \quad (7.38)$$

In the simplest versions of chaotic inflation with potentials  $M^2 \phi^2/2$  or  $\lambda \phi^4/4$  one has  $H_0 \sim 10^{14}$  GeV, which leads to the requirement  $T_R \lesssim 1$  GeV. But this equation shows that there is another way to relax the problem of the gravitational moduli production: one may consider models of inflation with a very small value of  $H_0$  [57]. For example, one may have  $n_\chi/s \sim 10^{-12}$  for  $T_R \sim H_0 \sim 10^7$  GeV.

However, this condition is not sufficient to resolve the moduli problem; the situation is more complicated. First of all, it is very difficult to find inflationary models where inflation occurs only during 60 e-foldings. Typically it lasts much longer, and the fluctuations of the light moduli fields will be much greater. This is especially

obvious in the theory of eternal inflation where the amplitude of fluctuations of the light moduli fields can become indefinitely large [3]. In particular, if the condition  $m_\chi^2 \sim m^2 + c^2 H^2$  with  $c \ll 1$  remains valid for  $\chi \gtrsim M_p$ , then one may expect the generation of moduli fields  $\chi > M_p$ . This should initiate inflation driven by the light moduli [47]. Then the situation would become even more problematic: we would need to find out how one could produce the baryon asymmetry of the universe after the light moduli decay and how one could obtain density perturbations  $\delta\rho/\rho \sim 10^{-4}$  in such a low-scale inflationary model.

One may expect that the region of values of  $\chi$  where its effective potential has small curvature  $m^2 \ll H^2$  may be limited, and may even depend on  $H$ . Then the existence of a long stage of inflation would push the fluctuations of the field  $\chi$  up to the region where its effective potential becomes curved, and instead of our results for  $\chi_0$  one should substitute the largest value of  $\chi$  for which  $m_\chi^2 < H^2$ . In such a situation one would have a mixture of problems that occur at  $c \ll 1$  and at  $c \sim 1$ .

Finally, I should emphasize that all our worries about quantum creation of moduli appear only after one makes the assumption that for whatever reason the initial value of the classical field  $\chi$  in the universe vanishes, i.e. that the classical version of the moduli problem has been resolved. We do not see any justification for this assumption in theories where the mass of the moduli field in the early universe is much smaller than  $H$ . Indeed, in such theories the classical field  $\chi$  initially can take *any* value, and this value is not going to change until the moment  $t \sim H^{-1} \sim m^{-1}$ . The main purpose of the research being reported on here was to demonstrate that even if one finds a solution to the light moduli problem at the classical level, the same problem will appear again because of quantum effects.

This does not mean that the moduli problem is unsolvable. One of the most interesting solutions is provided by thermal inflation [82, 83]. The Hubble constant during inflation in this scenario is very small, and the effects of moduli production there are rather insignificant. Another possibility is that moduli are very heavy in the early universe,  $m_\chi^2 = m^2 + c^2 H^2$ , with  $c > O(10)$ , in which case the moduli problem does not appear [84]. The main question is whether we really need to make the theory so complicated in order to avoid the cosmological problems associated with moduli.

Is it possible to find a simpler solution? One of the main results of our investigation is to confirm the conclusion of Ref. [57] that the simplest versions of inflationary theory do not help us to solve the moduli problem but rather aggravate it.

In conclusion I would like to note that the methods discussed here apply not only to the theory of moduli production but to other problems as well. For example, one may study the theory of gravitational production of superheavy scalar particles after inflation [35, 37]. If these particles are minimally coupled to gravity and have mass  $m \ll H$  during inflation, then one can use Eqs. (7.30), (7.33) to calculate the number of produced particles. These equations imply that the final result will strongly depend on  $\phi_0$ , i.e. on the duration of inflation. If inflation occurs for more than 60 Hubble times, the production of particles with  $m \ll H$  is much more efficient than was previously anticipated. As I just mentioned, if  $\phi_0$  is large enough then the production of fluctuations of the field  $\chi$  may even lead to a new stage of inflation driven by the field  $\chi$  [47]. On the other hand, if  $m$  is greater than the value of the Hubble constant at the very end of inflation, then quantum fluctuations are produced only at the early stages of inflation (when  $H > m$ ). These fluctuations oscillate and decrease exponentially during the last stages of inflation. In such cases the final number of produced particles will not depend on the duration of inflation and can be unambiguously calculated.

# Chapter 8

## Inflation After Preheating

*Note: This chapter is based on a paper by Gary Felder, Lev Kofman, Andrei Linde, and Igor Tkachev, available on the Los Alamos eprint server as hep-ph/0004024. The full citation appears in the bibliography [87].*

### Chapter Abstract

Preheating after inflation may lead to nonthermal phase transitions with symmetry restoration. These phase transitions may occur even if the total energy density of fluctuations produced during reheating is relatively small as compared with the vacuum energy in the state with restored symmetry. As a result, in some inflationary models one encounters a secondary, *nonthermal* stage of inflation due to symmetry restoration after preheating. Such secondary inflation could also provide a partial solution to the moduli problem. We review the theory of nonthermal phase transitions and make a prediction about the expansion factor during the secondary inflationary stage. We then present the results of lattice simulations that verify these predictions, and discuss possible implications of our results for the theory of formation of topological defects during nonthermal phase transitions.

## 8.1 Introduction

The theory of cosmological phase transitions is usually associated with symmetry restoration due to high temperature effects and the subsequent symmetry breaking that occurs as the temperature decreases in an expanding universe [88, 89, 90, 91, 92, 93, 3]. A particularly important version of this theory is the theory of first order cosmological phase transitions developed in [93]. It served as a basis for the first versions of inflationary cosmology [1, 13, 94], as well as for the theory of electroweak baryogenesis [95, 96].

Recently it was pointed out that preheating after inflation [5, 7] may rapidly produce a large number of particles that for a long time remain in a state out of thermal equilibrium. These particles may lead to specific *nonthermal* cosmological phase transitions [14, 15]. In some cases these phase transitions are first order [16, 97]; they occur by the formation of bubbles of the phase with spontaneously broken symmetry inside the metastable symmetric phase. If the lifetime of the metastable state is large enough for the energy density of fluctuations to be diluted, one may encounter a short secondary stage of inflation *after* preheating [14]. Such a secondary inflation stage, if it occurs late enough, could be important in solving the moduli and gravitino problems. In this respect secondary “nonthermal” inflation due to preheating may be an alternative to the “thermal inflation” [82], suggested for solving these problems.

In this chapter I will briefly present the theory of such phase transitions and then give the results of numerical lattice simulations that directly demonstrated the possibility of such brief inflation. I will also discuss possible implications of these results for the theory of formation of topological defects during nonthermal phase transitions. The lattice calculations reported here were done using the program LATTICEASY, described in part III of this thesis.



## 8.2 Theory of the phase transition

Consider a set of scalar fields with the potential

$$V(\phi, \chi) = \frac{\lambda}{4}(\phi^2 - v^2)^2 + \frac{g^2}{2}\phi^2\chi^2. \quad (8.1)$$

The inflaton field  $\phi$  has a double-well potential and interacts with an  $N$ -component scalar field  $\chi$ ;  $\chi^2 \equiv \sum_{i=1}^N \chi_i^2$ . For simplicity, the field  $\chi$  is taken to be massless and without self-interaction. The fields couple minimally to gravity in a FRW universe with a scale factor  $a(t)$ .

The potential  $V(\phi, \chi)$  has minima at  $\phi = \pm v$ ,  $\chi = 0$  and a local maximum in the  $\phi$  direction at  $\phi = \chi = 0$  with curvature  $V_{,\phi\phi} = -\lambda v^2$ . The effective potential acquires corrections due to quantum and/or thermal fluctuations of the scalar fields [88, 89, 93, 3],

$$\Delta V = \frac{3}{2}\lambda\langle\phi^2\rangle\phi^2 + \frac{g^2}{2}\langle\chi^2\rangle\phi^2 + \frac{g^2}{2}\langle\phi^2\rangle\chi^2 + \dots, \quad (8.2)$$

where I have written only the leading terms depending on  $\phi$  and  $\chi$ . The effective mass squared of the field  $\phi$  is given by

$$m_\phi^2 = -m^2 + 3\lambda\phi^2 + 3\lambda\langle\phi^2\rangle + g^2\langle\chi^2\rangle, \quad (8.3)$$

where  $m^2 = \lambda v^2$ . Symmetry is restored, i.e.  $\phi = 0$  becomes a stable equilibrium point, when the fluctuations  $\langle\phi^2\rangle, \langle\chi^2\rangle$  become sufficiently large to make the effective mass squared positive at  $\phi = 0$ .

For example, one may consider matter in thermal equilibrium. Then, in the large temperature limit, one has  $\langle\phi^2\rangle = \langle\chi_i^2\rangle = \frac{T^2}{12}$ . The effective mass squared of the field  $\phi$

$$m_{\phi,eff}^2 = -m^2 + 3\lambda\phi^2 + 3\lambda\langle\phi^2\rangle + g^2\langle\chi^2\rangle \quad (8.4)$$

is positive and symmetry is restored (i.e.  $\phi = 0$  is the stable equilibrium point) for  $T > T_c$ , where  $T_c^2 = \frac{12m^2}{3\lambda + Ng^2} \gg m^2$ . At this temperature the energy density of the gas

of ultrarelativistic particles is given by

$$\rho = \mathcal{N}(T_c) \frac{\pi^2}{30} T_c^4 = \frac{24 m^4 \mathcal{N}(T_c) \pi^2}{5 (3\lambda + N g^2)^2} . \quad (8.5)$$

Here  $\mathcal{N}(T)$  is the effective number of degrees of freedom at large temperature, which in realistic situations may vary from  $10^2$  to  $10^3$ . We will assume that  $N g^2 \gg \lambda$ , see below. For  $g^4 < \frac{96 \mathcal{N}(T_c) \pi^2}{5 N^2} \lambda$  the thermal energy at the moment of the phase transition is greater than the vacuum energy density  $V(0) = \frac{m^4}{4\lambda}$ , which means that the phase transition does not involve a stage of inflation.

In fact, the phase transition with symmetry breaking occurs not at  $T > T_c$ , but somewhat earlier [93]. To understand this effect let us compare the temperature  $T_c \sim m/(\sqrt{N}g)$  and the mass  $m_\chi = g\phi$  of the  $\chi$  particles in the minimum of the zero-temperature effective potential at  $\phi = v = m/\sqrt{\lambda}$ . One can easily see that  $m_\chi \gg T_c$  for  $N g^4 \gg \lambda$ . This means that for  $N g^4 \gg \lambda$  the temperature  $T_c$  is insufficient to excite perturbations of the fields  $\chi_i$  at  $\phi = v$ . As a result, these perturbations do not change the shape of the effective potential  $\phi = v$ . Thus the potential at  $T$  slightly above  $T_c$  has its old zero-temperature minimum at  $\phi = v$ , as well as the temperature-induced minimum at  $\phi = 0$ . Symmetry breaking occurs as a first-order phase transition due to formation of bubbles of the phase with  $\phi \approx v$  at some temperature above  $T_c$  when the minimum at  $\phi = v$  becomes deeper than the minimum at  $\phi = 0$ , and the probability of bubble formation becomes sufficiently large. A more detailed investigation in the case  $N = 1$  shows that the phase transition is first order under a weaker condition  $g^3 \gg \lambda$  [93].

In the case  $N g^4 > 10^2 \lambda$  the phase transition occurs after a secondary stage of inflation. In this regime radiative corrections are important. They lead to the creation of a local minimum of  $V(\phi, \chi)$  at  $\phi = 0$  even at zero temperature, and the phase transition occurs from a strongly supercooled state [93]. That is why the first models of inflation required supercooling at the moment of the phase transition [1, 13, 94].

In supersymmetric theories one may have  $N g^4 \gg 10^2 \lambda$  and still have a potential that is flat near the origin due to cancellation of quantum corrections of bosons and fermions [82]. In such cases the thermal energy becomes smaller than the vacuum

energy at  $T < T_0$ , where  $T_0^4 = \frac{15}{2N\pi^2}m^2v^2$ . Then one may have a short stage of inflation that begins at  $T \sim T_0$  and ends at  $T = T_c$ . During this time the universe may inflate by the factor

$$\frac{a_c}{a_0} = \frac{T_0}{T_c} \sim 10^{-1} \left( \frac{g^4}{\lambda} \right)^{1/4}. \quad (8.6)$$

Similar phase transitions may occur much more efficiently prior to thermalization, due to the anomalously large fluctuations  $\langle \phi^2 \rangle$  and  $\langle \chi^2 \rangle$  produced during preheating [14, 15]. These fluctuations can change the shape of the effective potential and lead to symmetry restoration. Afterwards, the universe expands, the values of  $\langle \phi^2 \rangle$  and  $\langle \chi^2 \rangle$  drop down, and the phase transition with symmetry breaking occurs.

An interesting feature of nonthermal phase transitions is that they may occur even in theories where the usual thermal phase transitions do not happen. The main reason can be understood as follows. Suppose reheating occurs due to the decay of a scalar field with energy density  $\rho$ . If this energy is instantly thermalized, then one obtains relativistic particles with energy density  $O(T^4)$  that in the first approximation can be represented as  $\rho \approx E^2(\langle \phi^2 \rangle + \langle \chi^2 \rangle)$ . Here  $E \sim T \sim \rho^{1/4}$  is a typical energy of a particle in thermal equilibrium. After preheating, however, one has particles  $\phi$  and  $\chi$  with much smaller energy but large occupation numbers. As a result, the same energy release may create much greater values of  $\langle \phi^2 \rangle$  and  $\langle \chi^2 \rangle$  than in the case of instant thermalization. This may lead to symmetry restoration after preheating even if the symmetry breaking occurs on the GUT scale,  $v \sim 10^{16}$  GeV [14, 15].

The main conclusions of [14, 15] have been confirmed by detailed investigation using lattice simulations in [16, 17, 98, 97]. One of the main results obtained in [16] was that for sufficiently large  $g^2$  nonthermal phase transitions are first order. They occur from a metastable vacuum at  $\phi = 0$  due to the creation of bubbles with  $\phi \neq 0$ . This result is very similar to the analogous result in the theory of thermal phase transitions [93]. According to [16], the necessary conditions for this transition to occur and to be of the first order can be formulated as follows:

(i) At the time of the phase transition, the point  $\phi = 0$  should be a local minimum of the effective potential. From (8.3), we see that this means that  $Ng^2\langle \chi_i^2 \rangle > \lambda v^2$ .

(ii) At the same time, the typical momentum  $p_*$  of  $\chi_i$  particles should be smaller

than  $gv$ . This is the condition of the existence of a potential barrier. Particles with momenta  $p < gv$  cannot penetrate the state with  $|\phi| \approx v$ , so they cannot change the shape of the effective potential at  $|\phi| \approx v$ . Therefore, if both conditions (i) and (ii) are satisfied, the effective potential has a local minimum at  $\phi = 0$  and two degenerate minima at  $\phi \approx \pm v$ .

(iii) Before the minima at  $\phi \approx \pm v$  become deeper than the minimum at  $\phi = 0$ , the inflaton's zero mode should decay significantly, so that it performs small oscillations near  $\phi = 0$ . Then, after the minimum at  $|\phi| \approx v$  becomes deeper than the minimum at  $\phi = 0$ , fluctuations of  $\phi$  drive the system over the potential barrier, creating an expanding bubble.

The investigation performed in [16] confirmed that for sufficiently large  $g^2$  and  $N$  these conditions are indeed satisfied and the phase transition is first order. One may wonder whether for  $g^2 \gg \lambda$  one may have a stage of inflation in the metastable vacuum  $\phi = 0$ .

Analytical estimates of Ref. [14] suggested that this is indeed the case, and the degree of this inflation for  $N = 1$  is expected to be

$$\frac{a_c}{a_0} \sim \left(\frac{g^2}{\lambda}\right)^{1/4}, \quad (8.7)$$

which is much greater than the number  $10^{-1} \left(\frac{g^4}{\lambda}\right)^{1/4}$  in the thermal inflation scenario. One could also expect that the duration of inflation, just like the strength of the phase transition, increases if one considers  $N$  fields  $\chi_i$  with  $N \gg 1$ .

However, the theory of preheating is extremely complicated, and there are some factors that could not be adequately taken into account in the simple estimates of [14]. The most important factor is the effect of rescattering of particles produced during preheating [99, 100]. This effect tends to shut down the resonant production of particles and thus shorten or prevent entirely the occurrence of a secondary stage of inflation. Thus the estimates above reflect the maximum degree of inflation possible for a given set of parameter values, but in practice the expansion factor will be somewhat smaller than these predictions. The only way to fully account for all the effects of backreaction and expansion is through numerical lattice simulations. In the

next section I will describe the basic features of our method and describe our main results.

### 8.3 Simulation Results and Their Interpretation

I take  $\lambda \approx 10^{-13}$ , which gives the proper magnitude of inflationary perturbations of density [3, 101]. I assume that  $g^2 \gg \lambda$ , and consider  $v \approx 10^{16}$  GeV, which corresponds to the GUT scale. A numerical investigation of preheating in the model (8.1) was first performed in [16]. The authors found a strongly first order phase transition. The strength of the phase transition increased with an increase of  $g^2/\lambda$  and of the number  $N$  of the fields  $\chi_i$ . However, for the parameters of the model studied in [16] ( $g^2/\lambda \approx 200$ ) there was no inflation during symmetry restoration. This is not unexpected because the estimates discussed above indicated that the expansion of the universe during the short stage of nonthermal inflation cannot be greater than  $(\frac{g^2}{\lambda})^{1/4}$ .

Keeping in mind that  $\lambda$  in this model is extremely small, one would expect that in realistic versions of this model one may have  $g^2/\lambda$  as large as  $10^{10}$ , which could lead to a relatively long stage of inflation. However, for very large  $g^2/\lambda$  our analytical estimates are unreliable, and lattice simulations become extremely difficult: One needs to have enormously large lattices to keep both infrared and ultraviolet effects under control.

To mimic the effects of large  $g^2$ , we considered a large number of the fields  $\chi_i$ . We performed simulations for  $g^2/\lambda = 800$  and  $N = 19$ . With these parameters the strength of the phase transition became much greater, and there was a short stage of inflation prior to the phase transition.

The details of our lattice calculations can be found in part III. Here I present only our main results for this model. These results were obtained using a grid of  $128^3$  points and a grid spacing of  $dx = .133 \frac{1}{\sqrt{\lambda\phi_0}}$  where  $\phi_0 = .342M_p$  is the value of the inflaton field at the end of inflation, and hence at the beginning of our simulation. These parameters correspond to a total box size roughly equal to 10 Hubble radii at the end of inflation.

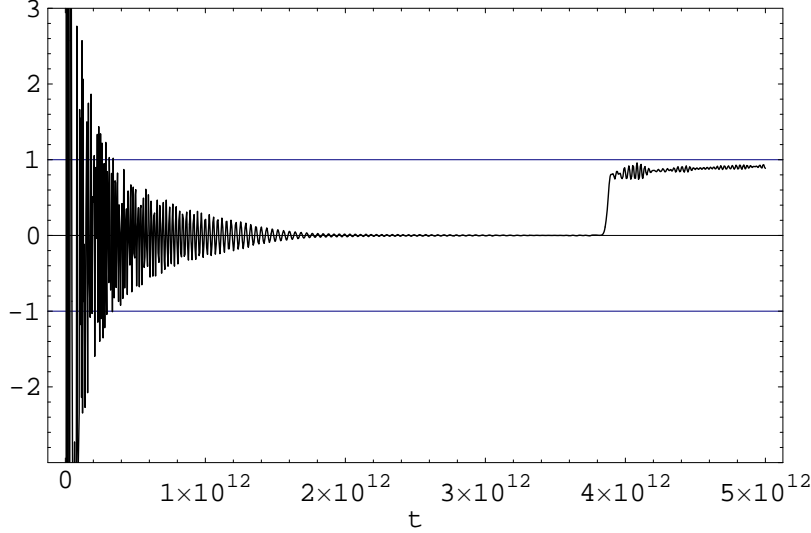


Figure 8.1: The spatial average of the inflation field  $\phi$  as a function of time. The field  $\phi$  is shown in units of  $v$ , the symmetry breaking parameter. Time is shown in Planck units.

The simulation showed that the oscillations of the inflaton field decreased until the field was trapped near zero. It remained there until the moment of the phase transition when it rapidly jumped to its symmetry breaking value, as shown in Fig. 8.1.

The trapping of the field occurred because of the corrections to the effective potential induced by the particles  $\phi$  and  $\chi$  produced during preheating, just like in the theory of high-temperature phase transitions. In this case, however, this effect has some unusual features.

To first order in  $g^2$ , the leading contribution to the equation of motion  $\ddot{\phi} = -V'$  is given by  $g^2\phi\langle\chi^2\rangle$ , where

$$\langle\chi^2\rangle \approx \frac{N}{2\pi^2} \int_0^\infty \frac{n_k k^2 dk}{\omega_k(\phi)}. \quad (8.8)$$

Here  $\omega_k = \sqrt{k^2 + g^2(\phi^2 + \langle\phi^2\rangle)}$  is the energy of  $\chi_i$  particles with momentum  $k$  and  $n_k$  is their occupation number;  $\phi$  is the homogeneous component of the field. For

$\phi \ll \sqrt{\langle \phi^2 \rangle}$ , one has

$$\langle \chi^2 \rangle_{\phi=0} \approx \frac{N}{2\pi^2} \int_0^\infty \frac{n_k k^2 dk}{\sqrt{k^2 + g^2 \langle \phi^2 \rangle}}. \quad (8.9)$$

This quantity does not depend on  $\phi$ ; it can be evaluated using our lattice simulations when the field  $\phi$  oscillates near  $\phi = 0$ . It leads to the usual quadratic correction to the effective potential, see Eq. (8.2). This correction adequately describes the change of the shape of the effective potential for  $\phi$  smaller than the amplitude of the oscillations of this field, because most of the time prior to the moment of the phase transition this amplitude is much smaller than  $\sqrt{\langle \phi^2 \rangle}$ .

However, if we want to evaluate the effective potential at all values of  $|\phi|$  from 0 to  $v$ , rather than for  $\phi$  similar to the amplitude of the oscillations, then one should take into account that for sufficiently large  $|\phi|$  the term  $g|\phi|$  becomes greater than  $g\sqrt{\langle \phi^2 \rangle}$  and than the typical momentum  $k$  of particles  $\chi_i$ . In this case the main contribution to  $\langle \chi^2 \rangle$  is given by nonrelativistic particles with  $\omega_k \approx +g|\phi|$ , and one has

$$\langle \chi^2 \rangle \approx \frac{N}{2\pi^2} \int_0^\infty \frac{n_k k^2 dk}{g|\phi|} = \frac{n_\chi}{g|\phi|}, \quad (8.10)$$

where  $n_\chi$  is the total density of all types of  $\chi_i$  particles. This implies that at large  $|\phi|$  the effective potential acquires a correction

$$\delta V \approx g|\phi|n_\chi. \quad (8.11)$$

Thus, instead of being quadratic or cubic in  $|\phi|$ , as one could expect from the analogy with the high-temperature theory [93, 97], the corrections to the effective potential at large  $|\phi|$  are proportional to  $|\phi|$  [5, 7].

The combination of these two types of corrections to the effective potential (quadratic at small  $|\phi|$  and linear at large  $|\phi|$ ) leads to the symmetry restoration that we have found in our lattice simulations.

It is instructive to look in a more detailed way at the small region near the time of the phase transition. The first of the graphs in Fig. 8.2 shows the oscillations of the field  $\phi$  soon before the phase transition, whereas the second one shows these

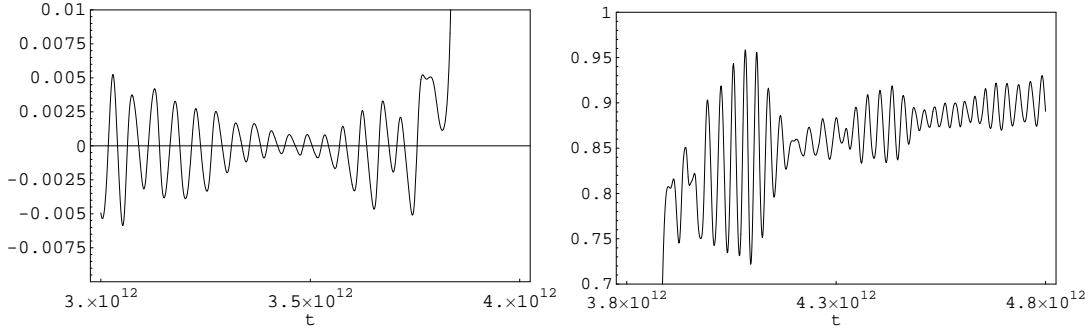


Figure 8.2: The spatial average of the inflation field  $\phi$  as a function of time in the vicinity of the phase transition. The left figure shows the field just before the phase transition and at the moment of the transition. The field oscillates with an amplitude approaching  $10^{-3}v$ . The right figure shows the field  $\phi$  after the phase transition, when it oscillates near the (time-dependent) position of the minimum of the effective potential at  $\phi \approx v$ . Time is shown in Planck units.

oscillations soon afterwards.

First of all, one can see that just before the phase transition the field oscillates with an amplitude three orders of magnitude smaller than  $v$ , which is a clear sign of symmetry restoration. Another interesting feature is that the frequency of oscillations does not vanish as we approach the phase transition, but remains nearly constant. Moreover, this frequency is only about two times smaller than the frequency of oscillations after the phase transition, which is equal to  $\sqrt{2}m$ . Note that the frequency of the oscillations is determined by the effective mass of the scalar field, which is given by the curvature of the effective potential:  $m_\phi^2 = V''$ . This means that at the moment of the phase transition the effective potential has a deep minimum at  $\phi = 0$  with curvature  $V'' \sim +m^2$ , i.e. the phase transition is strongly first order. Such phase transitions should occur due to the formation of bubbles containing nonvanishing field  $\phi$ .

Indeed, we found that this transition occurred in a nearly spherical region of the lattice that quickly grew to encompass the entire space. The growth of this region of the new phase is shown in Fig. 8.3. The nearly perfect sphericity of this region is an additional indication that the transition was strongly first-order. In comparison,



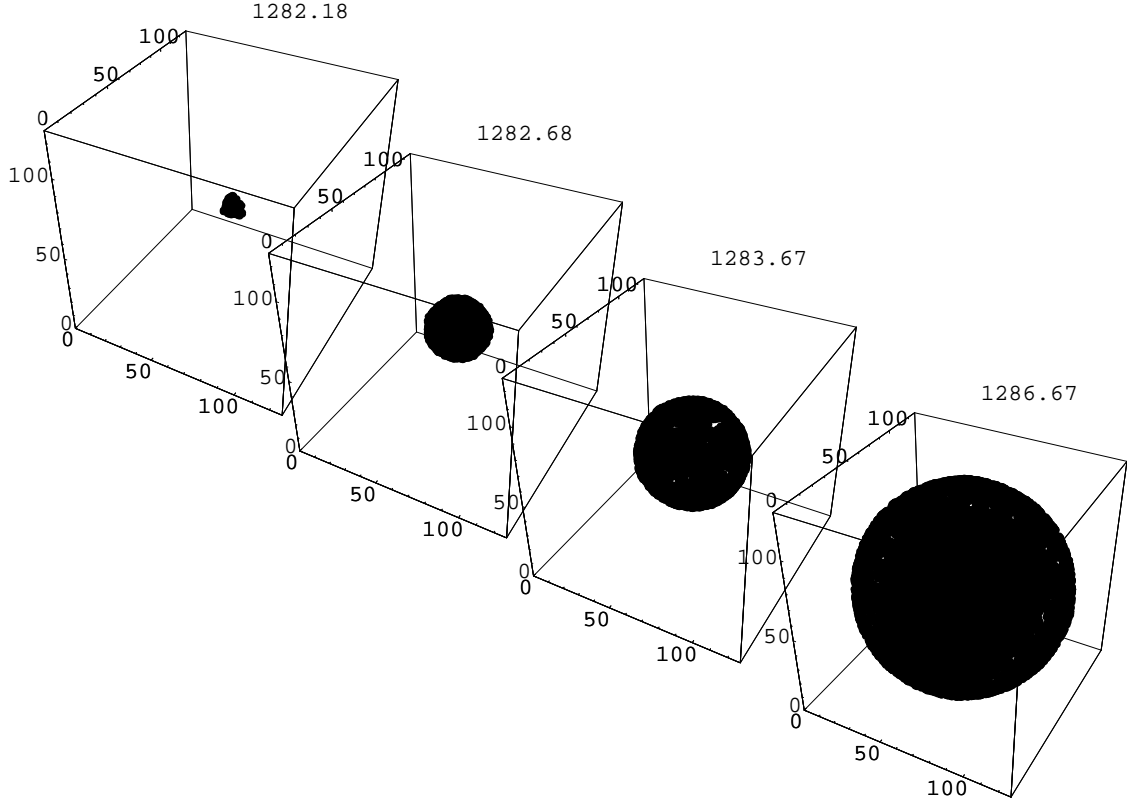


Figure 8.3: These plots show the region of space in which symmetry breaking has occurred at four successive times.

the bubble observed in the lattice simulations of [16] for  $g^2/\lambda \approx 200$  was not exactly spherically symmetric.

The first order phase transition and bubble formation seen in our simulations can be understood as a result of gradual accumulation of classical fluctuations  $\delta\phi(t, \vec{x})$ . These fluctuations stochastically climb up from  $\phi = 0$  towards the local maximum  $\phi_*$  of the effective potential. Consider the regions in which  $\delta\phi(t, \vec{x}) > \phi_*$ . If the probability of formation of such regions is small because they correspond to high peaks of the random field  $\phi$ , then these regions will have a nearly spherical shape and can be represented by spherical surfaces of radius  $R_*$  (bubbles). If the radius  $R_*$  is small, gradient terms will prevent the field  $\phi$  inside the region from rolling down towards the global minimum at  $\phi = v$  (subcritical bubble). If  $R_*$  is large enough,

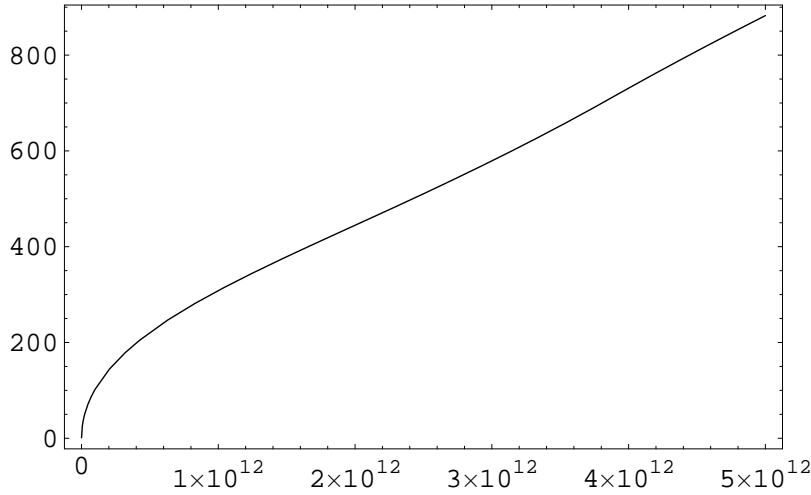


Figure 8.4: The scale factor  $a$  as a function of time. In the beginning  $a \sim \sqrt{t}$ , which is a curve with negative curvature, but then at some stage it begins to turn upwards, indicating a short stage of inflation.

the gradient terms cannot push the field back to the metastable state  $\phi = 0$  and the field inside the bubble rolls towards the global minimum, forming a bubble of ever increasing radius. This process can be described within the stochastic approach to tunneling proposed in [102]. Typically, the gradient terms cannot win over the potential energy terms if  $R_* > O(|m_\phi^{-1}|)$ , where  $m_\phi$  corresponds to the effective mass of the scalar field in the interior of the bubble. This provides an estimate for the initial size of the bubble  $R_* \sim O(|m_\phi^{-1}|)$ .

The phase transition occurs from a state with energy density dominated by the vacuum energy density  $V(0)$ . Figure 8.4 shows the scale factor  $a$  as a function of time. The curvature becomes slightly positive at the time before the phase transition, which indicates a short stage of exponential growth of the universe. Because the curvature is hard to see in figure 8.4 I have also plotted the second derivative  $\ddot{a}$  in figure 8.5. While the inflaton is trapped in the false vacuum state,  $\ddot{a}$  becomes positive, indicating a brief stage of inflation.

Another signature of inflation is an equation of state with negative pressure. Figure 8.6 shows the parameter  $\alpha = p/\rho$ , which becomes negative during the metastable phase. At the moment of the phase transition the universe becomes matter dominated

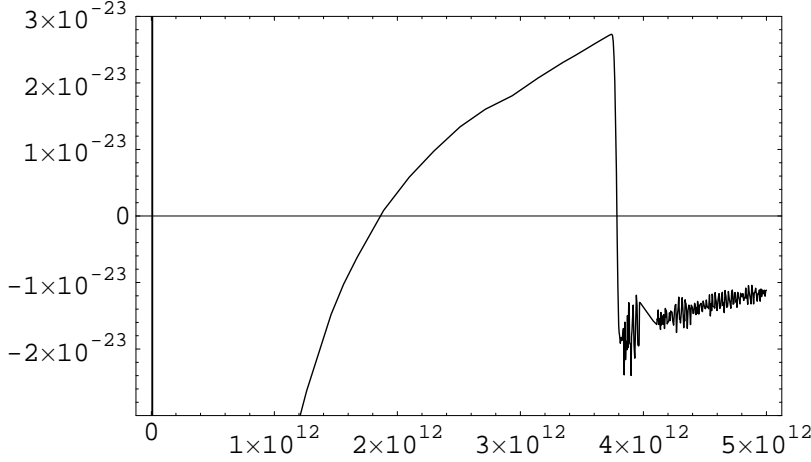


Figure 8.5: The second derivative of the scale factor,  $\ddot{a}$ . A universe dominated by ordinary matter (relativistic or nonrelativistic) will always have  $\ddot{a} < 0$ , whereas in an inflationary universe  $\ddot{a} > 0$ . We see that starting from the moment  $t \sim 2 \times 10^{12}$  (in Planck units) the universe experiences accelerated (inflationary) expansion.

and the pressure jumps to nearly 0.

From the beginning of this inflationary stage (roughly when the pressure becomes negative) to the moment of the phase transition the total expansion factor is 2.1. As expected this is of the same order but somewhat lower than the predicted maximum,  $\left(\frac{q^2}{\lambda}\right)^{1/4} \approx 5.3$ . We can thus conclude that it is possible to achieve inflation for parameters for which this would not have been possible in thermal equilibrium ( $g^4 \ll \lambda$ ). In our simulation we showed the occurrence of a very brief stage of inflation. This stage may be much longer for larger (realistic) values of  $g^2/\lambda$ . However, to check whether this is indeed the case one would need to perform a more detailed investigation on a lattice of a much greater size.

## 8.4 Nonthermal phase transitions and production of topological defects

In this section I would like to discuss possible implications of our investigation for the theory of production of topological defects after preheating [16, 17, 98].

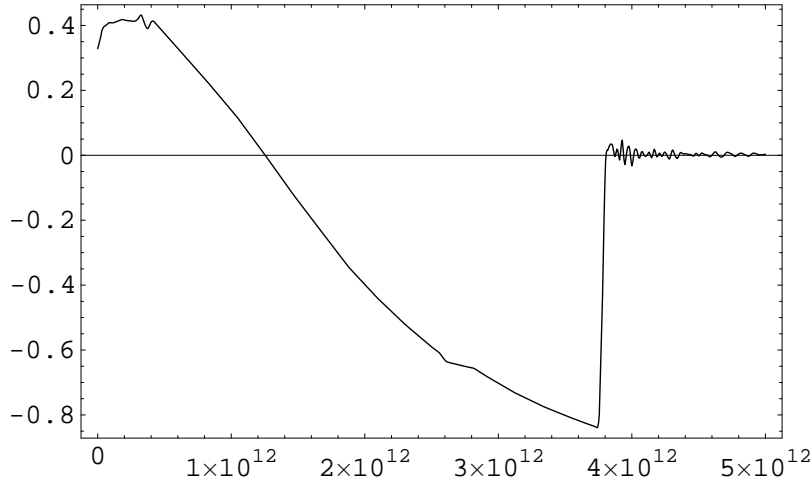


Figure 8.6: The ratio of pressure to energy density  $p/\rho$ . (Values were time averaged over short time scales to make the plot smoother and more readable.)

The bubbles that appear after the phase transition can contain either positive or negative field,  $\phi = \pm v$ . If bubbles of either type are formed with comparable probability, then after the phase transition the universe becomes divided into nearly equal numbers of domains with  $\phi = \pm v$ , separated by domain walls. Such domain walls would lead to disastrous cosmological consequences, which would rule out the models where this may happen [14, 15].

In general, the number of bubbles with  $\phi = +v$  may be much greater (or much smaller) than the number of bubbles with  $\phi = -v$ . Then the domain wall problem does not appear because the bubbles with  $\phi = +v$  would rapidly eat all their competitors with  $\phi = -v$  (or *vice versa*). This may happen, for example, if the moment of the bubble production is determined by the coherently oscillating scalar field  $\phi$ . In such a case, after oscillating a bit near the top of the effective potential, the field  $\phi$  may wind up in the same minimum of the effective potential everywhere in the universe.

To investigate the domain wall problem in our model one would need to repeat the calculation many times with slightly different initial conditions or to make them in a box of a much greater size that would allow one to see many bubbles simultaneously. Fortunately, the results obtained in our study may be sufficient to give an answer to

this question without extremely large simulations.

First of all, according to the stochastic approach [102] to the theory of tunneling with bubble formation [103, 104], the bubbles of the field  $\phi$  are created as a result of the accumulation of long-wavelength fluctuations of the scalar field with momenta  $k$  smaller than the typical mass scale  $m_\phi$  associated with this field, see Section 8.3. In our case this mass scale is related to the frequency of oscillations of the scalar field at the moment of the phase transition. At that moment the leading contribution to the fluctuations  $\langle\phi^2\rangle$  is given by fluctuations with momenta much smaller than  $m_\phi$ . We calculated the value of the long-wavelength component of  $\sqrt{\langle\phi^2\rangle}$  and found that it is (approximately) of the same order as the amplitude of oscillations of the field  $\phi$  at the moment of the phase transition. The existence of a first-order phase transition suggests that the probability of bubble formation must have been exponentially suppressed during the metastable stage. Such suppression would only occur only if the amplitude of fluctuations required to form a bubble of the new phase was much larger than  $\sqrt{\langle\phi^2\rangle}$  [102], which would in turn mean the required amplitude was much greater than the amplitude of oscillations of  $\phi$ . This suggests that the probability of the bubble formation is almost entirely determined by the incoherent fluctuations of the field  $\phi$  rather than by the small coherent oscillations of this field. Consequently, the probability of formation of bubbles containing  $\phi = +v$  in the first approximation must be equal to the probability of formation of bubbles containing  $\phi = -v$ .

To make this statement more reliable one would need to estimate the amplitude of the long-wavelength fluctuations of the field  $\phi$  in a more precise way, which would involve using lattices of a greater size. However, there is additional evidence suggesting that the number of bubbles with positive and negative  $\phi$  must be approximately equal to each other.

Indeed, as we have seen, the curvature of the effective potential remained approximately constant during dozens of oscillations of the field  $\phi$  prior to the moment of the phase transition. This suggests that the shape of the effective potential and, consequently, the probability of the tunneling, did not change much during a single oscillation. Therefore one may expect that, within a single oscillation, the probability of a bubble forming when the oscillating field  $\phi$  was negative was approximately the

same as the probability of the bubble forming when it was positive.

If the number of bubbles with positive and negative  $\phi$  are approximately equal to each other, the phase transition leads to the formation of dangerous domain walls, which rules out our model [105]. If correct, this is a rather important conclusion that shows that the investigation of nonthermal phase transition may rule out certain classes of inflationary models that otherwise would seem quite legitimate [14, 15].

But this conclusion does not imply that *all* theories where the nonthermal phase transition is strongly first order are ruled out. For example, one may consider a model (8.1) with  $\phi$  being not a real but a complex field,  $\phi = \frac{1}{\sqrt{2}}(\phi_1 + i\phi_2)$ ,  $|\phi|^2 = \frac{1}{2}(\phi_1^2 + \phi_2^2)$ . Since the main contribution to the effective potential of the field  $\phi$  in the theory (8.1) is given not by the field(s)  $\phi$  but by the fields  $\chi_i$ , we expect that this generalization will not lead to a qualitative modification of our results. In particular, we expect that for sufficiently large  $N$  and  $g^2/\lambda$  the phase transition will be strongly first order and there will be a short stage of inflation after preheating. However, in the new model we will have strings instead of domain walls.

A similar model in the absence of interaction of the fields  $\phi$  with the fields  $\chi$  was studied in [17, 98]. It was argued that even in this case infinite strings may be formed. The theory of galaxy formation due to cosmic strings is currently out of favor, but it is certainly true that cosmic strings produced after inflation may add new interesting features to the standard theory of formation of the large-scale structure of the universe [106, 107, 108, 109]

The possibility of strongly first order phase transitions induced by preheating in models with  $g^2 \gg \lambda$  adds new evidence that infinite strings can be produced after nonthermal phase transitions. Indeed, infinite strings may not be produced if the direction in which the field  $\phi$  falls from the point  $\phi = 0$  at the moment of the phase transition is determined by the oscillations of the field  $\phi$ . If, just as in the case discussed above, the amplitude of these oscillations are much smaller than  $\sqrt{\langle \phi^2 \rangle}$  at the moment of the phase transition, then infinite strings are indeed formed.

## 8.5 Conclusions

The results of our lattice simulation confirmed our expectations that preheating may lead to nonthermal phase transitions even in those theories where spontaneous symmetry breaking occurs at the GUT scale,  $v \sim 10^{16}$  GeV. Some time ago this question was intensely debated in the literature. Some authors claimed that nonthermal phase transitions induced by preheating are impossible, and the notion of the effective potential after preheating is useless. I believe that Figs. 1, 2 and 3 give a clear answer to this question. In particular, Fig. 1 shows that 90% of the time from the end of inflation to the moment of symmetry breaking the field  $\phi$  oscillates about  $\phi = 0$  with an amplitude much smaller than  $v$ . This could happen only because the corrections to the effective potential induced by particles  $\phi$  and  $\chi$  change the shape of  $V(\phi)$  near  $\phi = 0$ , turning its maximum into a deep local minimum.

In some theories, this effect may lead to production of superheavy strings, which may have important cosmological implications for the theory of formation of the large scale structure of the universe. In some other theories, these phase transitions may lead to excessive production of monopoles and domain walls. This may rule out a broad class of otherwise acceptable inflationary models.

In this paper we have shown that under certain conditions a nonthermal phase transition may lead to a short secondary stage of inflation. It would be interesting to study the possibility that a secondary stage of inflation induced by preheating could help solve the moduli and gravitino problems. The answer to this question will be strongly model-dependent because gravitinos can be produced by the oscillating scalar field even after the secondary inflation [61, 80]. Independently of all practical implications, the possibility of a secondary stage of inflation induced by preheating seems very interesting because it clearly demonstrates the potential importance of nonperturbative effects in post-inflationary cosmology.

# Chapter 9

## The Development of Equilibrium After Preheating

*Note: This chapter is based on a paper by Gary Felder and Lev Kofman, available on the Los Alamos eprint server as hep-ph/0011160. The full citation appears in the bibliography [110].*

### Chapter Abstract

In this chapter I present the results of a fully nonlinear study of the development of equilibrium after preheating. The rapid transfer of energy from the inflaton to other fields during preheating leaves these fields in a highly nonthermal state with energy concentrated in infrared modes. We performed lattice simulations of the evolution of interacting scalar fields during and after preheating for a variety of inflationary models. We formulated a set of generic rules that govern the thermalization process in all of these models. Notably, we found that once one of the fields is amplified through parametric resonance or other mechanisms it rapidly excites other coupled fields to exponentially large occupation numbers. These fields quickly acquire nearly thermal spectra in the infrared, which gradually propagate into higher momenta. Prior to the formation of total equilibrium, the excited fields group into subsets with almost identical characteristics (e.g. group effective temperature). The way fields



form into these groups and the properties of the groups depend on the couplings between them. We also studied the onset of chaos after preheating by calculating the Lyapunov exponent of the scalar fields.

## 9.1 Introduction

Reheating typically involves some form of rapid, non-perturbative preheating phase. The character of preheating may vary from model to model, e.g. parametric excitation in chaotic inflation [7] or tachyonic preheating in hybrid inflation (see chapter 10), but its distinct feature remains the same: rapid amplification of one or more bosonic fields to exponentially large occupation numbers. This amplification is eventually shut down by backreaction of the produced fluctuations. The end result of the process is a turbulent medium of coupled, inhomogeneous, classical waves far from equilibrium [99].

Despite the development of our understanding of preheating after inflation, the transition from this stage to a hot Friedmann universe in thermal equilibrium has remained relatively poorly understood. A theory of the thermalization of the fields generated from preheating is necessary to bridge the gap between inflation and the Hot Big Bang. The details of this thermalization stage depend on the constituents of the fundamental Lagrangian  $\mathcal{L}(\phi_i, \chi_i, \psi_i, A_\mu, h_{\mu\nu}, \dots)$  and their couplings, so at first glance it would seem that a description of this process would have to be strongly model-dependent. We found, however, that many features of this stage seem to hold generically across a wide spectrum of models. This fact is understandable because the conditions at the end of preheating are generally not qualitatively sensitive to the details of inflation. Indeed, at the end of preheating and beginning of the turbulent stage (denoted by  $t_*$ ), the fields are out of equilibrium. We examined many models and found that at  $t_*$  there is not much trace of the linear stage of preheating and conditions at  $t_*$  are not qualitatively sensitive to the details of inflation. We therefore found that this second, highly nonlinear, turbulent stage of preheating seemed to exhibit some universal, model-independent features.

Although a realistic model would include one or more Higgs-Yang-Mills sectors,

we treated the simpler case of interacting scalars. Within this context, however, we considered a number of different models including several chaotic and hybrid inflation scenarios with a variety of couplings between the inflaton and other matter fields.

There are many questions about the thermalization process that we set out to answer in our work. Could the turbulent waves that arise after preheating be described by the theory of (transient) Kolmogorov turbulence or would they directly approach thermal equilibrium? Could the relaxation time towards equilibrium be described by the naive estimate  $\tau \sim (n\sigma_{int})^{-1}$ , where  $n$  is a density of scalar particles and  $\sigma_{int}$  is a cross-section of their interaction? If the inflaton  $\phi$  were decaying into a field  $\chi$ , what effect would the presence of a decay channel  $\sigma$  for the  $\chi$  field have on the thermalization process? For that matter, would the presence of  $\sigma$  significantly alter the preheating of  $\chi$  itself, or even destroy it as suggested in [111]? How strongly model-dependent is the process of thermalization; are there any universal features across different models? Finally there's the question of chaos. It is known that Higgs-Yang-Mills systems display chaotic dynamics during thermalization [112]. The possibility of chaos in the case of a single, self-interacting inflaton was mentioned in passing in [99], but when we began our work it was unclear at what stage of preheating chaos might appear, and in what way.

Because the systems we studied involve strong, nonlinear interactions far from thermal equilibrium it is not possible to solve the equations of motion using linear analysis in Fourier space. Instead we solved the scalar field equations of motion directly in position space using lattice simulations. These simulations automatically take into account all nonlinear effects of scattering and backreaction. Using these numerical results we were able to formulate a set of empirical rules that seem to govern thermalization after inflation. These rules qualitatively describe thermalization in a wide variety of models. The features of this process are in some cases very different from our initial expectations.

Sections 9.2 and 9.3 describe the results of our numerical calculations. Section 9.2 describes one simple chaotic inflation model that we chose to focus on as a clear illustration of our results, while section 9.3 discusses how the thermalization process occurs in a variety of other models. Section 9.4 describes the onset of chaos during

preheating and includes a discussion of the measurement and interpretation of the Lyapunov exponent in this context. Section 9.5 contains a list of empirical rules that we formulated to describe thermalization after preheating. Section 9.6 discusses these results and other aspects of non-equilibrium scalar field dynamics.

## 9.2 Calculations in Chaotic Inflation

In this section I present the results of our numerical lattice simulations of the dynamics of interacting scalars after inflation. I discuss in detail one simple model that illustrates the general properties of thermalization after preheating. The next section will discuss thermalization in the context of other models.

### 9.2.1 Model

The example I have chosen to focus on is chaotic inflation with a quartic inflaton potential. The inflaton  $\phi$  has a four-legs coupling to another scalar field  $\chi$ , which in turn can couple to one or more other scalars  $\sigma_i$ . The potential for this model is

$$V = \frac{1}{4}\lambda\phi^4 + \frac{1}{2}g^2\phi^2\chi^2 + \frac{1}{2}h_i^2\chi^2\sigma_i^2. \quad (9.1)$$

The equations of motion for the model (9.1) are given by

$$\ddot{\phi} + 3\frac{\dot{a}}{a}\dot{\phi} - \frac{1}{a^2}\nabla^2\phi + \left(\lambda\phi^2 + g^2\chi^2\right)\phi = 0 \quad (9.2)$$

$$\ddot{\chi} + 3\frac{\dot{a}}{a}\dot{\chi} - \frac{1}{a^2}\nabla^2\chi + \left(g^2\phi^2 + h_i^2\sigma_i^2\right)\chi = 0 \quad (9.3)$$

$$\ddot{\sigma}_i + 3\frac{\dot{a}}{a}\dot{\sigma}_i - \frac{1}{a^2}\nabla^2\sigma_i + \left(h_i^2\chi^2\right)\sigma_i = 0. \quad (9.4)$$

We also included self-consistently the evolution of the scale factor  $a(t)$ . The model described by these equations is a conformal theory, meaning that the expansion of the universe can be (almost) eliminated from the equations of motion by an appropriate choice of variables [8].

A detailed explanation of our lattice simulations is in part III of this thesis. For the chaotic inflation potential described in this section we rescaled the variables from Planck units in the following ways

$$f_{pr} = \frac{a}{\phi_0} f; \quad \vec{x}_{pr} = \sqrt{\lambda} \phi_0 \vec{x}; \quad dt_{pr} = \sqrt{\lambda} \phi_0 \frac{dt}{a}, \quad (9.5)$$

where the subscript *pr* (for “program”) indicates the variables used in our calculations. The variable  $\phi_0 = .342 M_p$  is the initial value of  $\phi$  in the simulations. All plots in this chapter are shown in these program variables.

Preheating in this theory in the absence of the  $\sigma_i$  fields was described in [8]. For  $g^2 \gtrsim \lambda$  the field  $\chi$  will experience parametric amplification, rapidly rising to exponentially large occupation numbers. In the absence of the  $\chi$  field (or for sufficiently small  $g$ )  $\phi$  will be resonantly amplified through its own self-interaction, but this self-amplification is much less efficient than the two-field interaction. The results shown here are for  $\lambda = 9 \times 10^{-14}$  (for COBE normalization) and  $g^2 = 200\lambda$ . When I add a third field I take  $h_1^2 = 100g^2$  and when I add a fourth field I take  $h_2^2 = 200g^2$ .

### 9.2.2 The Output Variables

There are a number of ways to illustrate the behavior of scalar fields, and different ones are useful for exploring different phenomena. The raw data is the value of the field  $f(t, \vec{x})$ , or equivalently its Fourier transform  $f_k(t)$ . One of the simplest quantities one can extract from these values is the variance

$$\langle (f(t) - \bar{f}(t))^2 \rangle = \frac{1}{(2\pi)^3} \int d^3k |f_k(t)|^2, \quad (9.6)$$

where the integral does not include the contribution of a possible delta function at  $\vec{k} = 0$ , representing the mean value  $\bar{f}$ .

One of the most interesting variables to calculate is the (comoving) number density of particles of the  $f$ -field

$$n_f(t) \equiv \frac{1}{(2\pi)^3} \int d^3k n_k(t), \quad (9.7)$$

where  $n_k$  is the (comoving) occupation number of particles

$$n_k(t) \equiv \frac{1}{2\omega_k} |\dot{f}_k|^2 + \frac{\omega_k}{2} |f_k|^2 \quad (9.8)$$

$$\omega_k \equiv \sqrt{k^2 + m_{eff}^2} \quad (9.9)$$

$$m_{eff}^2 \equiv \frac{\partial^2 V}{\partial f^2} . \quad (9.10)$$

For the model (9.1) this effective mass is given by

$$m_{eff}^2 = \begin{cases} 3\lambda\langle\phi^2\rangle + g^2\langle\chi^2\rangle \\ g^2\langle\phi^2\rangle + h_i^2\langle\sigma_i^2\rangle \\ h_i^2\langle\chi^2\rangle \end{cases} \quad (9.11)$$

for  $\phi$ ,  $\chi$ , and  $\sigma_i$  respectively. For the classical waves of  $f$  that we are dealing with,  $n_k$  corresponds to an adiabatic invariant of the waves. Formula (9.8) can be interpreted as a particle occupation number in the limit of large amplitude of the  $f$ -field. As we will see below this occupation number spectrum contains important information about thermalization. Notice that the effective mass of the particles depends on the variances of the fields and may be significant and time-dependent. The momenta of the particles do not necessarily always exceed their masses, meaning the interacting scalar waves are not necessarily always in the kinetic regime. In particular this means that in general we cannot calculate the energies of the fields simply as  $\int d^3k \omega_k n_k$  because interaction terms between fields can be significant.

From here on I will use  $n$  without a subscript to denote the total number density for a field, and will use the subscript only to specify a particular field, e.g.  $n_\phi$ . I use  $n_{tot}$  to mean the sum of the total number density for all fields combined. Occupation number will always be written  $n_k$  and it should be clear from context which field is being referred to.

In practice it is not very important whether you consider the spectrum  $f_k$  and the variance of  $f$  or the spectrum  $n_k$  and the number density. Both sets of quantities qualitatively show the same behavior in the systems we considered. The variance and

number density grow exponentially during preheating and evolve much more slowly during the subsequent stage of turbulence. Most of our results are shown in terms of number density  $n_f$  and occupation number  $n_k$  because these quantities have obvious physical interpretations, at least in certain limiting cases. I shall occasionally show plots of variance for comparison purposes.

In what follows I discuss the evolution of  $n(t)$  and  $n_k(t)$ . The evolution of the total number density  $n_{tot}$  is an indication of the physical processes taking place. In the weak interaction limit the scattering of classical waves via the interaction term  $\frac{1}{2}g^2\phi^2\chi^2$  can be treated using a perturbation expansion with respect to  $g^2$ . The leading four-legs diagrams for this interaction corresponds to a two-particle collision ( $\phi\chi \rightarrow \phi\chi$ ), which conserves  $n_{tot}$ . The regime where such interactions dominate corresponds to “weak turbulence” in the terminology of the theory of wave turbulence [113]. If we see  $n_{tot}$  conserved it will be an indication that these two-particle collisions constitute the dominant interaction. Conversely, violation of  $n_{tot}(t) = const$  will indicate the presence of strong turbulence, i.e. the importance of many-particle collisions. Such higher order interactions may be significant despite the smallness of the coupling parameter  $g^2$  (and others) because of the large occupation numbers  $n_k$ . Later, when these occupation numbers are reduced by rescattering, the two-particle collision should become dominant and  $n_{tot}$  should be conserved.

For a bosonic field in thermal equilibrium with a temperature  $T$  and a chemical potential  $\mu$  the spectrum of occupation numbers is given by

$$n_k = \frac{1}{e^{\frac{\omega_k - \mu}{T}} - 1}. \quad (9.12)$$

(I use units in which  $\hbar = 1$ .) Preheating generates large occupation numbers for which equation (9.12) reduces to its classical limit

$$n_k \approx \frac{T}{\omega_k - \mu}, \quad (9.13)$$

which in turn reduces to  $n_k \propto 1/k$  for  $k \gg m, \mu$  and  $n_k \approx const.$  for  $k \ll m, \mu$ . We compared the spectrum  $n_k$  to this form to judge how the fields were thermalizing. Here

I consider the chemical potential of an interacting scalar fields as a free parameter.

Unless otherwise indicated all of our results are shown in comoving coordinates that, in the absence of interactions, would remain constant as the universe expanded. Note also that for most of the discussion I consider field spectra only as a function of  $|\vec{k}|$ , defined by averaging over spherical shells in  $k$  space. For a Gaussian field these spectra contain all the information about the field, and even for a non-Gaussian field most useful information is in these averages. This issue is discussed in more detail in section 9.4.

### 9.2.3 Results

The key results for this model are shown in Figures 9.12-9.19, which show the evolution of  $n(t)$  with time for each field and the spectrum  $n_k$  for each field at a time long after the end of preheating. These results are shown for runs with one field ( $\phi$  only), two fields ( $\phi$  and  $\chi$ ), and three and four fields (one and two  $\sigma_i$  fields respectively). I will begin by discussing some general features common to all of these runs, and then comment on the runs individually.

All of the plots of  $n(t)$  show an exponential increase during preheating, followed by a gradual decrease that asymptotically slows down. See for example Figure 9.1. This exponential increase is a consequence of explosive particle production due to parametric resonance. This regime is fairly well understood [8]. After preheating the fields enter a turbulent regime, during which  $n(t)$  decreases. This initial, fast decrease can be interpreted as a consequence of the many-particle interactions discussed above; as  $n_k$  shifts from low to high momenta the overall number decreases. Realistically, however, the onset of weak turbulence should be accompanied by the development of a compensating flow towards infrared modes, which we were unable to see because of our finite box size. Thus the continued, slow decrease in  $n(t)$  well into the weak turbulent regime is presumably a consequence of the lack of very long wavelength modes in our lattice simulations.

To see why this shift is occurring look at the spectra  $n_k$  (Figures 9.16-9.19, see also [111, 114]). Even long after preheating the infrared portions of some of these

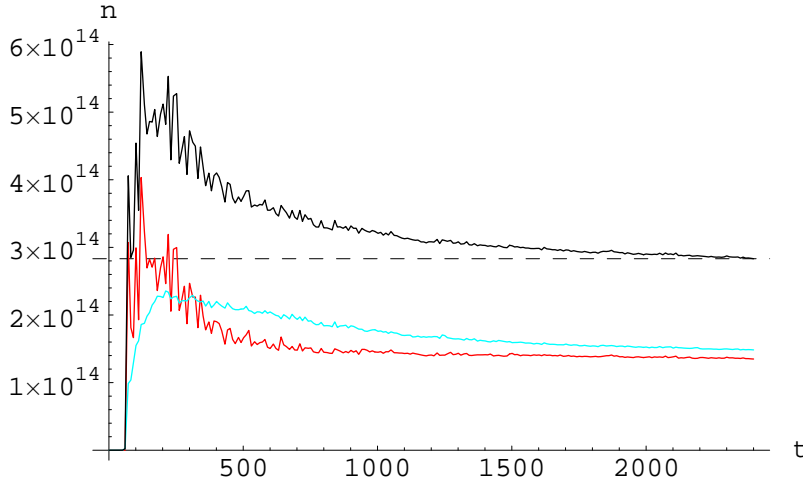


Figure 9.1: Number density  $n$  for  $V = \frac{1}{4}\lambda\phi^4 + \frac{1}{2}g^2\phi^2\chi^2$ . The plots are, from bottom to top at the right of the figure,  $n_\phi$ ,  $n_\chi$ , and  $n_{tot}$ . The dashed horizontal line is simply for comparison. The end of exponential growth and the beginning of turbulence (i.e. the moment  $t_*$ ) occurs around the time when  $n_{tot}$  reaches its maximum.

spectra are tilted more sharply than would be expected for a thermal distribution (9.13). Even more importantly, many of them show a cutoff at some momentum  $k$ , above which the occupation number falls off exponentially. Both of these features, the infrared tilt and the ultraviolet cutoff, indicate an excess of occupation number at low  $k$  relative to a thermal distribution. This excess occurs because parametric resonance is typically most efficient at exciting low momentum modes, and becomes completely inefficient above a certain cutoff  $k_*$ . A clear picture of how the flow to higher momenta reduces these features can be seen in Figure 9.2, which shows the evolution of the spectrum  $n_k$  for  $\chi$  in the two field model.

Figure 9.2 illustrates the initial excitation of modes in particular resonance bands, followed by a rapid smoothing out of the spectrum. The ultraviolet cutoff is initially at the momentum  $k_*$  where parametric resonance shuts down, but over time the cutoff moves to higher  $k$  as more modes are brought into the quasi-equilibrium of the infrared part of the spectrum. Meanwhile the infrared section is gradually flattening as it approaches a true thermal distribution. During preheating the excitation of the infrared modes drives this slope to large, negative values. From then on it gradually



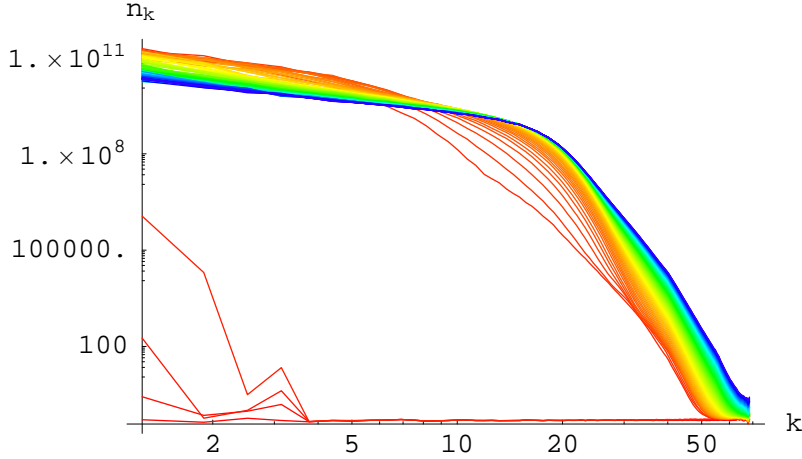


Figure 9.2: Evolution of the spectrum of  $\chi$  in the model  $V = \frac{1}{4}\lambda\phi^4 + \frac{1}{2}g^2\phi^2\chi^2$ . Red plots correspond to earlier times and blue plots to later ones. For black and white viewing: The sparse, lower plots all show early times. In the thick bundle of plots higher up the spectrum is rising on the right and falling on the left as time progresses.

approaches thermal equilibrium (i.e. a slope of  $-1$  to  $0$  depending on the chemical potential and the mass). The relaxation time for the equilibrium is significantly shorter than that given by formula  $1/n\sigma_{int}$ . This estimate is valid for dilute gases of particles, but in our case the large occupation numbers amplify the scattering amplitudes [7].

Figure 9.3 shows the evolution of the variances  $\langle (f - \bar{f})^2 \rangle$  for the two field model. As indicated above it shows all the same qualitative features as the evolution of  $n$  for that model.

I can now go on to point out some differences between the models, i.e. between runs with different numbers of fields. The one field model (pure  $\lambda\phi^4$ ) shows the basic features discussed above, but the tilt in the spectrum is still very large at the end of the simulation and  $n_\phi$  is decreasing very slowly compared to the spectral tilt and change in  $n$  we see in the two field case. This difference occurs because the interactions between  $\phi$  and  $\chi$  greatly speed up the thermalization of both fields. In the one field case  $\phi$  can only thermalize via its relatively weak self-interaction.

The spectra in the two field run also show a novel feature, namely that the spectra

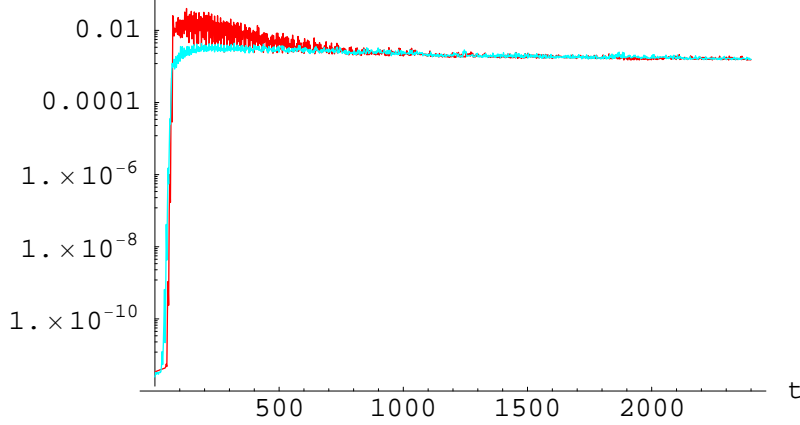


Figure 9.3: Variances for  $V = \frac{1}{4}\lambda\phi^4 + \frac{1}{2}g^2\phi^2\chi^2$ . The upper plot shows  $\langle(\phi - \bar{\phi})^2\rangle$  and the lower plot shows  $\langle(\chi - \bar{\chi})^2\rangle$ .

for  $\phi$  and  $\chi$  are essentially identical, which means among other things

$$n_\phi \approx n_\chi. \quad (9.14)$$

This matching of the two spectra occurs shortly after preheating and from then on the two fields evolve identically (except for the remaining homogeneous component of  $\phi$ ). A posteriori this result can be understood as follows. Looking at the potential  $\lambda\phi^4 + g^2\phi^2\chi^2$ , the second term dominates because of the hierarchy of coupling strengths  $g^2 = 200\lambda$ . So the potential  $V \approx g^2\phi^2\chi^2$  is symmetric with respect to the two fields, and therefore they act as a single effective field.

Figures 9.14 and 9.18 show the effects of adding an additional decay channel for  $\chi$ . The interaction of  $\chi$  and  $\sigma$  does not affect the preheating of  $\chi$ , but does drag  $\sigma$  exponentially quickly into an excited state. The field  $\sigma$  is exponentially amplified not by parametric resonance, but by its stimulated interactions with the amplified  $\chi$  field. Unlike amplification by preheating, this direct decay nearly conserves particle number, with the result that  $n_\chi$  decreases as  $\sigma$  grows, and the spectra of  $\phi$  and  $\chi$  are

no longer identical. Instead  $\chi$  and  $\sigma$  develop nearly identical spectra,

$$n_\chi \approx n_\sigma < n_\phi, \quad (9.15)$$

and they both thermalize (together) much more rapidly than  $\chi$  did in the absence of  $\sigma$ . There is a looser relationship  $n_\phi \approx n_\sigma + n_\chi$ , whose accuracy depends on the couplings. The inflaton, meanwhile, thermalizes much more slowly; note the low  $k$  of the cutoff in the  $\phi$  spectrum in Figure 9.18. By contrast, there is no visible cutoff in the spectra of  $\chi$  and  $\sigma$  and the tilt is relatively mild. The most striking property of this chain of interaction is the grouping of fields;  $\chi$  and  $\sigma$  behave identically to each other and differently from  $\phi$ . This again can be understood by the hierarchy of coupling constants,  $h^2 = 100g^2 = 20,000\lambda$ . The term  $h^2\chi^2\sigma^2$  is dominant and puts  $\chi$  and  $\sigma$  on an equal footing.

Varying the coupling  $h$  did not change the overall behavior of the system, but it changed the time at which  $\sigma$  grew. In the limiting case  $h \gg g$ ,  $\sigma$  grew with  $\chi$  during preheating and remained indistinguishable from it right from the start. (We found this, for example, for  $h^2 = 10,000g^2$ .)

When we added a second  $\sigma$  field we found that the  $\sigma$  field most strongly coupled to  $\chi$  would grow very rapidly and the more weakly coupled one would then grow relatively slowly. Note for example that  $n_{\sigma_2}$  in Figure 9.19 grows more slowly than  $n_\sigma$  in Figure 9.18 despite the fact that they have the same coupling to  $\chi$ . In the four field case  $n_\chi$  is reduced when the more strongly coupled  $\sigma$  field grows and this slows the growth of the more weakly coupled one. Nonetheless, the addition of another  $\sigma$  field once again sped up the thermalization of  $\chi$  and the  $\sigma$  fields. The three fields  $\chi$ ,  $\sigma_1$ , and  $\sigma_2$  once again have identical spectra

$$n_\chi \approx n_{\sigma_1} \approx n_{\sigma_2} < n_\phi, \quad (9.16)$$

but in the four field case by the end of the run they look indistinguishable from thermal spectra. If there is an ultraviolet cutoff for these spectra it is at momenta higher than can be seen on the lattice we were using. Again, we noticed a loose relationship  $n_\phi \approx n_\chi + n_{\sigma_1} + n_{\sigma_2}$ . in this case.

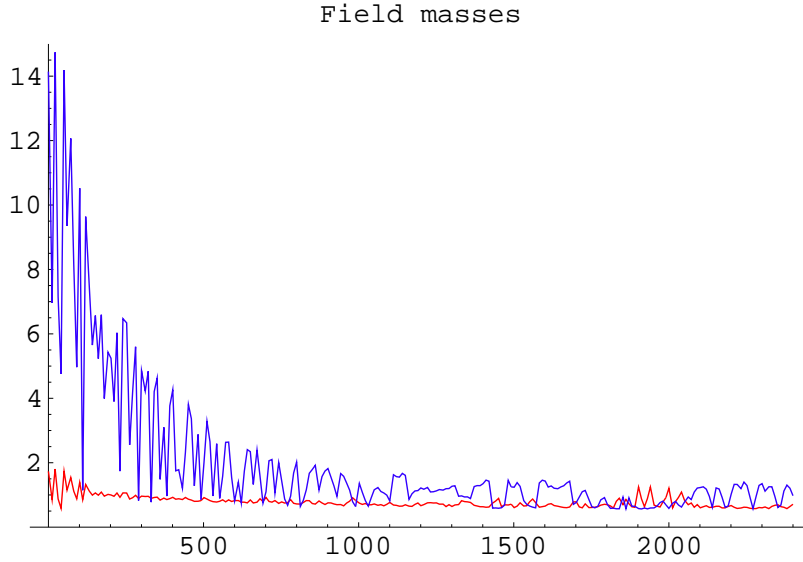


Figure 9.4: Effective masses for  $V = \frac{1}{4}\lambda\phi^4 + \frac{1}{2}g^2\phi^2\chi^2$  as a function of time in units of comoving momentum. The lower plot is  $m_\phi$  and the upper one is  $m_\chi$ .

I'll close this section with a few words about the effective masses of the fields, equation (9.10). All the masses are scaled in the comoving frame, i.e. I consider  $a^2 m_{eff}^2$ . Figure 9.4 shows the evolution of the effective masses in the two field model. Note that the vertical axis of these plots is in the same comoving units as the horizontal ( $k$ ) axes of the spectra plots. Since the momentum cutoff was of order  $k \sim 5 - 10$  (see Figure 9.2) the mass of  $\phi$  was consistently smaller than the typical momenta of the field. By contrast  $m_\chi$  started out much larger and only gradually decreased. The fluctuations of  $\chi$  remained massive through preheating (although with a physical mass  $\sim 1/a$ ) and for quite a while afterwards the typical momentum of these fluctuations was  $k \sim m$ .

Figure 9.5 shows the evolution of the effective masses for the three field model. Once again  $m_\phi$  remains small. Although  $m_\sigma$  grows large briefly it quickly subsides. However,  $m_\chi$ , with contributions from  $\sigma$  and  $\phi$ , remains relatively large. Note, however, that the spectrum of  $\chi$  has no clear cutoff after  $\sigma$  has grown, so it is difficult to say whether this mass exceeds a “typical” momentum scale or not.

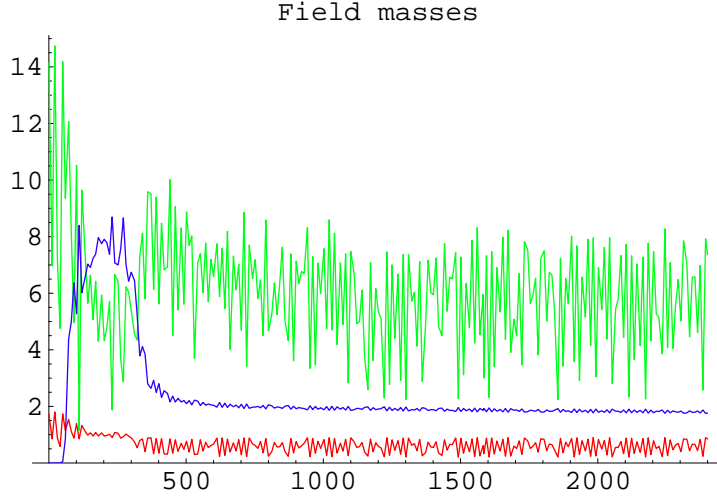


Figure 9.5: Time evolution of the effective masses for the model  $V = \frac{1}{4}\lambda\phi^4 + \frac{1}{2}g^2\phi^2\chi^2 + \frac{1}{2}h^2\chi^2\sigma^2$ . From bottom to top on the right hand side the plots show  $m_\phi$ ,  $m_\sigma$ , and  $m_\chi$ .

### 9.3 Other Models of Inflation and Interactions

The model (9.1) was chosen to illustrate our basic results because  $\lambda\phi^4$  inflation and preheating is relatively simple and well studied. Our main interest, however, was in universal features of thermalization. In this section I therefore more briefly discuss our results for a variety of other models. First I continue with  $\lambda\phi^4$  inflation by discussing variants on the interaction potential described above. Next I discuss thermalization in  $m^2\phi^2$  models of chaotic inflation. Finally I discuss hybrid inflation.

#### 9.3.1 Variations on Chaotic Inflation With a Quartic Potential

We looked at several simple variants of the potential (9.1). We considered a model with a further decay channel for  $\sigma$  so that the total potential was

$$V = \frac{1}{4}\lambda\phi^4 + \frac{1}{2}g^2\phi^2\chi^2 + \frac{1}{2}h_1^2\chi^2\sigma^2 + \frac{1}{2}h_2^2\sigma^2\gamma^2. \quad (9.17)$$

Setting  $h_1 = h_2$  we found that for this four field model the evolution of the field fluctuations, spectra, and number density were qualitatively similar to those in the

four field model (9.1). We found that at late times

$$n_\chi \approx n_\sigma \approx n_\gamma < n_\phi . \quad (9.18)$$

The fields  $\chi$ ,  $\sigma$ , and  $\gamma$  formed a group with nearly identical spectra and evolution and rapid thermalization, while  $\phi$  remained distinct and thermalized more slowly. Compare these results to the four field model results in Figures 9.15 and 9.19.

We also considered parallel decay channels for  $\phi$

$$V = \frac{1}{4}\lambda\phi^4 + \frac{1}{2}g_1^2\phi^2\chi^2 + \frac{1}{2}g_2^2\phi^2\gamma^2 + \frac{1}{2}h^2\chi^2\sigma^2. \quad (9.19)$$

Setting  $g_1 = g_2$  and  $h^2 = 100g_1^2$  we found that at late times

$$n_\phi \approx n_\gamma > n_\chi \approx n_\sigma . \quad (9.20)$$

In other words the four fields formed into two groups of two, with each group having a characteristic number density evolution.

Finally we looked at adding a self-interaction term for  $\chi$

$$V = \frac{1}{4}\lambda_\phi\phi^4 + \frac{1}{2}g^2\phi^2\chi^2 + \frac{1}{4}\lambda_\chi\chi^4 \quad (9.21)$$

with  $\lambda_\chi = g^2$  and found the results were essentially unchanged from those of the two field runs with no  $\chi^4$  term. The  $\chi$  self-coupling caused the spectra of  $\phi$  and  $\chi$  to deviate slightly from each other, but their overall evolution proceeded very similarly to the case with no  $\chi$  self-interaction term.

### 9.3.2 Chaotic Inflation with a Quadratic Potential

We also considered chaotic inflation models with an  $m^2\phi^2$  inflaton potential. Figures 9.20-9.23 show results for the model

$$V = \frac{1}{2}m^2\phi^2 + \frac{1}{2}g^2\phi^2\chi^2 + \frac{1}{2}h^2\chi^2\sigma^2, \quad (9.22)$$

with  $m = 10^{-6} M_p \approx 1.22 \times 10^{13} \text{ GeV}$  (for COBE),  $g^2 = 2.5 \times 10^5 m^2 / M_p^2$ , and  $h^2 = 100 g^2$ . The rescalings used for this model were

$$f_{pr} = \frac{a^{3/2}}{\phi_0} f; \quad \vec{x}_{pr} = m \vec{x}; \quad dt_{pr} = m dt, \quad (9.23)$$

and once again all plots here are shown in these rescaled variables. The initial value  $\phi_0$  was set to  $.193 M_p$ .

We considered separately the case of two fields  $\phi$  and  $\chi$  and three fields  $\phi$ ,  $\chi$ , and  $\sigma$ . This model exhibits parametric resonance similar to the resonance in quartic inflation [7], which results in the rapid growth of  $n$  seen in these figures. The spectra produced in this way are once again tilted towards the infrared. In the two field case,  $\phi$  and  $\chi$  do not have identical spectra as they did for quartic inflation. This is because the coupling term  $1/2 g^2 \phi^2 \chi^2$  redshifts more rapidly than the mass term  $1/2 m^2 \phi^2$ , so the latter remains dominant in the potential, which is therefore not symmetric between  $\phi$  and  $\chi$ . In the three field case we again see similar spectra for  $\chi$  and  $\sigma$ , although they are not as indistinguishable as they were in  $\lambda \phi^4$  theory. The basic features of rapid growth of  $n$ , high occupation of infrared modes, and then a flux of number density towards ultraviolet modes and a slow decrease in  $n_{tot}$  are all present as they were for  $\lambda \phi^4$  theory. The shape of the  $\phi$  spectrum does not appear thermal, but it is unclear if this spectrum is compatible with Kolmogorov turbulence.

### 9.3.3 Hybrid Inflation

Hybrid inflation models involve multiple scalar fields. The simplest potential for two-field hybrid inflation is

$$V(\phi, \sigma) = \frac{\lambda}{4} (\sigma^2 - v^2)^2 + \frac{g^2}{2} \phi^2 \sigma^2. \quad (9.24)$$

Inflation in this model occurs while the homogeneous  $\phi$  field slow rolls from large  $\phi$  towards the bifurcation point at  $\phi = \frac{\sqrt{\lambda}}{g} v$  (due to the slight lift of the potential in  $\phi$  direction). Once  $\phi(t)$  crosses the bifurcation point, the curvature of the  $\sigma$  field,  $m_\sigma^2 \equiv \partial^2 V / \partial \sigma^2$ , becomes negative. This negative curvature results in exponential

growth of  $\sigma$  fluctuations. Inflation then ends abruptly in a “waterfall” manner.

In chapter 10 I discuss preheating in hybrid inflation, which typically occurs via a mechanism called “tachyonic preheating.” Although this mechanism is very different in some ways from parametric resonance the result is quite similar; fluctuations of the fields are rapidly driven to a state with exponentially large occupation numbers up to some cutoff in momentum. I won’t discuss tachyonic preheating in any detail here. Rather my concern here is to note how thermalization occurs after preheating.

One reason to be interested in hybrid inflation is that it can be easily implemented in supersymmetric theories. In particular, for illustration I will use supersymmetric F-term inflation as an example of a hybrid model. The potential is

$$V = \frac{\lambda}{4} |4\bar{\Sigma}\Sigma - v^2|^2 + 4\lambda|\Phi|^2 (|\Sigma|^2 + |\bar{\Sigma}|^2) + h^2\chi^2|\Sigma|^2, \quad (9.25)$$

where  $\lambda = 2.5 \times 10^{-5}$  and  $h^2 = 2\lambda$ . Here  $\Phi$ ,  $\Sigma$  and  $\bar{\Sigma}$  are the complex scalar fields of the inflaton sector and  $\chi$  is an additional matter field. Inflation occurs along the  $\Phi$  direction for  $\langle\Phi\rangle \gg v$ , when  $\Sigma = \bar{\Sigma} = 0$ . When the magnitude of the slow-rolling field  $\Phi$  reaches the value  $\langle|\Phi_c|\rangle = \frac{v}{2}$  spontaneous symmetry breaking occurs and the  $\Sigma$  fields become excited. It can be shown that at the end of inflation and the start of symmetry breaking the complicated potential (9.25) can be effectively reduced to the simple two field potential (9.24) (where  $\phi$  and  $\sigma$  are combinations of  $\Phi$  and  $\Sigma$ ,  $\bar{\Sigma}$  and  $g^2 = \frac{1}{2}\lambda$ ) plus the coupling term with  $h^2\chi^2|\Sigma|^2$ .

Figure 9.6 show the evolution of the six degrees of freedom of the inflaton sector as well as the field  $\chi$ . We see that all of the inflaton fields except  $Im(\Phi)$  are excited very quickly. Later the fields  $\chi$  and  $Im(\Phi)$  are dragged into excited states as well. This dragging corresponds to preheating in the non-inflaton sector. The fields  $\chi$  and  $Im(\Phi)$  are excited by their stimulated interactions with the rest of the fields. The result of this amplification is a turbulent state that evolves towards equilibrium very similarly to the chaotic models. Although the details of inflation and preheating are very different in hybrid and chaotic models, we found that once a matter field has been amplified, the thermalization process proceeds in the same way.



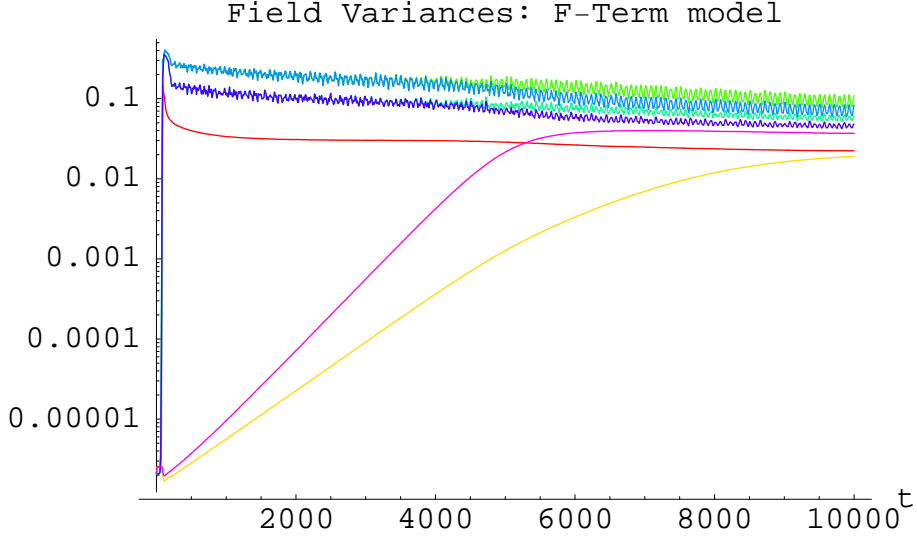


Figure 9.6: Evolution of variances of fields in the model (9.25). The two fields that grow at late times, in order of their growth, are  $\chi$  and  $Im(\Phi)$ .

## 9.4 The Onset of Chaos, Lyapunov Exponents and Statistics

Interacting waves of scalar fields constitute a dynamical system, meaning there is no dissipation and the system can be described by a Hamiltonian. Dynamical chaos is one of the features of wave turbulence. In this section I address the question if, how and when the onset of chaos takes place after preheating.

The scalar field fluctuations produced during preheating are generated in squeezed states [115, 7] that are characterized by correlations of phases between modes  $\vec{k}$  and  $-\vec{k}$ . Because of their large amplitudes we can consider these fluctuations to be standing classical waves with definite phases. During the linear stage of preheating, before interactions between modes becomes significant, the evolution of these waves may or may not show chaotic sensitivity to initial conditions. Indeed, for wide ranges of coupling parameters parametric resonance has stochastic features [7, 8], and prior to this work the issue of the numerical stability of parametric resonance had not been investigated. When interaction (rescattering) between waves becomes important, the

waves become decoherent. At this stage the waves have well defined occupation numbers but not well defined phases, and the random phase approximation can be used to describe the system. This transition signals the onset of turbulence, following which the system will gradually evolve towards thermal equilibrium.

To investigate the onset of chaos in this system we followed the time evolution of two initially nearby points in the phase space, see e.g. [112]. Consider two configurations of a scalar field  $f$  and  $f'$  that are identical except for a small difference of the fields at a set of points  $x_A$ . I use  $f(t, \vec{x}_A), \dot{f}(t, \vec{x}_A)$  to indicate the unperturbed field amplitude and field velocity at the point  $\vec{x}_A$  and  $f'(t, \vec{x}_A), \dot{f}'(t, \vec{x}_A)$  to indicate slightly perturbed values at this point. In other words, the field configurations with  $f(t, \vec{x}_A), \dot{f}(t, \vec{x}_A)$  and  $f'(t, \vec{x}_A), \dot{f}'(t, \vec{x}_A)$  are initially close points in the field phase space. We independently evolved these two systems (phase space points) and observe how the perturbed field values diverge from the unperturbed ones. Chaos can be defined as the tendency of such nearby configurations in phase space to diverge exponentially over time. This divergence is parametrized by the Lyapunov exponent for the system, defined as

$$\lambda \equiv \frac{1}{t} \log \frac{D(t)}{D_0} \quad (9.26)$$

where  $D$  is a distance between two configurations and  $D_0$  is the initial distance at time 0. Here we defined the distance  $D(t)$  simply as

$$D(t)^2 \equiv \sum_A (|f'_A - f_A|)^2 + (|\dot{f}'_A - \dot{f}_A|)^2, \quad (9.27)$$

where  $f_A \equiv f(t, \vec{x}_A)$  and the summation is taken over all the points where the configurations initially differed.

For illustration I present the calculations for the model  $V = \frac{1}{4}\lambda\phi^4 + \frac{1}{2}g^2\phi^2\chi^2$ . We did two lattice simulations of this model with initial conditions that were identical except that in one of them we multiplied the amplitude of  $\chi$  by  $1 + 10^{-6}$  at 8 evenly spaced points on the lattice. Figure 9.7 shows the Lyapunov exponent for both fields  $\phi$  and  $\chi$ . Note that the vertical axis is  $\lambda t$  rather than just  $\lambda$ . During the turbulent stage the parameter  $D(t)$  is artificially saturated to a constant because of the limited phase space volume of the system. Fortunately, the most interesting moment around

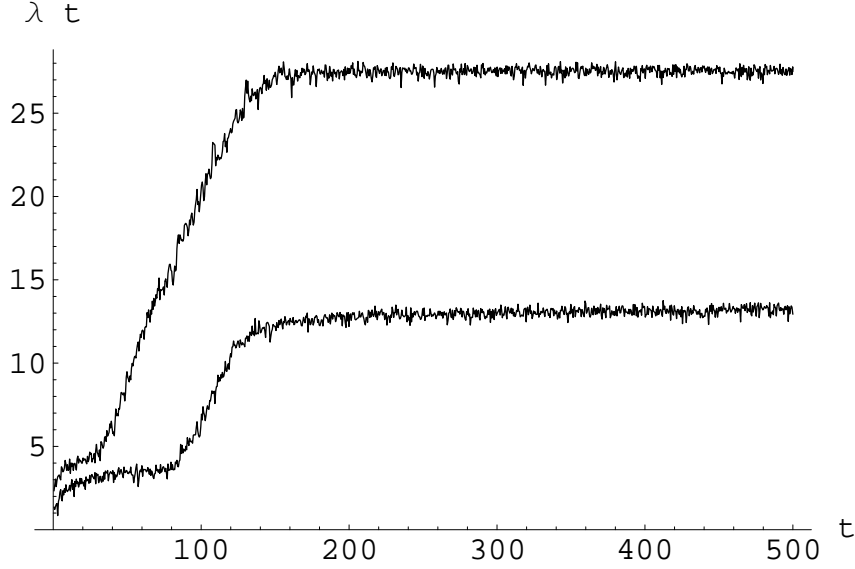


Figure 9.7: The Lyapunov exponent  $\lambda$  for the fields  $\phi$  (lower curve) and  $\chi$  (upper curve). The vertical axis is  $\lambda t$ .

$t_*$ , where the chaotic motion begins, is covered by this simple approach. Certainly, the field dynamics continue to be chaotic in subsequent stages of the turbulence, and one can use more sophisticated methods to calculate the Lyapunov exponent during these stages [116, 112]. However, this issue is less relevant for our study.

Both fields show roughly the same rate of growth of  $\lambda$ , but  $\lambda_\chi$  grows much earlier than  $\lambda_\phi$  and therefore reaches a higher level. The reason for this is simple. The amplitude of  $\chi$  is initially very small and grows exponentially, so even in the absence of chaos we would expect that during preheating the difference  $\chi'(t, \vec{x}_A) - \chi(t, \vec{x}_A)$  must grow exponentially, proportionally to  $\chi \sim e^{\int dt \mu(t)}$  itself. So this exponential growth is not a true indicator of chaos.

To get around this problem and define the onset of chaos in the context of preheating more meaningfully we introduced a normalized distance function

$$\Delta(t) \equiv \sum_A \left( \frac{f'_A - f_A}{f'_A + f_A} \right)^2 + \left( \frac{\dot{f}'_A - \dot{f}_A}{\dot{f}'_A + \dot{f}_A} \right)^2 \quad (9.28)$$

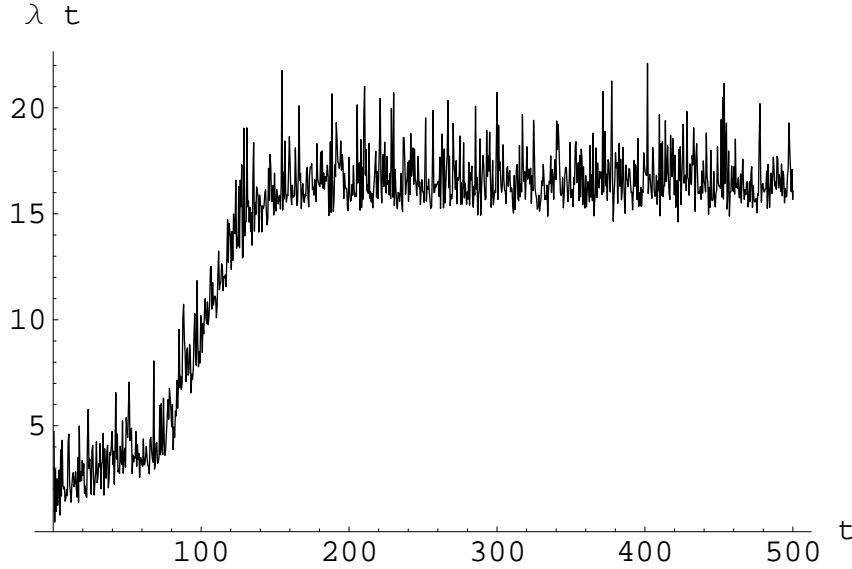


Figure 9.8: The Lyapunov exponent  $\lambda'$  for the fields  $\phi$  and  $\chi$  using the normalized distance function  $\Delta$ .

that is well regularized even while the field  $\chi$  is being amplified exponentially. Figure 9.8 shows the Lyapunov exponent  $\lambda' \equiv \frac{1}{t} \log \frac{\Delta(t)}{\Delta(t_0)}$  for  $\chi$ . In this case we see the onset of chaos only at the end of preheating. The plot for the  $\phi$  field is nearly identical. The Lyapunov exponents for the fields were  $\lambda'_\phi \approx \lambda'_\chi \approx 0.2$  (in the units of time adopted in the simulation). This corresponds to a very fast onset of chaos.

Thus we see that chaotic turbulence starts abruptly at the end of preheating. Initially wave turbulence is strong and rescattering does not conserve the total number of particles  $n_{tot}$ . The fastest variation in  $n_{tot}$  occurs at the same time as the onset of chaos,  $t_* \sim 100 - 200$ . We conjecture that the entropy of the system of interacting waves is generated around the moment  $t_*$ . As the particle occupation number drops, the turbulence will become weak and  $n_{tot}$  will be conserved. Figure 9.1 clearly shows this evolution of the total number of particles  $n_{tot}$  in the model.

We also considered the statistical properties of the interacting classical waves in the problem. The initial conditions of our lattice simulations correspond to random gaussian noise. In thermal equilibrium, the field velocity  $\dot{f}$  has gaussian statistics, while the field  $f$  itself departs from that unless it has high occupation numbers.

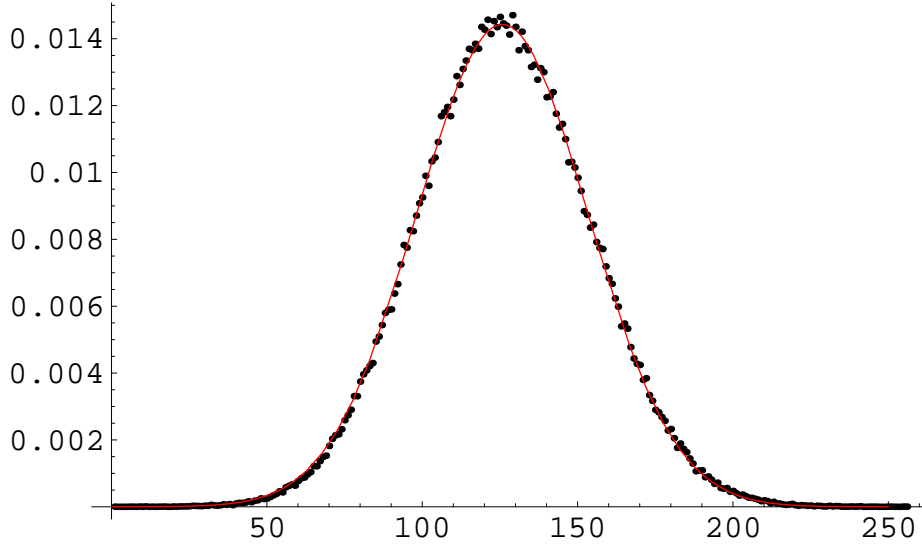


Figure 9.9: The probability distribution function for the field  $\chi$  after preheating. Dots show a histogram of the field and the solid curve shows a best-fit Gaussian.

Figure 9.9 shows the probability distribution of the field  $\chi$  during the weak turbulence stage after preheating, and indeed the distribution is nearly exactly gaussian. Thus, at this stage we can treat the superposition of classical scalar waves with large occupation numbers and random phases as random gaussian fields.

During preheating, however, this gaussian distribution is altered. A simple measure of the gaussianity of a field comes from examining its moments. For a gaussian field there is a fixed relationship between the two lowest nonvanishing moments, namely

$$3\langle\delta\phi^2\rangle^2 = \langle\delta\phi^4\rangle, \quad (9.29)$$

where  $\delta\phi \equiv \phi - \langle\phi\rangle$  and angle brackets denote ensemble averages or, equivalently, large spatial averages. We measured the ratio of the left and right hand sides of this equation for  $\phi$  and  $\chi$  and their time derivatives using spatial averages over the lattice. The results are shown in Figures 9.10 and 9.11. As expected, the fields are initially gaussian, deviate from it during preheating, and rapidly return to it afterwards. The plots for the moments of the field velocities are similar, although the field velocities remain closer to gaussianity.

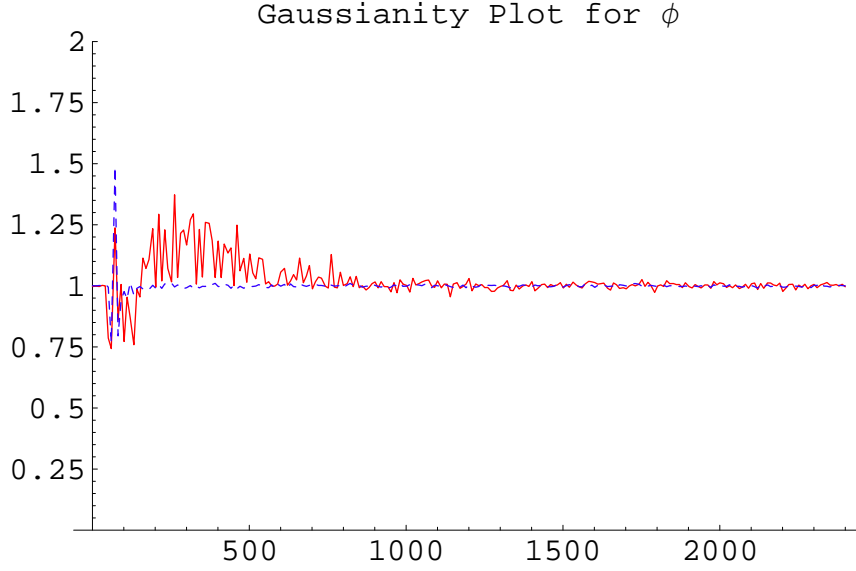


Figure 9.10: Deviations from Gaussianity for the field  $\phi$  as a function of time. The solid, red line shows  $3\langle\delta\phi^2\rangle^2/\langle\delta\phi^4\rangle$  and the dashed, blue line shows  $3\langle\delta\dot{\phi}^2\rangle^2/\langle\delta\dot{\phi}^4\rangle$ .

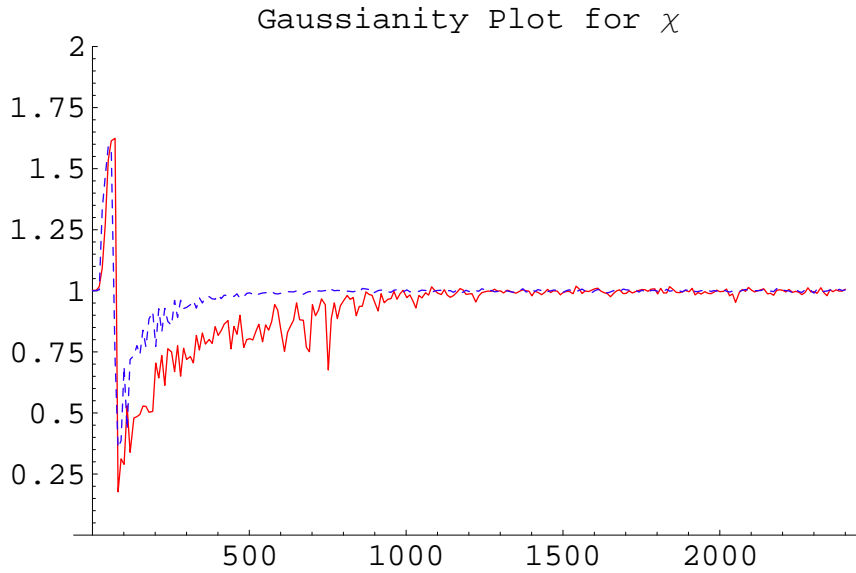


Figure 9.11: Deviations from Gaussianity for the field  $\chi$  as a function of time. The solid, red line shows  $3\langle\delta\chi^2\rangle^2/\langle\delta\chi^4\rangle$  and the dashed, blue line shows  $3\langle\delta\dot{\chi}^2\rangle^2/\langle\delta\dot{\chi}^4\rangle$ .

It is quite important to notice that gaussianity is broken around the end of preheating and the beginning of the strong turbulence. In particular, it makes invalid the use of the Hartree approximation beyond this point.

## 9.5 Rules of Thermalization

This research was primarily empirical. We numerically investigated the processes of preheating and thermalization in a variety of models and determined a set of rules that seem to hold generically. These rules can be formulated as follows:

*1. In many, if not all viable models of inflation there exists a mechanism for exponentially amplifying fluctuations of at least one field  $\chi$ . These mechanisms tend to excite long-wavelength excitations, giving rise to a highly infrared spectrum.*

The mechanism of parametric resonance in single-field models of inflation has been studied for a number of years. Contrary to the claims of some authors, this effect is quite robust. Adding additional fields (e.g. our  $\sigma$  fields) or self-couplings (e.g.  $\chi^4$ ) has little or no effect on the resonant period. Moreover, in many hybrid models a similar effect occurs due to other instabilities. The qualitative features of the fields arising from these processes seem to be largely independent of the details of inflation or the mechanisms used to produce the fields.

*2. Exciting one field  $\chi$  is sufficient to rapidly drag all other light fields with which  $\chi$  interacts into a similarly excited state.*

We saw this effect when multiple fields were coupled directly to  $\chi$  and when chains of fields were coupled indirectly to  $\chi$ . All it takes is one field being excited to rapidly amplify an entire sector of interacting fields. These second generation amplified fields will inherit the basic features of the  $\chi$  field, i.e. they will have spectra with more energy in the infrared than would be expected for a thermal distribution.

*3. The excited fields will be grouped into subsets with identical characteristics (spectra, occupation numbers, effective temperatures) depending on the coupling strengths.*

We saw this effect in a variety of models. For example in the models (9.1) and (9.17) the  $\chi$  and  $\sigma$  fields formed such a group. In general, fields that are interacting

in a group such as this will thermalize much more quickly than other fields, presumably because they have more potential to interact and scatter particles into high momentum states.

*4. Once the fields are amplified, they will approach thermal equilibrium by scattering energy into higher momentum modes.*

This process of thermalization involves a slow redistribution of the particle occupation number as low momentum particles are scattered and combined into higher momentum modes. The result of this scattering is to decrease the tilt of the infrared portion of the spectrum and increase the ultraviolet cutoff of the spectrum. Within each field group the evolution proceeds identically for all fields, but different groups can thermalize at very different rates.

## 9.6 Discussion

We investigated the dynamics of interacting scalar fields during post-inflationary preheating and the development of equilibrium immediately after preheating. We used three dimensional lattice simulations to solve the non-linear equations of motion of the classical fields.

There are a number of problems both from the point of view of realistic models of early universe preheating and from the point of view of non-equilibrium quantum field theory that I have not yet addressed. In this section I shall discuss some of them.

Although we considered a series of models of inflation and interactions, we mostly restricted ourselves to four-legs interactions. (The sole exception was the hybrid inflation model, which develops a three-legs interaction after symmetry breaking.) This meant we still had a residual homogeneous or inhomogeneous inflaton field. In realistic models of inflation and preheating we expect the complete decay of the inflaton field. (There are radical suggestions to use the residuals of the inflaton oscillations as dark matter or quintessence, but these require a great deal of fine tuning.) The problem of residual inflaton oscillations can be easily cured by three-legs interactions. In the scalar sector three-legs interactions of the type  $g^2 v \phi \chi^2$  may result



in stronger preheating. Yukawa couplings  $h\bar{\psi}\phi\psi$  will lead to parametric excitations of fermions [32, 117].

There are subtle theoretical issues related to the development of precise thermal equilibrium in quantum and classical field theory due to the large number of degrees of freedom, see e.g. [118]. In our simulations we see the flattening of the particle spectra  $n_k$  and we describe this as an approach to thermal equilibrium, but in light of these subtleties we should clarify that we mean *approximate* thermal equilibrium.

Often classical scalar fields in the kinetic regime display transient Kolmogorov turbulence, with a cascade towards both infrared and ultraviolet modes [119, 113]. In our systems it appears that the flux towards ultraviolet modes is occurring in such a way as to bring the fields closer to thermal equilibrium (9.13). Indeed, the slope of the spectra  $n_k$  at the end of our simulations is close to  $-1$ . However, given the size of the box in these simulations we were not able to say much about the phase space flux in the direction of infrared modes. This question could be addressed, for example, with the complementary method of chains of interacting oscillators, see [119]. This is an interesting problem because an out-of-equilibrium bose-system of interacting scalars with a conserved number of particles can, in principle, develop a bose-condensate. It would be interesting to see how the formation of this condensate would or would not take place in the context of preheating in an expanding universe. One highly speculative possibility is that a cosmological bose condensate could play the role of a late-time cosmological constant.

The highlights of our study for early universe phenomenology are the following. The mechanism of preheating after inflation is rather robust and works for many different systems of interacting scalars. There is a stage of turbulent classical waves where the initial conditions for preheating are erased. Initially, before all the fields have settled into equilibrium with a uniform temperature, the reheating temperature may be different in different subgroups of fields. The nature of these groupings is determined by the coupling strengths.

### Number Density vs. Time

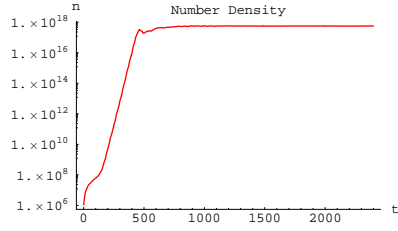


Figure 9.12:  $V = 1/4\lambda\phi^4$ . (Note that the vertical scale is larger than for the subsequent plots.)

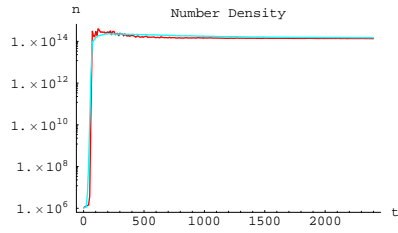


Figure 9.13:  $V = 1/4\lambda\phi^4 + 1/2g^2\phi^2\chi^2$ ,  $g^2/\lambda = 200$ . The upper curve represents  $n_\chi$ .

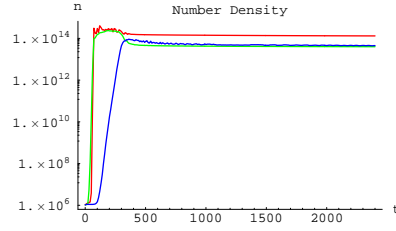


Figure 9.14:  $V = 1/4\lambda\phi^4 + 1/2g^2\phi^2\chi^2 + 1/2h^2\chi^2\sigma^2$ ,  $g^2/\lambda = 200$ ,  $h^2 = 100g^2$ . The highest curve is  $n_\phi$ . The number density of  $\chi$  diminishes when  $n_\sigma$  grows.

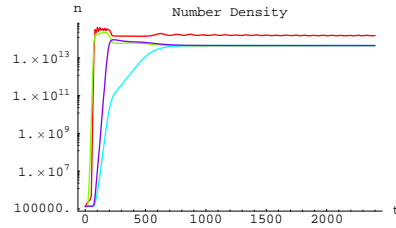
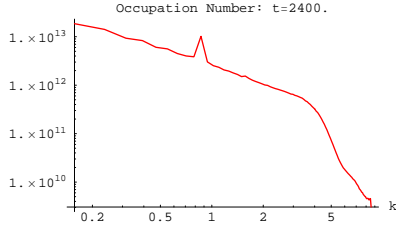
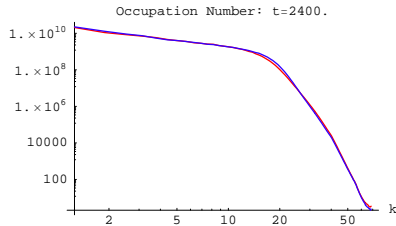
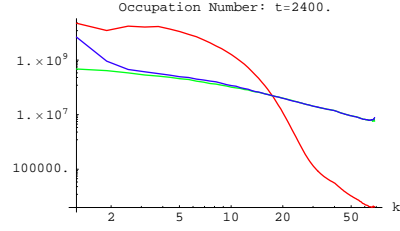
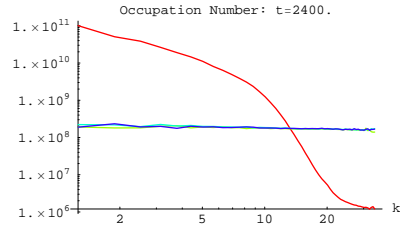


Figure 9.15:  $V = 1/4\lambda\phi^4 + 1/2g^2\phi^2\chi^2 + 1/2h_i^2\chi^2\sigma_i^2$ ,  $g^2/\lambda = 200$ ,  $h_1^2 = 200g^2$ ,  $h_2^2 = 100g^2$ . The pattern is similar to the three-field case until the growth of  $\sigma_2$ .

## Occupation Number vs. Momentum

Figure 9.16:  $V = 1/4\lambda\phi^4$ .Figure 9.17:  $V = 1/4\lambda\phi^4 + 1/2g^2\phi^2\chi^2$ ,  $g^2/\lambda = 200$ . The spectra of  $\phi$  and  $\chi$  are nearly identical.Figure 9.18:  $V = 1/4\lambda\phi^4 + 1/2g^2\phi^2\chi^2 + 1/2h^2\chi^2\sigma^2$ ,  $g^2/\lambda = 200$ ,  $h^2 = 100g^2$ . The  $\chi$  and  $\sigma$  spectra are similar, but  $\sigma$  rises in the infrared). The spectrum of  $\phi$  is markedly different from the others.Figure 9.19:  $V = 1/4\lambda\phi^4 + 1/2g^2\phi^2\chi^2 + 1/2h_1^2\chi^2\sigma_1^2 + 1/2h_2^2\chi^2\sigma_2^2$ ,  $g^2/\lambda = 200$ ,  $h_1^2 = 200g^2$ ,  $h_2^2 = 100g^2$ . All fields other than the inflaton have nearly identical spectra.

## Number Density vs. Time

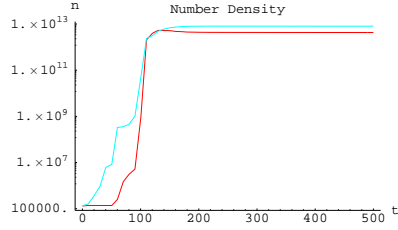


Figure 9.20:  $V = 1/2m^2\phi^2 + 1/2g^2\phi^2\chi^2$ ,  $g^2M_p^2/m^2 = 2.5 \times 10^5$ . The upper curve represents  $n_\chi$ .

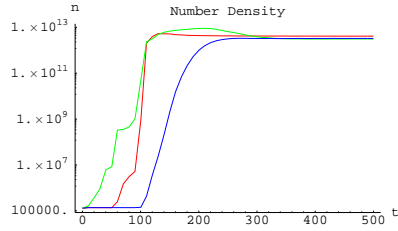


Figure 9.21:  $V = 1/2m^2\phi^2 + 1/2g^2\phi^2\chi^2 + 1/2h^2\chi^2\sigma^2$ ,  $g^2M_p^2/m^2 = 2.5 \times 10^5$ ,  $h^2 = 100g^2$ . The highest curve is  $n_\chi$ . The field that grows latest is  $\sigma$ .

## Number Density vs. Momentum

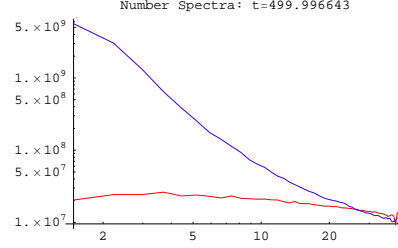


Figure 9.22:  $V = 1/2m^2\phi^2 + 1/2g^2\phi^2\chi^2$ ,  $g^2M_p^2/m^2 = 2.5 \times 10^5$ . The upper curve represents the spectrum of  $\chi$ .

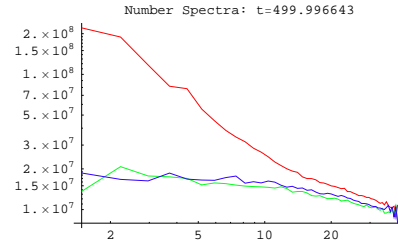


Figure 9.23:  $V = 1/2m^2\phi^2 + 1/2g^2\phi^2\chi^2 + 1/2h^2\chi^2\sigma^2$ ,  $g^2M_p^2/m^2 = 2.5 \times 10^5$ ,  $h^2 = 100g^2$ . The  $\chi$  and  $\sigma$  spectra are similar, while the spectrum of  $\phi$  rises much higher in the infrared.

## Chapter 10

# Dynamics of Symmetry Breaking and Tachyonic Preheating

*Note: This chapter is based on a paper by Gary Felder, Juan Garcia-Bellido, Patrick Greene, Lev Kofman, Andrei Linde, and Igor Tkachev, available on the Los Alamos eprint server as hep-ph/0012142. The full citation appears in the bibliography [120].*

### Chapter Abstract

We reconsidered the old problem of the dynamics of spontaneous symmetry breaking using 3d lattice simulations, and developed a theory of tachyonic preheating, which occurs due to the spinodal instability of the scalar field. Tachyonic preheating is so efficient that symmetry breaking typically completes within a single oscillation of the field distribution as it rolls towards the minimum of its effective potential. As an application of this theory we considered preheating in the hybrid inflation scenario, including SUSY-motivated F-term and D-term inflationary models. We showed that preheating in hybrid inflation is typically tachyonic and the stage of oscillations of a homogeneous component of the scalar fields driving inflation ends after a single oscillation. Our results may also be relevant for the theory of the formation of disoriented chiral condensates in heavy ion collisions.

## 10.1 Introduction

Spontaneous symmetry breaking is a basic feature of all realistic theories of elementary particles. In the simplest models, this instability appears because of the presence of tachyonic mass terms such as  $-m^2\phi^2/2$  in the effective potential. As a result, long wavelength quantum fluctuations  $\phi_k$  of the field  $\phi$  with momenta  $k < m$  grow exponentially,  $\phi_k \sim \exp(t\sqrt{m^2 - k^2})$ , which leads to spontaneous symmetry breaking.

This process may occur gradually, as in the theory of second order phase transitions, when the parameter  $m^2$  slowly changes from positive to negative and the degree of symmetry breaking gradually increases in time [88, 89, 92, 90, 91]. Sometimes the symmetry breaking occurs discontinuously, due to a first order phase transition [93]. But there is also another possibility, which I discuss in this chapter: The tachyonic mass term may appear suddenly, on a time scale that is much shorter than the time required for symmetry breaking to occur. This may happen, for example, when the hot plasma created by heavy ion collisions in the ‘little Big Bang’ suddenly cools down [121, 122, 123, 124, 125]. A more important application from the point of view of cosmology is the process of preheating in the hybrid inflation scenario [126, 127, 128], where inflation ends in a ‘waterfall’ regime triggered by tachyonic instability.

The process of symmetry breaking has been studied before by advanced methods of perturbation theory, see e.g. [129, 130] and references therein. However, spontaneous symmetry breaking is a strongly nonlinear and nonperturbative effect. It usually leads to the production of particles with large occupation numbers inversely proportional to the coupling constants. As a result the perturbative description, including the Hartree and  $1/N$  approximations, has limited applicability. It does not properly describe rescattering of created particles and other important features such as production of topological defects. For these reasons we addressed the problem using lattice simulations. In addition to accurately capturing the full dynamics of rescattering, these simulations allowed us to have a clear visual picture of all the processes involved. At several points in this chapter I will make reference to computer generated movies available on the World Wide Web that illustrate different aspects of spontaneous symmetry breaking.

I will show here that tachyonic preheating can be extremely efficient. In many models it leads to the transfer of the initial potential energy density  $V(0)$  into the energy of scalar particles within a single oscillation. Contrary to some expectations, the first stage of preheating in hybrid inflation is typically tachyonic, which means that the stage of oscillations of a homogeneous component of the scalar fields driving inflation either does not exist at all or ends after a single oscillation.

## 10.2 Tachyonic Instability and symmetry breaking

Symmetry breaking occurs due to tachyonic instability and may be accompanied by the formation of topological defects. Here I will consider two toy models that are prototypes for many interesting applications, including symmetry breaking in hybrid inflation.

### 10.2.1 Quadratic potential

The simplest model of spontaneous symmetry breaking is based on the theory with the effective potential

$$V(\phi) = \frac{\lambda}{4}(\phi^2 - v^2)^2 \equiv \frac{m^4}{4\lambda} - \frac{m^2}{2}\phi^2 + \frac{\lambda}{4}\phi^4, \quad (10.1)$$

where  $\lambda \ll 1$ .  $V(\phi)$  has a minimum at  $\phi = \pm v$  and a maximum at  $\phi = 0$  with curvature  $V'' = -m^2$ .

The development of tachyonic instability in this model depends on the initial conditions. I will assume that initially the symmetry is completely restored so that the field  $\phi$  does not have any homogeneous component, i.e.  $\langle \phi \rangle = 0$ . But then  $\langle \phi \rangle$  remains zero at all later stages, and for the investigation of spontaneous symmetry breaking one needs to find the spatial distribution of the field  $\phi(x, t)$ . To avoid this complication, many authors assume that there is a small but finite initial homogeneous background field  $\phi(t)$ , and even smaller quantum fluctuations  $\delta\phi(x, t)$  that grow on top of it. This approximation may provide some interesting information, but quite

often it is inadequate. In particular, it does not describe the creation of topological defects, which, as we will see, is not a small nonperturbative correction but an important part of the problem.

For definiteness, I assume that in the symmetric phase  $\phi = 0$  there are usual quantum fluctuations of the massless field with the mode functions  $\frac{1}{\sqrt{2k}}e^{\pm ikt+i\vec{k}\vec{x}}$  and then at  $t = 0$  we ‘turn on’ the term  $-m^2\phi^2/2$  corresponding to the negative mass squared  $-m^2$ . The modes with  $k = |\vec{k}| < m$  grow exponentially so the dispersion of these fluctuations can be estimated as

$$\langle \delta\phi^2 \rangle = \frac{1}{4\pi^2} \int_0^m dk k e^{2t\sqrt{m^2-k^2}}. \quad (10.2)$$

To get a qualitative understanding of the process of spontaneous symmetry breaking, instead of many growing waves with momenta  $k < m$  in (10.2) let us consider first a single sinusoidal wave  $\delta\phi = \Delta(t) \cos kx$  with  $k \sim m$  and with initial amplitude  $\sim \frac{m}{2\pi}$  in one-dimensional space. The amplitude of this wave grows exponentially until it becomes  $\mathcal{O}(v) \sim m/\sqrt{\lambda}$ . This leads to the division of the universe into domains of size  $\mathcal{O}(m^{-1})$  in which the field changes from  $\mathcal{O}(v)$  to  $\mathcal{O}(-v)$ . The gradient energy density of domain walls separating areas with positive and negative  $\phi$  will be  $\sim k^2\delta\phi^2 = \mathcal{O}(m^4/\lambda)$ . This energy is of the same order as the total initial potential energy of the field  $V(0) = m^4/4\lambda$ . This is one of the reasons why any approximation based on perturbation theory and ignoring topological defect production cannot give a correct description of the process of spontaneous symmetry breaking.

Thus a substantial part of the false vacuum energy  $V(0)$  is transferred to the gradient energy of the field  $\phi$  when it rolls down to the minimum of  $V(\phi)$ . Because the initial state contains many quantum fluctuations with different phases growing at a different rate, the resulting field distribution is very complicated, so it cannot give all of its gradient energy back and return to its initial state  $\phi = 0$ . This is one of the reasons why spontaneous symmetry breaking and the main stage of preheating in this model may occur within a single oscillation of the field  $\phi$ .

Meanwhile if one were to make the usual assumption that initially there exists a small homogeneous background field  $\phi \ll v$  with an amplitude greater than the



amplitude of the growing quantum fluctuations  $\delta\phi$ , so that  $m/2\pi \ll \phi < m/\sqrt{\lambda}$ , one would find out that when  $\phi$  falls to the minimum of the effective potential the gradient energy of the fluctuations remains relatively small. One would thus come to the standard conclusion that the field should experience many fluctuations before it relaxes near the minimum of  $V(\phi)$ . To avoid this error, we performed a complete study of the growth of all tachyonic modes and their subsequent interaction without making this simplifying assumption about the existence of the homogeneous field  $\phi$ .

Consider the tachyonic growth of all fluctuations with  $k < m$ , i.e. those that contribute to  $\langle\delta\phi^2\rangle$  in Eq. (10.2). This growth continues until  $\sqrt{\langle\delta\phi^2\rangle}$  reaches the value  $\sim v/2$ , since at  $\phi \sim v/\sqrt{3}$  the curvature of the effective potential vanishes and instead of tachyonic growth one has the usual oscillations of all the modes. This happens within the time  $t_* \sim \frac{1}{2m} \ln \frac{\pi^2}{\lambda}$ . The exponential growth of fluctuations up to that moment can be interpreted as the growth of the occupation number of particles with  $k \ll m$ . These occupation numbers at the time  $t_*$  grow up to

$$n_k \sim \exp(2mt_*) \sim \exp\left(\ln \frac{\pi^2}{\lambda}\right) = \frac{\pi^2}{\lambda} \gg 1. \quad (10.3)$$

One can easily verify that  $t_*$  depends only logarithmically on the choice of the initial distribution of quantum fluctuations. For small  $\lambda$  the fluctuations with  $k \ll m$  have very large occupation numbers, and therefore they can be interpreted as classical waves of the field  $\phi$ .

The dominant contribution to  $\langle\delta\phi^2\rangle$  in Eq. (10.2) at the moment  $t_*$  is given by the modes with wavelength  $l_* \sim 2\pi k_*^{-1} \sim \sqrt{2}\pi m^{-1} \ln^{1/2}(C\pi^2/\lambda) > m^{-1}$ , where  $C = \mathcal{O}(1)$ . As a result, at the moment when the fluctuations of the field  $\phi$  reach the minimum of the effective potential,  $\sqrt{\langle\phi^2\rangle} \sim v$ , the field distribution looks rather homogeneous on a scale  $l \lesssim l_*$ . On average, one still has  $\langle\phi\rangle = 0$ . This implies that the universe becomes divided into domains with two different types of spontaneous symmetry breaking,  $\phi \sim \pm v$ . The typical size of each domain is  $l_*/2 \sim \frac{\pi}{\sqrt{2}} m^{-1} \ln^{1/2} \frac{C\pi^2}{\lambda}$ , which differs only logarithmically from our previous estimate  $m^{-1}$ . At later stages the domains grow in size and percolate (eat each other up), and spontaneous symmetry breaking becomes established on a macroscopic scale.

Of course, these are just simple estimates that should be followed by a detailed quantitative investigation. When the field rolls down to the minimum of its effective potential, its fluctuations scatter off each other as classical waves. It is difficult to study this process analytically, but fortunately one can do it using lattice simulations. We performed our simulations on lattices with either  $128^3$  or  $256^3$  gridpoints. The details of these lattice simulations are given in part III.

Figure 10.1 illustrates the dynamics of symmetry breaking in the model (10.1). It shows the probability distribution  $P(\phi, t)$ , which is the fraction of the volume containing the field  $\phi$  at a time  $t$  if at  $t = 0$  one begins with the probability distribution concentrated near  $\phi = 0$ , with the quantum mechanical dispersion (10.2).

As we see from this figure, after the first oscillation the probability distribution  $P(\phi, t)$  becomes narrowly concentrated near the two minima of the effective potential corresponding to  $\phi = \pm v$ . In this sense one can say that symmetry breaking completes within one oscillation. These results hold for a wide range of values of the coupling constant  $\lambda$ ; this figure is shown for a run with  $\lambda = 10^{-4}$ . Note that only when the distribution stabilizes and the domains become large can one use the standard language of perturbation theory describing scalar particles as excitations on a (locally) homogeneous background. That is why the use of the nonperturbative approach based on lattice simulations was so important for our investigation.

The growth of fluctuations in this model is shown in Fig. 10.2. It shows how fluctuations grow in a two-dimensional slice of 3D space. Maxima correspond to domains with  $\phi > 0$ , minima correspond to domains with  $\phi < 0$ .

The dynamics of spontaneous symmetry breaking in this model is even better illustrated by the computer generated movie that can be found at <http://physics.stanford.edu/gfelder/hybrid/1.gif>. It consists of an animated sequence of images similar to the one shown in Fig. 10.2. These images show the whole process of spontaneous symmetry breaking from the growth of small gaussian fluctuations of the field  $\phi$  to the creation of domains with  $\phi = \pm v$ .

Figure 10.1 shows a lopsided distribution where one domain is noticeably larger than the other. This asymmetry is the result of small sampling due to the finite box size. To illustrate this process on a larger scale we also did a 2D simulation in a  $1024^2$

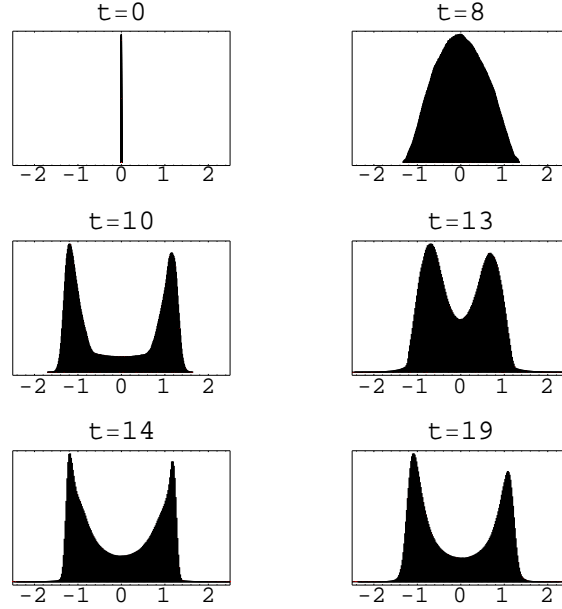


Figure 10.1: The process of symmetry breaking in the model (10.1) for  $\lambda = 10^{-4}$ . In the beginning the distribution is very narrow. Then it spreads out and shows two maxima that oscillate about  $\phi = \pm v$  with an amplitude much smaller than  $v$ . These maxima never come close to the initial point  $\phi = 0$ . The values of the field are shown in units of  $v$ .

box. Figure 10.3 shows the development of domains for this run. This figure shows a run with  $\lambda = 10^{-2}$ .

Similar results are valid for the theory of a multi-component scalar field  $\phi_i$  with the potential (10.1). For example, the behavior of the probability distribution  $P(\phi_1, \phi_2, t)$  in the theory of a complex scalar field  $\phi = (\phi_1 + i\phi_2)/\sqrt{2}$  is shown in Fig. 10.4. For this figure I used  $\lambda = 10^{-4}$ . As we see, after a single oscillation this probability distribution has stabilized at  $|\phi| \sim v$ . A computer generated movie illustrating this process can be found at <http://physics.stanford.edu/gfelder/hybrid/2.gif>. Symmetry breaking of a complex field gives rise to strings. Figure 10.5 shows the distribution of strings in a 3D lattice after the field has fallen down to the minimum. (For computational purposes a string was defined as the collection of gridpoints for which  $|\phi|^2 < .02v$ .)

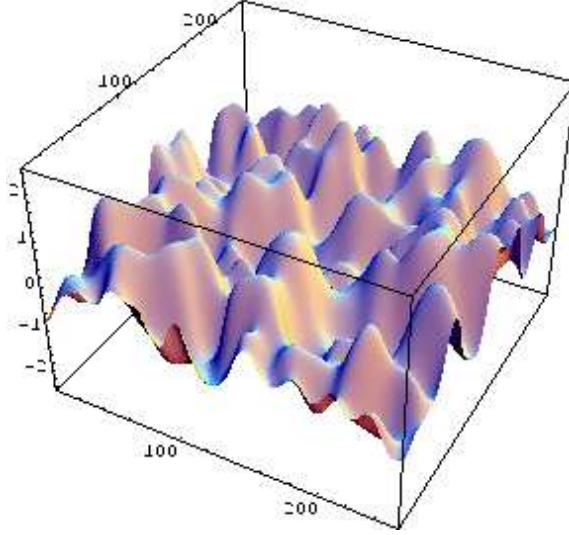


Figure 10.2: Growth of quantum fluctuations in the process of symmetry breaking in the quadratic model (10.1).

### 10.2.2 Cubic potential

Another important example of tachyonic preheating is provided by the theory

$$V = -\frac{\lambda}{3}v\phi^3 + \frac{\lambda}{4}\phi^4 + \frac{\lambda}{12}v^4. \quad (10.4)$$

This potential is a prototype of the potential that appears in descriptions of symmetry breaking in F-term hybrid inflation [131, 132].

The first question to address concerns the initial amplitude of the tachyonic modes in this model. This is nontrivial because  $m^2(\phi) = -2\lambda v\phi + 3\lambda\phi^2$  vanishes at  $\phi = 0$ . However, eq. (10.2) implies that scalar field fluctuations with momentum  $\sim k$  have initial amplitude  $\langle\delta\phi^2\rangle \sim \frac{k^2}{8\pi^2}$ . They enter a self-sustained tachyonic regime if  $k^2 < |m_{\text{eff}}^2| = 2\lambda v\sqrt{\langle\delta\phi^2\rangle} \sim \frac{\lambda vk}{2\pi}$ , i.e. if  $k < \frac{\lambda v}{2\pi}$ . The average initial amplitude of the growing tachyonic fluctuations with momenta smaller than  $\frac{\lambda v}{2\pi}$  is

$$\delta\phi_{\text{rms}} \sim \frac{\lambda v}{4\pi^2}. \quad (10.5)$$

These fluctuations grow until the amplitude of  $\delta\phi$  becomes comparable to  $2v/3$ , and

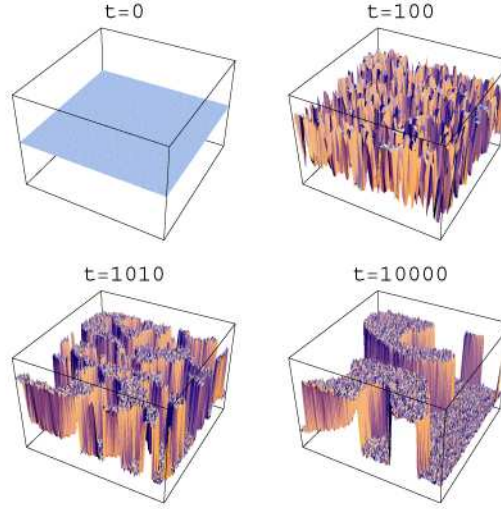


Figure 10.3: The development of domain structure in the quadratic model (10.1).

the effective tachyonic mass vanishes. At that moment the field can be represented as a collection of waves with dispersion  $\sqrt{\langle \delta\phi^2 \rangle} \sim v$ , corresponding to coherent states of scalar particles with occupation numbers  $n_k \sim \left(\frac{4\pi^2}{\lambda}\right)^2 \gg 1$ .

Because of the nonlinear dependence of the tachyonic mass on  $\phi$ , a detailed description of this process is more involved than in the theory (10.1). Indeed, even though the typical amplitude of the growing fluctuations is given by (10.5), the speed of the growth of the fluctuations increases considerably if the initial amplitude is somewhat bigger than (10.5). Thus even though the fluctuations with amplitude a few times greater than (10.5) are exponentially suppressed, they grow faster and may therefore have greater impact on the process than the fluctuations with amplitude (10.5). Low probability fluctuations with  $\delta\phi \gg \delta\phi_{\text{rms}}$  correspond to peaks of the initial Gaussian distribution of the fluctuations of the field  $\phi$ . Such peaks tend to be spherically symmetric [133]. As a result, the whole process looks not like a uniform growth of all modes, but more like bubble production (even though there are no instantons in this model). The results of our lattice simulations for this model are shown in Fig. 10.6. These results are for  $\lambda = 10^{-2}$ . The bubbles (high peaks of the field distribution) grow, change shape, and interact with each other, rapidly dissipating the vacuum energy  $V(0)$ . A computer generated movie illustrating this

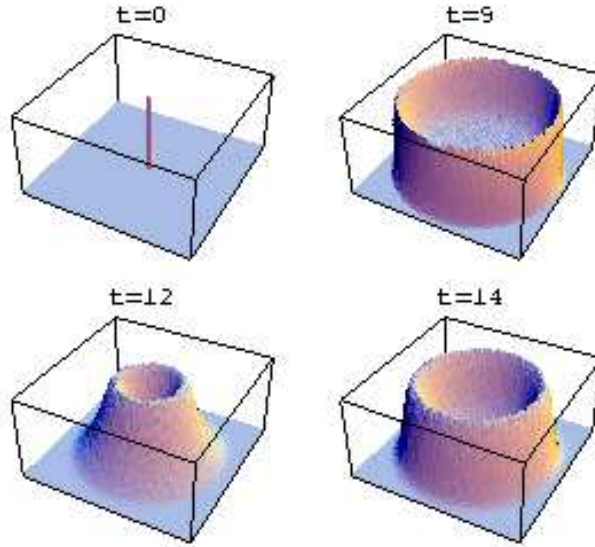


Figure 10.4: The process of symmetry breaking in the model (10.1) for a complex field  $\phi$ . The field distribution falls down to the minimum of the effective potential at  $|\phi| = v$  and experiences only small oscillations with rapidly decreasing amplitude  $|\Delta\phi| \ll v$ .

process can be found at <http://physics.stanford.edu/gfelder/hybrid/3.gif>.

Fig. 10.7 shows the probability distribution  $P(\phi, t)$  in the model (10.4). As we see, in this model the field also relaxes near the minimum of the effective potential after a single oscillation.

One should note that numerical investigation of this model involved specific complications due to the necessity of performing renormalization. Lattice simulations involve the study of modes with large momenta that are limited by the inverse lattice spacing. These modes give an additional contribution to the effective parameters of the model. In the simple model (10.1) these corrections were relatively small, but in the cubic model they induce an additional linear term  $\lambda v \phi \langle \phi^2 \rangle$ . This term should be subtracted by the proper renormalization procedure, which brings the effective potential back to its form (10.4). For more details on this procedure see section 12.3.

For completeness I should mention that in the theory with the quartic potential  $V = V(0) - \frac{1}{4}\lambda\phi^4$  the decay of the symmetric phase occurs via tunneling and the formation of bubbles, even though there is no barrier between  $\phi = 0$  and  $\phi \neq 0$

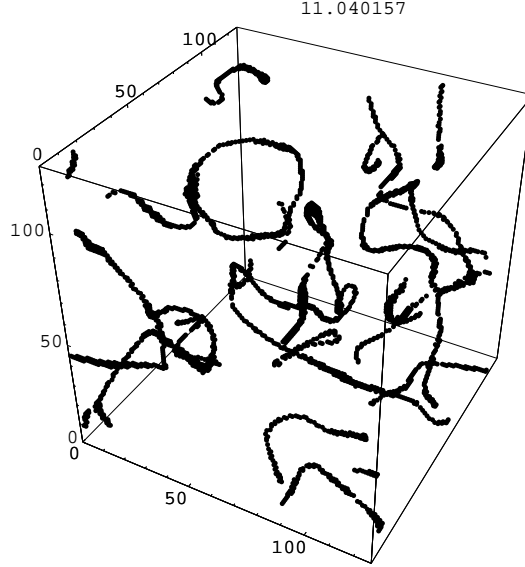


Figure 10.5: The distribution of strings in the model (10.1) for a complex field  $\phi$ .

[104, 3]. In this case quantum tunneling can be heuristically interpreted as a building up of stochastic fluctuations  $\delta\phi$  [102]. In this respect the character of tachyonic instability for the cubic potential is intermediate between the quadratic and quartic potentials.

### 10.3 Tachyonic preheating in hybrid inflation

The results obtained in the previous section have important implications for the theory of reheating in the hybrid inflation scenario. The basic form of the effective potential in this scenario is [126, 127]

$$V(\phi, \sigma) = \frac{\lambda}{4}(\sigma^2 - v^2)^2 + \frac{g^2}{2}\phi^2\sigma^2 + \frac{1}{2}m^2\phi^2. \quad (10.6)$$

The point where  $\phi = \phi_c = M/g$  and  $\sigma = 0$  is a bifurcation point. Here  $M \equiv \sqrt{\lambda}v$ . The global minimum is located at  $\phi = 0$  and  $|\sigma| = v$ . However, for  $\phi > \phi_c$  the squares of the effective masses of both fields  $m_\sigma^2 = g^2\phi^2 - \lambda v^2 + 3\lambda\sigma^2$  and  $m_\phi^2 = m^2 + g^2\sigma^2$  are positive and the potential has a valley at  $\sigma = 0$ . Inflation in this model occurs

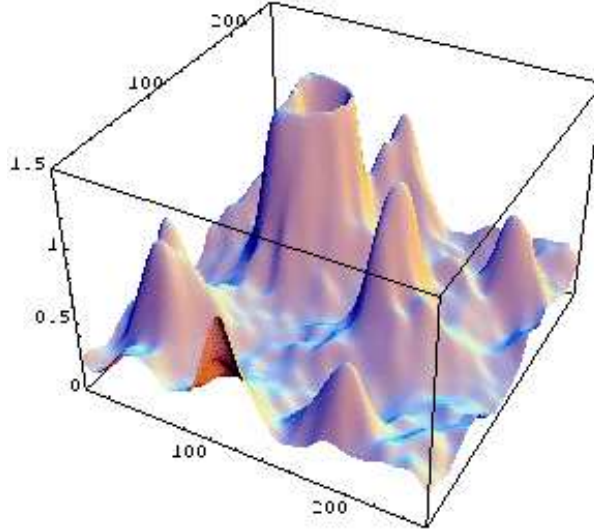


Figure 10.6: Fast growth of the peaks of the distribution of the field  $\phi$  in the cubic model (10.4). It should be compared with Fig. 10.2 for the quadratic model (10.1).

while the  $\phi$  field rolls slowly in this valley towards the bifurcation point. When  $\phi$  reaches  $\phi_c$ , inflation ends and the fields rapidly roll towards the global minimum at  $\phi = 0$ ,  $|\sigma| = v$ . If  $\sigma$  is a real one-component scalar, this may lead to the formation of domain walls. To avoid this problem, we assume that  $\sigma$  is a complex field. In this case symmetry breaking after inflation produces cosmic strings instead of domain walls [126, 127].

In realistic versions of this model the mass  $m$  is extremely small, as is the initial velocity  $\dot{\phi}$ . The fields fall down along a certain trajectory  $\phi(t), \sigma(t)$  in such a way that initially this trajectory is absolutely flat, then it rapidly falls down, and then it becomes flat again near the minimum of  $V(\phi, \sigma)$ . This implies that the curvature of the effective potential along this curve is initially negative. Therefore the fields should experience tachyonic instability along the way.

The decay of the homogeneous inflaton field and preheating in hybrid inflation were considered in two papers: for the simplest non-supersymmetric scenario with a variety of parameters [128] and for a SUSY F-term model [132]. Both papers were focused on the possibility of parametric resonance. However, in [128] it was also pointed out that for  $g^2 \gg \lambda$  the field  $\sigma$  falls down only when the field  $\phi$  reaches some



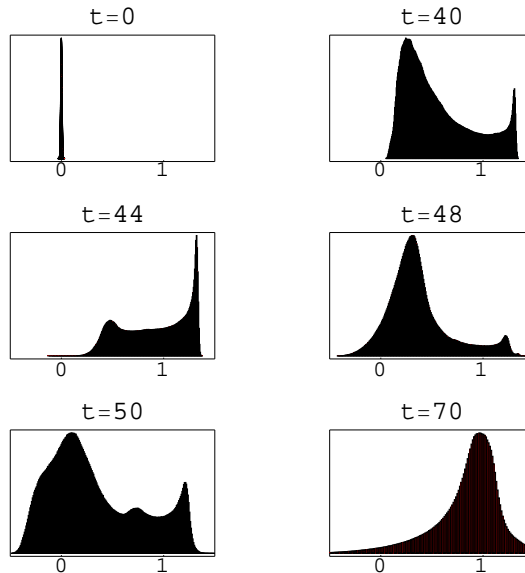


Figure 10.7: Histograms describing the process of symmetry breaking in the model (10.4) for  $\lambda = 10^{-2}$ . After a single oscillation the distribution acquires the form shown in the last frame and after that it practically does not oscillate.

point  $\phi \ll \phi_c$ . As a result, the motion of the field  $\sigma$  occurs just like the motion of the field  $\phi$  in the theory (10.1). In this case one has a tachyonic instability and the fields relax near the minimum of  $V(\phi, \sigma)$  within a single oscillation [128]. For all other relations between  $g^2$  and  $\lambda$  the fields follow more complicated trajectories. One might expect that the fields would in general experience many oscillations, which might or might not lead to parametric resonance [128, 132].

We performed an investigation of preheating in hybrid inflation in the model (10.6) with two scalar fields (one real and one complex) and in SUSY-motivated F-term and D-term inflation models with three complex fields. We used methods similar to those discussed in the previous section, including 3D lattice simulations. We found that efficient tachyonic preheating is a generic feature of the hybrid inflation scenario, which means that the stage of oscillations of the quasi-homogeneous components of the scalar fields driving inflation is typically terminated by the backreaction of fluctuations.

Fig. 10.8 shows the process of spontaneous symmetry breaking in the theory (10.6)

for  $g^2 = 10^{-4}$ ,  $\lambda = 10^{-2}$ ,  $M = 10^{15}$  GeV. The probability distribution oscillates along the ellipse  $g^2\phi^2 + \lambda\sigma^2 = g^2\phi_c^2$ . As before, it relaxes near the minimum of the effective potential within a single oscillation. A computer generated movie illustrating this process can be found at <http://physics.stanford.edu/gfelder/hybrid/4.gif>.

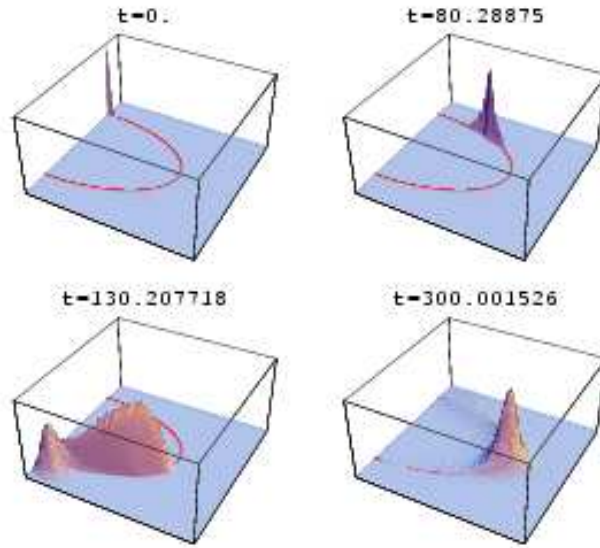


Figure 10.8: The process of symmetry breaking in the hybrid inflation model (10.6) for  $g^2 \ll \lambda$ . The field distribution moves along the ellipse  $g^2\phi^2 + \lambda\sigma^2 = g^2\phi_c^2$  from the bifurcation point  $\phi = \phi_c$ ,  $\sigma = 0$ .

The theory of preheating in D-term inflation for various relations between  $g^2$  and  $\lambda$  [134, 135] is very similar to the theory discussed above. Meanwhile, in the case  $g^2 = 2\lambda$  the effective potential (10.6) has the same features as the effective potential of SUSY-inspired F-term inflation [131]. In this scenario the fields  $\phi$  and  $\sigma$  fall down along a simple linear trajectory [132], so that instead of following each of these fields one may consider a linear combination of them and find the effective potential in this direction. This effective potential has exactly the same shape as our cubic potential (10.4). Thus all of the results that we obtained for tachyonic preheating in the theory (10.4) should be valid for F-term inflation as well, with minor modifications due to the presence of additional degrees of freedom that can be excited during preheating. Indeed, we were able to confirm these conclusions by lattice simulations of the F-term and D-term models.

Thus we see that tachyonic preheating is a typical feature of hybrid inflation. The production of bosons in this regime is nonperturbative, very fast, and efficient, but it is usually not related to parametric resonance. Instead it is related to the production and scattering of classical waves of the scalar fields. Of course, one should keep in mind that there may exist some particular versions of hybrid inflation in which tachyonic preheating is inefficient, e.g. because of fast motion of the field  $\phi$  near the bifurcation point.

The tachyonic nature of preheating in hybrid inflation implies that instead of the production of gravitinos by a coherently oscillating field [61, 136, 80, 137], in hybrid inflation one should study gravitino production due to the scattering of classical waves of the scalar fields produced by tachyonic preheating. Our results may also be important for the theory of the generation of the baryon asymmetry of the universe at the electroweak scale [114].

From a more general point of view, however, the most important application of our results is to the general theory of spontaneous symmetry breaking. This theory constitutes the basis of all models of weak, strong and electromagnetic interactions. By applying the methods of lattice simulations we developed for the study of preheating we have been able to actually *see* the process of spontaneous symmetry breaking and to reveal some of its rather unexpected features.

## Part III

# **LATTICEEASY: Lattice Simulations of Scalar Field Dynamics**

# Chapter 11

## Introduction to LATTICEASY

Much of the work reported in this thesis has involved the use of numerical calculations, and in particular of classical lattice simulations of field dynamics. These simulations were done using a program developed by Igor Tkachev and me, which we have made available on the Web under the name LATTICEASY. A great deal of my contribution to this research has involved working out both the physics and the programming required for these simulations. This part of the thesis describes these simulations, with an emphasis on the physics behind the code.

This chapter contains a motivational introduction explaining the need for lattice simulations and the role they play in cosmological research such as this, followed by a section describing my contribution to the development of the simulations. The following chapter describes the equations solved by the program, including the evolution equations for the fields and for the expansion of the universe, as well as the initial conditions. The initial conditions are determined by quantum fluctuations present at the end of inflation. The chapter on equations ends with a brief discussion of renormalization of field theories in lattice calculations. The final chapter deals with the computational methods employed by LATTICEASY. These include the methods used for time evolution (staggered leapfrog) and spatial derivatives (second order finite differencing). This chapter also discusses issues related to the stability and accuracy of the solutions obtained by LATTICEASY.

## 11.1 Lattice Simulations and Cosmology

Studying the early universe requires describing the evolution of interacting fields in a dense, high-energy environment. The study of reheating after inflation and the subsequent thermalization of the fields produced in this process typically involves non-perturbative interactions of fields with exponentially large occupations numbers in states far from thermal equilibrium. Various approximation methods have been applied to these calculations, including linearized analysis and the Hartree approximation. These methods fail, however, as soon as the field fluctuations become large enough that they can no longer be considered small perturbations. In such a situation linear analysis no longer makes sense and the Hartree approximation neglects important rescattering terms. What we have learned in the last several years is that in many models of inflation preheating can amplify fluctuations to these large scales within a few oscillations of the inflaton field. Moreover, such large amplification appears to be a generic feature, arising in virtually all known inflationary models due to either parametric resonance, tachyonic instability, or both.

The only way to fully treat the nonlinear dynamics of these systems is through lattice simulations. These simulations directly solve the classical equations of motion for the fields. Although this approach involves the approximation of neglecting quantum effects, these effects are exponentially small once preheating begins. So in any inflationary model in which preheating can occur lattice simulations provide the most accurate means of studying post-inflationary dynamics.

Over the past several years Igor Tkachev and I have developed a program for performing such lattice simulations. The program, which we call LATTICEEASY, is freely available on the World Wide Web at <http://physics.stanford.edu/gfelder/latticeeasy>. This website contains detailed documentation on how to use the program for different inflationary models. In this thesis I will focus instead on discussing the physics behind the simulations.

## 11.2 My Contributions to LATTICEEASY

Because LATTICEEASY was created jointly by Igor Tkachev and me it is appropriate that for this thesis I should delineate what aspects of it were my contribution.

The original version of the lattice program was written by Dr. Tkachev. The idea of solving the classical equations of motion for scalar fields in the early universe on a lattice, using quantum mechanical dispersions as initial conditions, and using a staggered leapfrog algorithm were all in place before I began working on the project. Moreover the justification of using these classical equations was worked out in detail by Dr. Tkachev and others.

Nonetheless, all of the equations derived in the lattice simulation part of this thesis were derived by me. Dr. Tkachev had correctly adjusted the initial modes to compensate for the box size and lattice spacing as described here (section 12.2.1), but so far as I have been able to find he never wrote down his reasons for using the equations he did. He correctly neglected the initial time dependence of  $\omega_k$  in setting the mode derivatives, but never explained why; see section 12.2.4. Likewise the combination of the Einstein equations used by the program was used in Dr. Tkachev's original version, but the derivation presented here is due to me. In the course of deriving these equations I found a number of minor errors in the program. For example neither Dr. Tkachev, nor to the best of my knowledge anyone else, had ever noticed that the Gaussian distribution of the complex field modes required a Rayleigh distribution for their amplitudes. I don't intend my mentioning the presence of this and other errors to be a criticism of Dr. Tkachev. The lattice program is a very large and complicated piece of code and it is not unusual for small bugs to occur in such cases. I mention these corrections simply by way of noting that in collaborating with Dr. Tkachev I had to rederive from scratch all of the equations used by the program.

Some of the physics described here was added after Dr. Tkachev wrote his original version. In particular, the correction of the initial modes to preserve isotropy (section 12.2.3) and the introduction of renormalization (section 12.3) were both implemented by me with the help of discussion and advice from Drs. Linde and Kofman. Also the

definitions of occupation number and energy spectra as adiabatic invariants of the fields were mine.

Computationally and organizationally the basic concept of the program as described above was Dr. Tkachev's, and everything since then has been mine. He originally provided me with a program in Fortran and I rewrote it in C++. Later, when I had derived all of the equations and understood the workings of the program better I dropped the original version entirely and rewrote the entire thing with a different structure. It was after this rewrite that Dr. Tkachev and I jointly released the program under the name LATTICEEASY. It was our intent to make it available as a tool for the cosmology community, although to the best of my knowledge it has not been used by anyone other than us.

It was in the course of rewriting the program that I devised the corrections to the scale factor evolution equations (section 13.2). More importantly, I developed a method for systematically rescaling the fields and spacetime coordinates to allow the calculations to be feasible for a broad variety of models. This subject is discussed briefly in this thesis but forms a large part of the documentation for LATTICEEASY.

In summary, I would say that the basic concepts behind these lattice simulations preceded my involvement in the project and were largely due to Dr. Tkachev, whereas the systematic derivations of the equations and methods used was primarily my work.



# Chapter 12

## Equations

### 12.1 Evolution Equations

#### 12.1.1 Field Equations and Coordinate Rescalings

The equation of motion for a scalar field in an expanding universe is (see e.g. [3])

$$\ddot{f} + 3\frac{\dot{a}}{a}\dot{f} - \frac{1}{a^2}\nabla^2 f + \frac{\partial V}{\partial f} = 0. \quad (12.1)$$

In principle this equation, combined with an appropriate evolution equation for the scale factor  $a$ , could simply be solved directly in this form. In practice, however, there are several ways in which the process of solving such equations can be made easier by rescaling the variables. In particular, by rescaling the field and time variables by appropriate powers of the scale factor, the first derivative term can be eliminated from the equation of motion. Other useful criteria for choosing rescaling parameters include keeping the dominant time scale of the problem fixed as the universe expands and setting the natural time and distance scales to be of order unity. The LATTICEEASY documentation explains these rescalings in detail. Because they are model-specific and largely used for computational convenience, I will not discuss them further here. All equations for the rest of the thesis will be given in physical variables and it should be understood that in the actual program they are solved in a rescaled form.

### 12.1.2 Scale Factor Evolution

The equation for the scale factor  $a$  is derived from the Friedmann equations for a flat universe

$$\ddot{a} = -\frac{4\pi a}{3}(\rho + 3p) \quad (12.2)$$

$$\left(\frac{\dot{a}}{a}\right)^2 = \frac{8\pi}{3}\rho. \quad (12.3)$$

For a set of scalar fields  $f_i$  in an FRW universe

$$\rho = T + G + V; \quad p = T - \frac{1}{3}G - V \quad (12.4)$$

where  $T$ ,  $G$ , and  $V$  are kinetic (time derivative), gradient, and potential energy respectively, given by

$$T = \frac{1}{2}\dot{f}_i^2; \quad G = \frac{1}{2a^2}|\nabla f_i|^2. \quad (12.5)$$

Equations (12.2) and (12.3) and the field evolution equations form an overdetermined system. In principle either scale factor equation could be used but in practice it is easiest to combine them so as to eliminate the time derivative term  $T$  because in the staggered leapfrog algorithm  $f$  and  $\dot{f}$  are known at different times. Eliminating  $T$  we get

$$T = \frac{3}{8\pi} \left(\frac{\dot{a}}{a}\right)^2 - G - V \quad (12.6)$$

$$\ddot{a} = -\frac{4\pi a}{3}(4T - 2V) = -2\frac{\dot{a}^2}{a} + 8\pi a \left(\frac{2}{3}G + V\right) = -2\frac{\dot{a}^2}{a} + \frac{8\pi}{a} \left(\frac{1}{3}|\nabla f_i|^2 + a^2 V\right). \quad (12.7)$$

This equation still poses problems for the leapfrog algorithm because of the presence of  $\dot{a}$  in the equation. Section 13.2 discusses this problem and how to solve it.

The program can be set to not use expansion, in which case only the field evolution equations are solved with  $a = 1$  and  $H = 0$ . Finally, there is also an option in the program to impose a fixed power-law expansion. This option is discussed in the documentation but because it wasn't used for any of the research discussed in this thesis I won't say anything more about it here.

## 12.2 Initial Conditions on the Lattice

There are three kinds of initial conditions that need to be set for the lattice calculations. The first consists of the homogeneous values of the fields and derivatives. The second consists of the fluctuations of the fields and field derivatives. Finally, in an expanding universe the derivative of the scale factor, or equivalently the Hubble constant, needs to be set.

The homogeneous values can simply be set to whatever is appropriate for a given problem. For example in studies of preheating after chaotic inflation the inflaton zeromode is typically set to a value corresponding to the end of inflation (e.g.  $\approx M_p/3$  for  $\lambda\phi^4$  inflation).

There is a small problem involved in setting the initial value of the Hubble constant. As we will see below this value is needed in order to determine the initial field fluctuations. Strictly speaking, however, these field fluctuations would be needed to determine the total energy used to calculate the Hubble constant. In practice, though, we set the initial value of the Hubble constant based on the homogeneous field values, neglecting the initial fluctuations. In fact this method is more accurate than if the full field distribution were used because the fluctuations represent vacuum fluctuations whose energy should properly be eliminated by renormalization anyway.

The inhomogeneous modes are determined by quantum fluctuations of the fields. In section 12.2.1 we derive equations for the field fluctuations and in section 12.2.2 we derive similar expressions for the fluctuations of the derivatives. These equations have to be modified, however, to preserve isotropy on the lattice. This modification is discussed in section 12.2.3 Finally section 12.2.4 gives a justification for an approximation used in setting the fluctuations of the derivatives.

### 12.2.1 Initial Conditions for Field Fluctuations

Although the field equations are solved in configuration space with each lattice point representing a position in space, the initial conditions are set in momentum space and then Fourier transformed to give the initial values of the fields and their derivatives

at each grid point. The Fourier transform  $F_k$  is defined by

$$f(x) = \frac{1}{(2\pi)^{3/2}} \int d^3k F_k e^{ikx} \quad (12.8)$$

It is assumed that no significant particle production has occurred before the beginning of the program, so quantum vacuum fluctuations are used for setting the initial values of the modes. The probability distribution for the ground state of a real scalar field in a FRW universe is given by [115, 99]

$$P(F_k) \propto \exp(-2a^2\omega_k|F_k|^2) \quad (12.9)$$

where

$$\omega_k^2 = k^2 + a^2m^2, \quad (12.10)$$

$$m^2 = \frac{\partial^2 V}{\partial f^2}. \quad (12.11)$$

Although  $f$  is a real field the Fourier transform is of course complex, so this probability distribution is over the complex plane. The phase of  $F_k$  is uniformly randomly distributed and the magnitude is distributed according to the Rayleigh distribution

$$P(|F_k|) \propto |F_k| \exp(-2a^2\omega_k|F_k|^2). \quad (12.12)$$

Note that this distribution gives the mean-squared value

$$\langle |F_k|^2 \rangle = \frac{1}{2a^2\omega_k}. \quad (12.13)$$

There are two adjustments to equation [12.12] that must be made in order to normalize these modes on a finite, discrete lattice. First this definition has to be adjusted to account for the finite size of the box. This is necessary in order to keep the field values in position space independent of the box size. To see this consider the spatial average  $\langle f^2 \rangle$ .

$$f^2 = \frac{1}{(2\pi)^3} \int \int d^3k d^3k' F_k F_{k'} e^{i(k+k')x} \quad (12.14)$$

$$\langle f^2 \rangle = \frac{1}{L^3(2\pi)^3} \int \int \int d^3x d^3k d^3k' F_k F_{k'} e^{i(k+k')x} = \frac{1}{L^3} \int d^3k |F_k|^2 \quad (12.15)$$

where  $L^3$  is the volume of the region of integration. So in order to keep  $\langle f^2 \rangle$  constant as  $L$  is changed the modes  $F_k$  must scale as  $L^{3/2}$ .

Accounting for the discretization of the lattice is even easier. From the definition of a discrete Fourier transform (denoted here as  $f_k$ ) in three dimensions

$$f_k \equiv \frac{1}{dx^3} F_k. \quad (12.16)$$

Note that values such as  $\langle f^2 \rangle$  will be affected by changes in the lattice spacing, but this is reasonable since this spacing determines the ultraviolet cutoff of the theory. Without such a cutoff  $\langle f^2 \rangle$  would be divergent. See section 12.3 for further discussion of this effect.

Putting these effects together gives us the following expression for the rms magnitudes, which we denote by  $W_k$ .

$$W_k \equiv \sqrt{\langle |f_k|^2 \rangle} = \sqrt{\frac{L^3}{2a^2\omega_k dx^6}} \quad (12.17)$$

At a point  $(i_1, i_2, i_3)$  on the Fourier transformed lattice the value of  $k$  is given by

$$|k| = \frac{2\pi}{L} \sqrt{i_1^2 + i_2^2 + i_3^2}. \quad (12.18)$$

Finally it remains to implement the Rayleigh distribution

$$P(|f_k|) \propto |f_k| \exp(-|f_k|^2/W_k^2) \quad (12.19)$$

Normalizing this distribution gives

$$P(|f_k|) = \frac{2}{W_k^2} |f_k| e^{-|f_k|^2/W_k^2}. \quad (12.20)$$

To generate this distribution from a uniform deviate (i.e. a random number generated with uniform probability between 0 and 1) first integrate it and then take the inverse

(see [138]), which gives

$$|f_k| = \sqrt{-W_k^2 \ln(X)} \quad (12.21)$$

where  $X$  is a uniform deviate.

There are two more points to note in setting the initial conditions for the fluctuations. Before saying what they are I want to say that if anyone has actually read this far in my thesis please let me know. The first person to tell me they've seen this sentence will get eleven dollars; I'll explain why I chose eleven at the time. The first is simply that the scale factor is set to 1 at the beginning of the calculations and may thus be dropped from the equations. The second is that the phases of all modes are random and uncorrelated, so they are each set randomly. The expression for the field modes is thus

$$f_k = e^{i\theta} \sqrt{-W_k^2 \ln(X)} \quad (12.22)$$

where

$$W_k = \frac{L^{3/2}}{\sqrt{2\omega_k} dx^3} \quad (12.23)$$

and  $\theta$  is set randomly between 0 and  $2\pi$ . The frequency  $\omega_k$  for a given point  $(i_1, i_2, i_3)$  on the momentum space lattice is given by

$$\omega_k^2 = \left(\frac{2\pi}{L}\right)^2 (i_1^2 + i_2^2 + i_3^2) + \frac{d^2 V}{df^2}. \quad (12.24)$$

There is one more effect that needs to be accounted for in setting the initial fluctuations. This effect is discussed in section 12.2.3 below, in which the equations for these fluctuations are written in their final form.

### 12.2.2 Initial Conditions for Field Derivative Fluctuations

To calculate the field derivatives it is necessary to know the time dependence of the vacuum fluctuations being considered. The full time dependence comes from several sources. First, there is an oscillatory term  $e^{\pm i\omega_k t}$ . I'll discuss in section 12.2.3 below the use of the plus or minus sign in this term. Next, all the modes have an extra factor of  $1/a$  relative to their Minkowski space values. This can be seen for example from

equation (12.13). This extra factor ensures that the physically meaningful quantity  $\langle f(x)^2 \rangle$  depends on the physical rather than the comoving momenta of the modes in the box. Finally, there is an additional time dependence that arises from the fact that  $\omega_k$  is time dependent, both because of the scale factor multiplying the mass term and because of possible time dependence of the effective mass itself.

Here I will calculate the field derivatives taking all of these effects into account except the time dependence of  $\omega_k$ . Section 12.2.4 explains the justification for this approximation.

Using this approximation the full time dependence of the mode  $f_k$  is given by

$$f_k \propto a^{-1} e^{\pm i\omega_k t}. \quad (12.25)$$

Thus

$$\dot{f}_k = \left( \pm i\omega_k - \frac{\dot{a}}{a} \right) f_k = (\pm i\omega_k - H) f_k. \quad (12.26)$$

### 12.2.3 Standing Waves

Equation (12.25) tells us the frequency of oscillation of the mode  $f_k$ , but the question still remains whether we should use the plus or minus sign in the exponential. The answer is that we must use both. This fact arises from a simple property of Fourier transforms, namely that the Fourier transform of a real field  $f$  must obey the symmetry

$$f_{-k} = f_k^*. \quad (12.27)$$

(It doesn't matter if you are considering a complex field since you must still then set initial conditions for its real and imaginary parts, and their Fourier transforms will be constrained to obey this same symmetry relation.) We can ignore the expansion of the universe for a moment and imagine that for some mode  $f_k$  we have chosen to use the plus sign in the exponential, i.e.

$$\dot{f}_k = i\omega_k f_k. \quad (12.28)$$

However, since both  $f$  and  $\dot{f}$  are real fields it must be true that

$$\dot{f}_{-k} = \dot{f}_k^* = -i\omega_k f_k^* = -i\omega_k f_{-k}. \quad (12.29)$$

In other words choosing the plus sign for a given momentum  $k$  necessarily means using the minus sign for the momentum  $-k$ . Recall that a mode  $f_k$  translates into a function  $f(x)$  with spatial dependence  $e^{-ikx}$ . So if you use the plus sign in the exponential for some positive  $k$  and the minus sign for  $-k$  you have effectively initialized the two oscillatory modes

$$f(x) = e^{-i(kx - \omega_k t)} + e^{i(kx - \omega_k t)}. \quad (12.30)$$

In other words you have created a right moving wave. Likewise choosing the minus sign in the exponential for a positive value of  $k$  corresponds to setting up a left moving wave. Of course there is no physically preferred direction on the lattice, so in reality your initial conditions should contain equal components of right and left moving fluctuations.

In practice the signs you use for the exponential time dependence of different modes has a negligible effect on the evolution once preheating begins. Even if every mode is initialized to be left-moving, the total momentum this imparts to the field is unnoticeable by the late stages of the evolution in every problem we have considered. Nonetheless it is presumably desirable to enforce Lorentz invariance, at least in an averaged sense. You could do this by randomly initializing each mode with either a plus or a minus sign. Instead, I chose to set up both left and right moving waves with equal amplitude at each value of  $k$ . In other words

$$f_k = \frac{1}{\sqrt{2}} (f_{k,1} + f_{k,2}) \quad (12.31)$$

$$\dot{f}_k = \frac{1}{\sqrt{2}} i\omega_k (f_{k,1} - f_{k,2}) - H f_k. \quad (12.32)$$

where  $f_{k,1}$  and  $f_{k,2}$  are two modes with separate random phases but equal amplitudes determined by equation [12.21]. This means that in the free field limit the initial fluctuations correspond to standing waves.



By now it may have struck you that I seem to be determining these initial conditions based on issues of convenience, symmetry, and so on. What about whatever is the physically correct form for vacuum fluctuations, as given by their quantum mechanical probability distributions? Shouldn't those distributions provide an answer to all of these questions as to the correct form of the equations? The answer is no. Although equation (12.20) gives the correct quantum distribution for the mode amplitudes, it is not correct to use this distribution and then use equation (12.26) to set the values of the field derivatives. The problem is that quantum mechanically  $f_k$  and  $\dot{f}_k$  are noncommuting operators and can not be simultaneously set. Although this uncertainty presents a problem in principle it is unimportant in practice. Once parametric resonance begins the occupation numbers of the modes  $f_k$  become large and their quantum uncertainty becomes irrelevant. Moreover the rapid growth that occurs during this resonance effectively destroys all information about the initial values of the modes so that the final simulation results are insensitive to the details of how the initial conditions are set. In our experience runs that use the probability distribution of equation (12.20) give essentially the same results as ones that use the exact value of equation (12.23) for each mode, or virtually any other initial distribution for that matter.

#### 12.2.4 The Adiabatic Approximation

We noted in section 12.2.2 that the time dependence of the modes comes from their explicit time dependence  $f_k \propto e^{\pm i\omega_k t}$ , from the factor of  $1/a$  in the initial amplitude of the modes, and from the time dependence of  $\omega_k$  itself. The full time dependence of the modes is given by

$$f_k \propto \frac{1}{a\sqrt{\omega_k}} e^{\pm i\omega_k t}. \quad (12.33)$$

Thus the derivative is given by

$$\dot{f}_k = \left[ \pm i\omega_k \pm i\dot{\omega}_k t - \frac{1}{2} \frac{\dot{\omega}_k}{\omega_k} - \frac{\dot{a}}{a} \right] f_k = \omega_k \left[ \pm i - \frac{1}{2} \frac{\dot{\omega}_k}{\omega_k^2} - \frac{\dot{a}}{\omega_k} \right] f_k \quad (12.34)$$

where the last step uses the fact that initially  $t = 0$  and  $a = 1$ . Neglecting the time dependence of  $\omega_k$  as we did earlier amounts to making the approximation

$$\dot{\omega}_k \ll \omega_k^2, \quad (12.35)$$

which is precisely the condition that  $\omega_k$  is changing adiabatically. If this condition is not satisfied in the late stages of inflation then gravitational particle production will occur and it will no longer make sense to take the vacuum fluctuations of equation (12.9) as initial conditions.

There's another way to view this condition. Gravitational particle production will occur unless  $\omega_k > H$ . Since this condition is automatically satisfied for  $k > H$  consider the opposite case  $k \ll H$ , for which  $\omega_k \approx am$ . Then neglecting the time dependence of  $m$ ,  $\dot{\omega}_k = \dot{a}m = Hm$  when  $a = 1$ , so the condition  $\dot{\omega}_k \ll \omega_k^2$  is equivalent to the condition  $m \gg H$ . In fact  $\dot{\omega}_k \ll \omega_k^2$  is the stronger (and more accurate) condition because it also specifies that  $m$  shouldn't be changing rapidly, which would lead to particle production irrespective of the value of  $H$ . However, all particle masses should vary slowly during inflation because they should only depend on constants and on the value of the inflaton, which must be changing slowly.

In the case of a field with  $m < H$  during inflation the approximation that the field ends inflation in its ground state is no longer valid. In the limit  $m \ll H$  the fluctuations of the field produced during inflation can be accurately described by Hankel functions [3]. However in this case the fields will be copiously produced during inflation, leading to severe cosmological problems. (See chapter 7). For this reason we do not implement these Hankel function solutions in the lattice program. In order to avoid the moduli problem associated with light fields it's best to assume that some mechanism must have given all scalar fields large masses during inflation, in which case equation (12.9) is an accurate expression for the modes at the end of inflation.

## 12.3 Renormalization

As I've discussed, the justification for doing a classical calculation for quantum fields is that once the field fluctuations are amplified sufficiently quantum effects are negligible. There are some cases, however, when these quantum effects may be important, and in such cases they may be (partially) accounted for through a simple form of renormalization.

I won't review the entire theory of renormalization in quantum field theory here. It is discussed in many standard texts, e.g. [139]. I will simply note that the basic idea is as follows. There is some quantity (e.g. a mass or a coupling constant) whose bare value formally receives infinitely large quantum mechanical corrections. Although the difference between the bare and measured values of this quantity may be infinite, the differences between any two measurable quantities (e.g. the effective coupling at two different energy scales) should remain finite and calculable. In practice these calculations can be performed by adding to the Lagrangian terms that cancel these infinite corrections. These cancellations can be tuned so as to fix the value of one measurement, e.g. by matching the measured coupling at some particular energy.

Consider how this applies to the lattice calculations discussed here. Initially the field fluctuations are only those representing quantum vacuum states. These fluctuations affect couplings, masses, and the total energy of the system in a way that is dependent on the lattice spacing. For example, consider the theory

$$V = \lambda \phi^4 \tag{12.36}$$

and rewrite the field  $\phi$  as the sum of a homogeneous component  $\Phi$  and fluctuations  $\delta\phi$ . The effective potential felt by the homogeneous field  $\Phi$  will receive a correction from the fluctuations equal to

$$\delta V \approx \frac{3}{2} \lambda \langle \delta\phi^2 \rangle \Phi^2. \tag{12.37}$$

(The  $3/2$  arises from combinatorics.) I'm assuming all odd powers of  $\delta\phi$  vanish on average. This correction represents an unphysical effect in the sense that its

strength depends on the ultraviolet cutoff imposed by the lattice. In the limit of zero lattice spacing where arbitrarily large momenta would be included on the lattice this correction would become infinite. This effect could be eliminated, however, by adding a renormalization term

$$V_{renormalization} = -\frac{3}{2}\lambda < \delta\phi^2 > \phi^2 \quad (12.38)$$

or equivalently by adding the term

$$-3\lambda < \delta\phi^2 > \phi \quad (12.39)$$

to the equation of motion for  $\phi$ . Note that  $< \delta\phi^2 >$  in this case refers to the initial value that arises from quantum fluctuations, not to a dynamic quantity that changes as the field evolves. Such changes represent physical effects and should not be eliminated. In effect this correction would fix the effective mass for  $\Phi$  (i.e.  $\partial^2 V / \partial \Phi^2$ ) to be flat at  $\Phi = 0$  when the field is in the vacuum state.

The above example illustrates how a simple form of renormalization can be implemented on the lattice. This procedure could in principle be used to renormalize any mass, coupling constant, or energy term in the theory. Ordinarily these corrections are not important because the quantum effects are quickly swamped as the fluctuations become amplified. In some cases, however, quantum effects can change the initial behavior of the system in important ways. For example in the theory

$$V = \frac{1}{4}\lambda\phi^4 - \frac{1}{3}\lambda v\phi^3 + \frac{1}{12}\lambda v^4 \quad (12.40)$$

the cubic term contributes a linear term to  $V_{eff}(\Phi)$  that causes the field to initially start rolling away from zero. In this case we found it useful to eliminate this term by adding

$$V_{renormalization} = \lambda v < \delta\phi^2 > \quad (12.41)$$

to the equation of motion for  $\phi$ . See chapter 10.

## Chapter 13

# Computational Methods Used by LATTICEASY

### 13.1 Time Evolution: The Staggered Leapfrog Method

LATTICEASY uses a method called “staggered leapfrog” for solving differential equations. In order to solve a second order (in time) equation you need to store the value of the variable and its first time derivative at each step, and use these to calculate the value of the second time derivative. The idea of staggered leapfrog is to store the variables (i.e. the field values) and their derivatives at different times. Specifically, if the program is using a time step  $dt$  and the field values are known at a time  $t$  then the derivatives will initially be known at a time  $t - dt/2$ . Using the field values the program can then calculate the second derivative  $\ddot{f}$  at time  $t$  and use this to advance  $\dot{f}$  to  $t + dt/2$ . This value of  $\dot{f}$  can in turn be used to advance  $f$  to  $t + dt$ , thus restarting the process. Schematically, this looks like

$$\begin{aligned} f(t) &= f(t - dt) + dt\dot{f}(t - dt/2) \\ \dot{f}(t + dt/2) &= \dot{f}(t - dt/2) + dt\ddot{f}[f(t)] \\ f(t + dt) &= f(t) + dt\dot{f}(t + dt/2) \end{aligned} \tag{13.1}$$

Because each step advances  $f$  or  $\dot{f}$  in terms of its derivative at a time in the *middle* of the step this method has higher order accuracy and greater stability than a simple Euler method. However, the method relies on being able to calculate  $\ddot{f}$  in terms of  $f$  at the time  $t$ , so both accuracy and stability are generally lost if  $\ddot{f}$  depends on the first derivative  $\dot{f}$ . This is the reason we choose our rescalings so as to eliminate first derivative terms in the equations of motion. Note that the evolution equation for the scale factor does have a first derivative in it. Section 13.2 describes how this problem is solved in the program.

To set the initial conditions for the staggered leapfrog calculations the field values and derivatives must be desynchronized. The initial conditions are set at  $t = 0$  and then the fields are advanced by an Euler step of size  $dt/2$  to begin the leapfrog. Thereafter all calculations are done in full, staggered steps.

## 13.2 Correction to the Scale Factor Evolution Equation to Account for Staggered Leapfrog

Using a staggered leapfrog algorithm means that in solving for  $\ddot{a}(t)$  the value of  $\dot{a}$  is known at  $t - d/2$  where  $d$  is the time step. See section 13.1 for more details. The solution to this problem is to use the two equations

$$\dot{a}_+ \approx \dot{a}_- + d\ddot{a}; \quad \dot{a} \approx \frac{1}{2}(\dot{a}_+ + \dot{a}_-) \quad (13.2)$$

where  $\dot{a}_+$  and  $\dot{a}_-$  refer to the values of  $\dot{a}$  at  $t + d/2$  and  $t - d/2$  respectively and all other variables are evaluated at time  $t$ .<sup>1</sup> Take the evolution equation to be

$$\ddot{a} = -C_1 \frac{\dot{a}^2}{a} + C_2. \quad (13.3)$$

---

<sup>1</sup>Thanks to Julian Borrill for suggesting this solution.

Plugging this form into equation (13.2) and eliminating  $\dot{a}$  gives

$$\dot{a}_+ \approx \dot{a}_- + d \left( -\frac{C_1}{4a} (\dot{a}_+ + \dot{a}_-)^2 + C_2 \right) = -\frac{dC_1}{4a} \dot{a}_+^2 - \frac{dC_1}{2a} \dot{a}_+ \dot{a}_- - \frac{dC_1}{4a} \dot{a}_-^2 + dC_2 + \dot{a}_- \quad (13.4)$$

$$\begin{aligned} \dot{a}_+ &\approx -\frac{2a}{dC_1} \left( \frac{dC_1}{2a} \dot{a}_- + 1 \pm \sqrt{\frac{d^2 C_1^2}{4a^2} \dot{a}_-^2 + \frac{dC_1}{a} \dot{a}_- + 1 - \frac{d^2 C_1^2}{4a^2} \dot{a}_-^2 + \frac{d^2 C_1 C_2}{a} + \frac{dC_1}{a} \dot{a}_-} \right) \\ &= -\dot{a}_- - \frac{2a}{dC_1} \pm \frac{2a}{dC_1} \sqrt{1 + \frac{2dC_1}{a} \dot{a}_- + \frac{d^2 C_1 C_2}{a}}. \end{aligned} \quad (13.5)$$

To determine whether to use the plus or minus sign in equation (13.5) consider the limit as  $d \rightarrow 0$ . In this limit

$$\dot{a}_+ \approx -\dot{a}_- - \frac{2a}{dC_1} \pm \frac{2a}{dC_1} \sqrt{1 + \frac{2dC_1}{a} \dot{a}_-} \approx -\dot{a}_- - \frac{2a}{dC_1} \pm \left( \frac{2a}{dC_1} + 2\dot{a}_- \right). \quad (13.6)$$

This suggests that the plus sign must be used in order to reduce to the limit  $\dot{a}_+ \approx \dot{a}_-$ . Hence

$$\dot{a}_+ \approx -\dot{a}_- - \frac{2a}{dC_1} \left( 1 - \sqrt{1 + \frac{2dC_1}{a} \dot{a}_- + \frac{d^2 C_1 C_2}{a}} \right). \quad (13.7)$$

In the program it's useful to calculate  $\ddot{a}$ , which is roughly  $(\dot{a}_+ - \dot{a}_-)/d$ , so

$$\ddot{a} \approx \frac{1}{d} \left[ -2\dot{a}_- - \frac{2a}{dC_1} \left( 1 - \sqrt{1 + \frac{2dC_1}{a} \dot{a}_- + \frac{d^2 C_1 C_2}{a}} \right) \right]. \quad (13.8)$$

Thus equation (12.7) becomes

$$\ddot{a} \approx \frac{1}{d} \left\{ -2\dot{a}_- - \frac{a}{d} \left[ 1 - \sqrt{1 + \frac{4d\dot{a}_-}{a} + d^2 \frac{16\pi}{A^2} a^{-2} \left( \frac{1}{3} |\nabla f_i|^2 + a^2 V \right)} \right] \right\}. \quad (13.9)$$

### 13.3 Spatial Derivatives

There are two contexts in which the lattice program needs to calculate spatial derivatives. The first is in the evolution equations, which include a Laplacian term  $\nabla^2 f$ . The second is in calculating the field gradients  $|\nabla f|^2$ , both for total energy and for

the scale factor evolution.

The Laplacian is calculated using a simple nearest-neighbor scheme

$$\nabla^2 f(x, y, z) \equiv \frac{\partial^2 f}{\partial x^2} + \frac{\partial^2 f}{\partial y^2} + \frac{\partial^2 f}{\partial z^2} \approx \frac{1}{dx^2} \left( \sum_{\text{neighbors}} f - 6f(x, y, z) \right) \quad (13.10)$$

where  $dx$  is the lattice spacing and the sum over neighbors is taken over the six lattice points adjacent to  $(x, y, z)$ . We tried on several occasions using a higher order scheme involving twice removed neighbors, but never found any noticeable difference in the results.

Gradients could be calculated using a similar formula, but it turns out there is a more accurate way that is no more computationally expensive.<sup>2</sup> This simplification is made possible by the fact that the gradients are only needed for sums over the entire lattice. Since the lattice is periodic we can use integration by parts with no surface term, i.e.

$$\sum_{\text{lattice}} |\nabla f|^2 = - \sum_{\text{lattice}} f \nabla^2 f. \quad (13.11)$$

We can thus use the Laplacian formula above for the gradients as well. Switching from a direct calculation of the gradients to this indirect method improved our calculation of the total energy so much that the amount of energy nonconservation in our runs decreased by more than an order of magnitude!

## 13.4 The Accuracy of the Simulations

### 13.4.1 The Classical Approximation

As mentioned before, frequently used approximation schemes such as linear analysis or the Hartree approximation are inadequate for preheating problems, which typically involve significant rescattering. Lattice simulations automatically account for all rescattering effects, but one may legitimately ask whether these simulations involve other, potentially dangerous approximations.

---

<sup>2</sup>Thanks to Ue-Li Pen for this suggestion.



Of course any numerical calculations suffer from a certain amount of inaccuracy. In addition to simple roundoff errors lattice simulations also contain errors due to their inherent ultraviolet (grid spacing) and infrared (box size) cutoffs. Section 13.4.2 discusses how such errors are monitored and controlled in our simulations.

On a more fundamental level, however, simulations such as ours employ the classical approximation. In other words we simply solve the classical equations of motion for the fields in our system, neglecting all quantum mechanical effects. This approximation may seem unjustifiable, particularly given that the initial fluctuations that seed reheating in inflationary cosmology are quantum mechanical in origin. In preheating, however, these fluctuations are rapidly amplified to exponentially large amplitudes, which permits us to neglect quantum effects.

More precisely, the classical limit of a field theory occurs when the occupation number becomes much larger than one. For a scalar field  $\phi$  the occupation number of a particular mode  $\phi_k$  is given by

$$n_k = \frac{1}{2} \left( \omega_k |\phi_k|^2 + \frac{1}{\omega_k} |\dot{\phi}_k|^2 \right), \quad (13.12)$$

where

$$\omega_k \equiv \sqrt{k^2 + m^2}. \quad (13.13)$$

In the vacuum the field has expectation values

$$\langle |\phi_k|^2 \rangle = \frac{1}{2\omega_k} \quad (13.14)$$

$$\langle |\dot{\phi}_k|^2 \rangle = \frac{\omega_k}{2} \quad (13.15)$$

and thus

$$\langle n_k \rangle = \frac{1}{2}. \quad (13.16)$$

In all of our simulations preheating rapidly drives the fields to a state where  $n_k \gg 1$ .

In fact it turns out that not all modes on the lattice are amplified in this way, but the ones that aren't make an exponentially small contribution to the field dynamics. More specifically, preheating amplifies infrared modes, so for any particular model

there will be a certain cutoff in momentum space above which the modes aren't amplified. To ensure that all relevant physics is included in the simulation the lattice spacing should be small enough to include all modes below this cutoff. Then the small wavelength modes that remain unamplified make no appreciable difference. This assertion can (and should) always be checked for a given model by verifying that the results are insensitive to the exact lattice spacing used.

Finally, one might wonder if the initial stages of the calculation are a source for concern since in these stages all of the fluctuations have small occupation numbers. While this concern is valid in principle, it turns out to be irrelevant in practice. The final outcome of preheating in a particular model is determined by feedback mechanisms that come into play when the fluctuations are large and rescattering important. In all of the models we have examined to date the final results proved to be extremely insensitive to the details of the initial conditions, which leads us to believe that any potential inaccuracies in our treatment of the first stages of preheating should have little or no effect on our conclusions. Nonetheless such concerns are ultimately valid ones and must be rechecked for each model that one wishes to examine using the classical approximation.

### 13.4.2 Numerical Accuracy

There are numerous ways to monitor the numerical accuracy of a calculation. These include straightforward, “brute-force” methods of trial and error. For example one should always vary quantities such as the time step and random number seeds (used in the initial conditions, see section 12.2.1) to make sure that the final results are insensitive to changes in these quantities.

Another useful trick is to monitor one or more conserved quantities. In the case of field theory in Minkowski space it is a straightforward task to compute the total energy on the lattice. All of our Minkowski space simulations conserve total energy to within a few percent, and virtually all of them do so to within at most a few tenths of a percent.

Minkowski space is only an approximation, however, useful in cases where expansion can be neglected. In an expanding universe the situation is a little more complicated because energy density is not conserved, but rather decreases in a way determined by the expansion rate and the equation of state of the fields. This red-shifting of energy is described by the continuity equation

$$\dot{\rho} + 3\frac{\dot{a}}{a}(\rho + 3p) = 0. \quad (13.17)$$

Equation (13.17) can be derived from the Friedmann equations, so if these are being solved exactly then the continuity equation will be obeyed as well. So a simple way to check energy conservation in an expanding universe is to use one of the Friedmann equations, equations (12.2) and (12.3) to evolve the scale factor and then check if the other is being satisfied as well. In practice the program uses a combination of these two equations so either one can be used as a check of energy conservation. We use equation (12.3), i.e.

$$\left(\frac{\dot{a}}{a}\right)^2 = \frac{8\pi}{3}\rho. \quad (13.18)$$

So when expansion is being included in a simulation the program periodically calculates

$$H^2 / \left(\frac{8\pi}{3}\rho\right). \quad (13.19)$$

This quantity should remain close to 1 throughout the run. We have generally found that the deviation of this ratio from one is comparable to the lack of energy conservation for runs done with the same models without expansion. We have also checked that using the second Friedmann equation, equation (12.2), gives essentially the same results as this method.

Finally, even assuming all the numerics are done accurately, there is an inherent inaccuracy in any lattice calculation related to the ultraviolet and infrared cutoffs imposed by the lattice. A cubic lattice in position space will have a discrete Fourier transform corresponding to a cubic lattice in momentum space. The largest momentum modes will have a wavelength of the order of the lattice spacing, and the smallest

momentum modes will have a wavelength of the order of the total box size.<sup>3</sup> This means that if there is significant physics occurring at wavelengths outside this range the lattice will simply not see it, no matter how small a time step you use.

There are a number of ways to minimize the effect of this problem. The first is to know the physics of the system you are considering. For all the problems we have solved on the lattice the relevant wavelengths could be approximately calculated analytically, and the lattice could be used to verify these calculations. Note that such considerations may limit the range of parameter space available for lattice calculations. If a problem has two important wavelengths that differ by ten orders of magnitude then a lattice simulation such as ours can not possibly hope to include them both. As long as all the most important wavelengths occur within a couple of orders of magnitude of each other, though, they can typically be treated accurately.

Secondly, as with variables such as the time step, there's no substitute for a little trial and error. As much as possible we would vary the size of our box and lattice spacing to make sure that we were in a realm where our results were insensitive to such changes. This procedure doesn't guard against relevant effects occurring far outside the range of the simulations, but it at least ensures that in the general area of momentum space being considered the lattice isn't imposing any limitations.

Finally, it's important to monitor the spectrum of the fields in order to see which modes are playing the most significant roles. In the case of preheating the spectrum typically looks relatively flat at long wavelengths and then has an exponential cutoff at some point. Thus as long as we kept the lattice spacing small enough to include modes up to the cutoff in momentum space we felt confident we weren't missing important ultraviolet physics.<sup>4</sup>

---

<sup>3</sup>Strictly speaking this is not true because the lowest momentum mode is  $k = 0$ , corresponding to a perfectly homogeneous field. The lowest *nonzero* momentum, however, will correspond to a wavelength comparable to the box size.

<sup>4</sup>Note that in the limit of zero lattice spacing these ultraviolet modes would make an infinitely large contribution to the field dynamics. For more discussion of this issue see section 12.3 on renormalization.

## **Part IV**

# **Conclusion: My Philosophical Ramblings**

Working in cosmology has one great advantage over work in many other areas of physics. In all areas of physics the mathematical and other tools used can be complicated and often provide a barrier between those working in the field and others who might be interested in the results of that work. It is difficult for most working physicists to explain to someone outside the field what they do, or sometimes even why the questions they are working on are interesting and worth pursuing. In many cases this difficulty arises not because the problems are unimportant but simply because there is a great deal of technical background required to understand them. In cosmology it is still true that the tools we use are often highly technical and mathematically complex. However the questions we are trying to answer are in many cases the same questions that people have always wondered about.

Has the universe been here forever or did it have a beginning? Is it infinite or finite? Where did all the different things in it come from? Will the universe be here forever or someday be destroyed? Is our position in the universe unusual or typical? All of these and many other questions like them seem so basic to human nature that in general it requires no explanation for people to understand why we in the field consider these problems worth pursuing.

I am not claiming that cosmology has answered these questions, or even that it ever will. I do believe, however, that whether or not we ever achieve a complete understanding of these issues we can make progress on refining our understanding of them. What will be the fate of the universe? Our current theories and observations seem to indicate that it will expand forever. Where did all the matter in the universe come from? If inflationary theory is correct it came from the decay of the energy of a single field. Where did that field originally come from? That is one of the many questions we don't have an answer to. And if we ever have a complete physical theory of the universe from beginning to end we will still be left with the question of why that theory should be true, and not some other. I don't believe science can in principle address that question.

On the whole, however, I believe that science is capable of making progress on answering many of the basic questions that humans have wondered about throughout the ages. I think that the last century has seen tremendous progress in that direction,

and the century to come will see even more than that. Ultimately, it is these questions that have motivated me in all the work presented here.

“I want to know God’s thoughts. The rest are details.” - Albert Einstein





# Bibliography

- [1] A. H. Guth, Phys. Rev. **D23**, 347 (1981).
- [2] A. D. Linde, Phys. Lett. **B129**, 177 (1983).
- [3] A. Linde, *Particle Physics and Inflationary Cosmology* (Harwood, Chur, Switzerland, 1990).
- [4] A. Albrecht, P. J. Steinhardt, M. S. Turner, and F. Wilczek, Phys. Rev. Lett. **48**, 1437 (1982).
- [5] L. Kofman, A. Linde, and A. A. Starobinsky, Phys. Rev. Lett. **73**, 3195 (1994), hep-th/9405187.
- [6] L. Landau and E. Lifshitz, *Mechanics* (Pergamon Press, Oxford, 1960).
- [7] L. Kofman, A. Linde, and A. A. Starobinsky, Phys. Rev. **D56**, 3258 (1997), hep-ph/9704452.
- [8] P. B. Greene, L. Kofman, A. Linde, and A. A. Starobinsky, Phys. Rev. **D56**, 6175 (1997), hep-ph/9705347.
- [9] G. Felder, L. Kofman, and A. Linde, Phys. Rev. **D59**, 123523 (1999), hep-ph/9812289.
- [10] A. D. Dolgov and A. D. Linde, Phys. Lett. **B116**, 329 (1982).
- [11] L. F. Abbott, E. Farhi, and M. B. Wise, Phys. Lett. **B117**, 29 (1982).

- [12] A. A. Starobinsky, (1984), In \*Moscow 1981, Proceedings, Quantum Gravity\*, 103-128.
- [13] A. D. Linde, Phys. Lett. **B108**, 389 (1982).
- [14] L. Kofman, A. Linde, and A. A. Starobinsky, Phys. Rev. Lett. **76**, 1011 (1996), hep-th/9510119.
- [15] I. I. Tkachev, Phys. Lett. **B376**, 35 (1996), hep-th/9510146.
- [16] S. Khlebnikov, L. Kofman, A. Linde, and I. Tkachev, Phys. Rev. Lett. **81**, 2012 (1998), hep-ph/9804425.
- [17] I. Tkachev, S. Khlebnikov, L. Kofman, and A. Linde, Phys. Lett. **B440**, 262 (1998), hep-ph/9805209.
- [18] E. W. Kolb, A. Linde, and A. Riotto, Phys. Rev. Lett. **77**, 4290 (1996), hep-ph/9606260.
- [19] E. W. Kolb, A. Riotto, and I. I. Tkachev, Phys. Lett. **B423**, 348 (1998), hep-ph/9801306.
- [20] S. Y. Khlebnikov and I. I. Tkachev, Phys. Lett. **B390**, 80 (1997), hep-ph/9608458.
- [21] B. R. Greene, T. Prokopec, and T. G. Roos, Phys. Rev. **D56**, 6484 (1997), hep-ph/9705357.
- [22] I. Zlatev, G. Huey, and P. J. Steinhardt, Phys. Rev. **D57**, 2152 (1998), astro-ph/9709006.
- [23] D. J. H. Chung, (1998), hep-ph/9809489.
- [24] L. H. Ford, Phys. Rev. **D35**, 2955 (1987).
- [25] B. Spokoiny, Phys. Lett. **B315**, 40 (1993), gr-qc/9306008.
- [26] M. Joyce, Phys. Rev. **D55**, 1875 (1997), hep-ph/9606223.

- [27] M. Joyce and T. Prokopec, Phys. Rev. **D57**, 6022 (1998), hep-ph/9709320.
- [28] P. J. E. Peebles and A. Vilenkin, Phys. Rev. **D59**, 063505 (1999), astro-ph/9810509.
- [29] R. R. Caldwell, R. Dave, and P. J. Steinhardt, Phys. Rev. Lett. **80**, 1582 (1998), astro-ph/9708069.
- [30] A. Berera and T. W. Kephart, Phys. Lett. **B456**, 135 (1999), hep-ph/9811295.
- [31] J. Baacke, K. Heitmann, and C. Patzold, Phys. Rev. **D58**, 125013 (1998), hep-ph/9806205.
- [32] P. B. Greene and L. Kofman, Phys. Lett. **B448**, 6 (1999), hep-ph/9807339.
- [33] V. Berezhinsky, M. Kachelriess, and A. Vilenkin, Phys. Rev. Lett. **79**, 4302 (1997), astro-ph/9708217.
- [34] V. A. Kuzmin and V. A. Rubakov, Phys. Atom. Nucl. **61**, 1028 (1998), astro-ph/9709187.
- [35] D. J. H. Chung, E. W. Kolb, and A. Riotto, Phys. Rev. **D59**, 023501 (1999), hep-ph/9802238.
- [36] V. Kuzmin and I. Tkachev, JETP Lett. **68**, 271 (1998), hep-ph/9802304.
- [37] V. Kuzmin and I. Tkachev, Phys. Rev. **D59**, 123006 (1999), hep-ph/9809547.
- [38] D. J. H. Chung, E. W. Kolb, and A. Riotto, Phys. Rev. **D60**, 063504 (1999), hep-ph/9809453.
- [39] E. W. Kolb, D. J. H. Chung, and A. Riotto, (1998), hep-ph/9810361.
- [40] K. Greisen, Phys. Rev. Lett. **16**, 748 (1966).
- [41] G. T. Zatsepin and V. A. Kuzmin, JETP Lett. **4**, 78 (1966).
- [42] C. M. Hull and P. K. Townsend, Nucl. Phys. **B451**, 525 (1995), hep-th/9505073.

- [43] E. Witten, Nucl. Phys. **B443**, 85 (1995), hep-th/9503124.
- [44] K. Intriligator and N. Seiberg, Nucl. Phys. Proc. Suppl. **45BC**, 1 (1996), hep-th/9509066.
- [45] M. Shifman, Prog. Part. Nucl. Phys. **39**, 1 (1997), hep-th/9704114.
- [46] J. Polchinski, *String Theory* (Cambridge University Press, Cambridge, 1998).
- [47] G. Felder, L. Kofman, and A. Linde, Phys. Rev. **D60**, 103505 (1999), hep-ph/9903350.
- [48] Y. B. Zeldovich and A. A. Starobinsky, Sov. Phys. JETP **34**, 1159 (1972).
- [49] L. P. Grishchuk, Sov. Phys. JETP **40**, 409 (1975).
- [50] L. P. Grishchuk, Nuovo Cim. Lett. **12**, 60 (1975).
- [51] S. G. Mamaev, V. M. Mostepanenko, and A. A. Starobinsky, Zh. Eksp. Teor. Fiz. **70**, 1577 (1976).
- [52] A. A. Grib, S. G. Mamaev, and V. M. Mostepanenko, Gen. Rel. Grav. **7**, 535 (1976).
- [53] A. A. Grib, S. G. Mamaev, and V. M. Mostepanenko, *Vacuum Quantum Effects in Strong Fields* (Energoatomizdat, Moscow, 1988).
- [54] L. A. Kofman and A. D. Linde, Nucl. Phys. **B282**, 555 (1987).
- [55] M. Dine, W. Fischler, and D. Nemeschansky, Phys. Lett. **B136**, 169 (1984).
- [56] G. D. Coughlan, R. Holman, P. Ramond, and G. G. Ross, Phys. Lett. **B140**, 44 (1984).
- [57] A. S. Goncharov, A. D. Linde, and M. I. Vysotsky, Phys. Lett. **B147**, 279 (1984).
- [58] G. Dvali, (1995), hep-ph/9503259.

- [59] M. Dine, L. Randall, and S. Thomas, Phys. Rev. Lett. **75**, 398 (1995), hep-ph/9503303.
- [60] J. Ellis, G. B. Gelmini, J. L. Lopez, D. V. Nanopoulos, and S. Sarkar, Nucl. Phys. **B373**, 399 (1992).
- [61] R. Kallosh, L. Kofman, A. Linde, and A. V. Proeyen, Phys. Rev. **D61**, 103503 (2000), hep-th/9907124.
- [62] J. Ellis, A. D. Linde, and D. V. Nanopoulos, Phys. Lett. **B118**, 59 (1982).
- [63] L. M. Krauss, Nucl. Phys. **B227**, 556 (1983).
- [64] D. V. Nanopoulos, K. A. Olive, and M. Srednicki, Phys. Lett. **B127**, 30 (1983).
- [65] M. Y. Khlopov and A. D. Linde, Phys. Lett. **B138**, 265 (1984).
- [66] J. Ellis, J. E. Kim, and D. V. Nanopoulos, Phys. Lett. **B145**, 181 (1984).
- [67] M. Kawasaki and T. Moroi, Prog. Theor. Phys. **93**, 879 (1995), hep-ph/9403364.
- [68] G. Felder, L. Kofman, and A. Linde, JHEP **02**, 027 (2000), hep-ph/9909508.
- [69] C. Pathinayake and L. H. Ford, Phys. Rev. **D35**, 3709 (1987).
- [70] M. Bronstein, Zh. Eksp. Teor. Fiz. **3**, 73 (1933).
- [71] M. Ozer and M. O. Taha, Nucl. Phys. **B287**, 776 (1987).
- [72] K. Freese, F. C. Adams, J. A. Frieman, and E. Mottola, Nucl. Phys. **B287**, 797 (1987).
- [73] C. Wetterich, Nucl. Phys. **B302**, 668 (1988).
- [74] B. Ratra and P. J. E. Peebles, Phys. Rev. **D37**, 3406 (1988).
- [75] J. A. Frieman, C. T. Hill, A. Stebbins, and I. Waga, Phys. Rev. Lett. **75**, 2077 (1995), astro-ph/9505060.

- [76] P. G. Ferreira and M. Joyce, Phys. Rev. Lett. **79**, 4740 (1997), astro-ph/9707286.
- [77] E. J. Copeland, A. R. Liddle, and D. Wands, Phys. Rev. **D57**, 4686 (1998), gr-qc/9711068.
- [78] D. Huterer and M. S. Turner, (1998), astro-ph/9808133.
- [79] L. min Wang, R. R. Caldwell, J. P. Ostriker, and P. J. Steinhardt, Astrophys. J. **530**, 17 (2000), astro-ph/9901388.
- [80] G. F. Giudice, I. Tkachev, and A. Riotto, JHEP **08**, 009 (1999), hep-ph/9907510.
- [81] G. D. Coughlan, W. Fischler, E. W. Kolb, S. Raby, and G. G. Ross, Phys. Lett. **B131**, 59 (1983).
- [82] D. H. Lyth and E. D. Stewart, Phys. Rev. Lett. **75**, 201 (1995), hep-ph/9502417.
- [83] D. H. Lyth and E. D. Stewart, Phys. Rev. **D53**, 1784 (1996), hep-ph/9510204.
- [84] A. Linde, Phys. Rev. **D53**, 4129 (1996), hep-th/9601083.
- [85] T. Asaka and M. Kawasaki, Phys. Rev. **D60**, 123509 (1999), hep-ph/9905467.
- [86] L. Randall and S. Thomas, Nucl. Phys. **B449**, 229 (1995), hep-ph/9407248.
- [87] G. Felder, L. Kofman, A. Linde, and I. Tkachev, JHEP **08**, 010 (2000), hep-ph/0004024.
- [88] D. A. Kirzhnits, JETP Lett. **15**, 529 (1972).
- [89] D. A. Kirzhnits and A. D. Linde, Phys. Lett. **B42**, 471 (1972).
- [90] S. Weinberg, Phys. Rev. **D9**, 3357 (1974).
- [91] L. Dolan and R. Jackiw, Phys. Rev. **D9**, 3320 (1974).
- [92] D. A. Kirzhnits and A. D. Linde, Sov. Phys. JETP. **40**, 628 (1975).

- [93] D. A. Kirzhnits and A. D. Linde, *Ann. Phys.* **101**, 195 (1976).
- [94] A. Albrecht and P. J. Steinhardt, *Phys. Rev. Lett.* **48**, 1220 (1982).
- [95] V. A. Kuzmin, V. A. Rubakov, and M. E. Shaposhnikov, *Phys. Lett.* **B155**, 36 (1985).
- [96] M. E. Shaposhnikov, *JETP Lett.* **44**, 465 (1986).
- [97] A. Rajantie and E. J. Copeland, *Phys. Rev. Lett.* **85**, 916 (2000), hep-ph/0003025.
- [98] S. Kasuya and M. Kawasaki, *Phys. Rev.* **D61**, 083510 (2000), hep-ph/9903324.
- [99] S. Y. Khlebnikov and I. I. Tkachev, *Phys. Rev. Lett.* **77**, 219 (1996), hep-ph/9603378.
- [100] S. Y. Khlebnikov and I. I. Tkachev, *Phys. Rev. Lett.* **79**, 1607 (1997), hep-ph/9610477.
- [101] E. Kolb and M. Turner, *The Early Universe* (Addison-Wesley, Redwood City, CA, 1990).
- [102] A. Linde, *Nucl. Phys.* **B372**, 421 (1992), hep-th/9110037.
- [103] S. Coleman, *Phys. Rev.* **D15**, 2929 (1977).
- [104] A. D. Linde, *Nucl. Phys.* **B216**, 421 (1983).
- [105] Y. B. Zeldovich, I. Y. Kobsarev, and L. B. Okun, *Phys. Lett.* **B50**, 340 (1974).
- [106] A. Linde and A. Riotto, *Phys. Rev.* **D56**, 1841 (1997), hep-ph/9703209.
- [107] C. Contaldi, M. Hindmarsh, and J. Magueijo, *Phys. Rev. Lett.* **82**, 2034 (1999), astro-ph/9809053.
- [108] R. A. Battye and J. Weller, *Phys. Rev.* **D61**, 043501 (2000), astro-ph/9810203.
- [109] R. A. Battye, J. Magueijo, and J. Weller, (1999), astro-ph/9906093.

- [110] G. Felder and L. Kofman, (2000), hep-ph/0011160.
- [111] T. Prokopec and T. G. Roos, Phys. Rev. **D55**, 3768 (1997), hep-ph/9610400.
- [112] T. Biro, S. Matinyan, and B. Muller, *Chaos and Gauge Field Theory* (World Scientific, Singapore, 1994).
- [113] V. Zakharov, V. L'vov, and G. Falkovich, *Kolmogorov Spectra of Turbulence* (Springer-Verlag, 1992).
- [114] J. Garcia-Bellido, D. Y. Grigoriev, A. Kusenko, and M. Shaposhnikov, Phys. Rev. **D60**, 123504 (1999), hep-ph/9902449.
- [115] D. Polarski and A. A. Starobinsky, Class. Quant. Grav. **13**, 377 (1996), gr-qc/9504030.
- [116] U. Heinz, C. R. Hu, S. Leupold, S. G. Matinian, and B. Muller, Phys. Rev. **D55**, 2464 (1997), hep-th/9608181.
- [117] P. B. Greene and L. Kofman, Phys. Rev. **D62**, 123516 (2000), hep-ph/0003018.
- [118] G. Aarts, G. F. Bonini, and C. Wetterich, Nucl. Phys. **B587**, 403 (2000), hep-ph/0003262.
- [119] D. V. Semikoz and I. I. Tkachev, Phys. Rev. **D55**, 489 (1997), hep-ph/9507306.
- [120] G. Felder *et al.*, (2000), hep-ph/0012142.
- [121] A. A. Anselm and M. G. Ryskin, Phys. Lett. **B266**, 482 (1991).
- [122] J. D. Bjorken, K. L. Kowalski, and C. C. Taylor, Presented at 7th Les Rencontres de Physique de la Vallee d'Aoste: Results and Perspectives in Particle Physics, La Thuile, Italy, 7-13 Mar 1993.
- [123] K. Rajagopal and F. Wilczek, Nucl. Phys. **B399**, 395 (1993), hep-ph/9210253.
- [124] K. Rajagopal and F. Wilczek, Nucl. Phys. **B404**, 577 (1993), hep-ph/9303281.



- [125] D. Boyanovsky, H. J. de Vega, and R. Holman, Phys. Rev. **D51**, 734 (1995), hep-ph/9401308.
- [126] A. Linde, Phys. Lett. **B259**, 38 (1991).
- [127] A. Linde, Phys. Rev. **D49**, 748 (1994), astro-ph/9307002.
- [128] J. Garcia-Bellido and A. Linde, Phys. Rev. **D57**, 6075 (1998), hep-ph/9711360.
- [129] D. Boyanovsky, M. D’Attanasio, H. J. de Vega, R. Holman, and D. S. Lee, Phys. Rev. **D52**, 6805 (1995), hep-ph/9507414.
- [130] D. Boyanovsky, H. J. de Vega, and R. Holman, (1999), hep-ph/9903534.
- [131] E. J. Copeland, A. R. Liddle, D. H. Lyth, E. D. Stewart, and D. Wands, Phys. Rev. **D49**, 6410 (1994), astro-ph/9401011.
- [132] M. Bastero-Gil, S. F. King, and J. Sanderson, Phys. Rev. **D60**, 103517 (1999), hep-ph/9904315.
- [133] J. M. Bardeen, J. R. Bond, N. Kaiser, and A. S. Szalay, Astrophys. J. **304**, 15 (1986).
- [134] P. Binetruiy and G. Dvali, Phys. Lett. **B388**, 241 (1996), hep-ph/9606342.
- [135] E. Halyo, Phys. Lett. **B387**, 43 (1996), hep-ph/9606423.
- [136] R. Kallosh, L. Kofman, A. Linde, and A. V. Proeyen, Class. Quant. Grav. **17**, 4269 (2000), hep-th/0006179.
- [137] G. F. Giudice, A. Riotto, and I. Tkachev, JHEP **11**, 036 (1999), hep-ph/9911302.
- [138] W. Press *et al.*, *Numerical Recipes in C: The Art of Scientific Computing, Second Edition* (Cambridge University Press, Melbourne, Australia, 1992).
- [139] M. E. Peskin and D. V. Schroeder, *An Introduction to Quantum Field Theory* (Addison Wesley, Reading, Massachusetts, 1995).